Characterization of The SPOC Regulatory Function of Bud14

by

Hüseyin Karabürk

A Dissertation Submitted to the
Graduate School of Sciences and Engineering
in Partial Fulfillment of the Requirements for
the Degree of

Master of Science

in

Molecular Biology and Genetics

KOÇ
ÜNİVERSİTESİ

August 2021

Characterization of The SPOC Regulatory Function of Bud14

Koç University

Graduate School of Sciences and Engineering

This is to certify that I have examined this copy of a master's thesis by

Hüseyin Karabürk

and have found that it is complete and satisfactory in all respects,
and that any and all revisions required by the final
examining committee have been made.

Committee Members:

Assistant Prof. Dr. Ayşe Koca Çaydaşı (Advisor-Koç University)

Associate Prof. Dr. Elif Nur Fırat Karalar (Koç University)

Prof. Dr. Ayşe Elif Erson Bensan (Middle East Technical University)

Date:06/08/2021

To my family, and everyone else who supported me during this journey

ABSTRACT

Characterization of The SPOC Regulatory Function of Bud14

Hüseyin Karabürk

Master of Science in Molecular Biology and Genetics

August 6, 2021

Saccharomyces cerevisiae, also known as the budding yeast, is a commonly used model organism to study the orientation of mitotic spindle and its effects on asymmetric cell division. The mitotic spindle of budding yeast needs to be oriented in the mother-to-daughter polarity axis in order to segregate one copy of its genomic DNA to the daughter cell during the cell cycle. Spindle Position Checkpoint (SPOC) is a surveillance mechanism that inhibits the progression of cell cycle upon spindle mispositioning. Cells with deficient SPOC lose their genomic integrity, eventually resulting in multiploidy and aneuploidy. Therefore, SPOC is necessary for the maintenance of ploidy in budding yeast. However, so far it has not been completely enlightened how the SPOC mechanism functions. In this thesis, we showed that Bud14 is a novel component of SPOC. We showed that deletion of *BUD14* promotes the growth of cells with impaired mitotic exit, indicating Bud14 is an inhibitor of mitotic exit. We demonstrated that *bud14Δ* cells are SPOC deficient, accumulating multinucleated cell populations in the presence of spindle misalignment. Our data showed that SPOC regulatory function of Bud14 is not dependent on its role in formin-dependent actin polymerization regulation. We identified that Bud14-Glc7 interaction is required for the mitotic exit inhibitory function of Bud14 because a temperature sensitive mutant version of Glc7 (*glc7-12*) that cannot bind to Bud14 resulted in SPOC deficiency in the presence of *BUD14* upon spindle misalignment. Our data indicate that Bud14-Glc7 limits the SPB-bound levels of Bfa1-Bub2 complex in metaphase and anaphase. We identified that Bud14 falls off from the bud cortex, spreading through the cell during late anaphase. We showed that phosphatase Bud14-Glc7 and the SPOC kinase Kin4 have different and additive molecular roles in SPOC. We proposed a model in which Bud14-Glc7 complex acts on Bfa1 with a parallel pathway to Kin4 in order to block the cell cycle progression in response to spindle misorientation.

ÖZETÇE

Bud14'ün SPOC Mekanizmasını Kontrol Eden Görevinin Karakterizasyonu

Hüseyin Karabürk

Moleküler Biyoloji ve Genetik, Yüksek Lisans

6 Ağustos 2021

Ekmek mayası olarak da adlandırılan *Saccharomyces cerevisiae*, mitotik iğ ipliği oryantasyonun ve de bu oryantasyonun asimetrik hücre döngüsü üzerindeki etkilerini araştırmak için oldukça ideal bir organizmadır. Anne ve yavru hücrenin her birine eşit birer DNA kopyasının aktarılması için, ekmek mayasının mitotik iğ iplikleri polarite ekseninde hizalanmak zorundadır. İğ ipliği yönü kontrol noktası (SPOC) hücre dögüsünün ilerleyişini iğ ipliklerinin yanlış yönde hizalanmasına bağlı olarak durdurur. Bu mekanizmadaki sorunların hücrenin genomik kararlılığının bozulmasına ve de sonuç olarak poliploidi ve anöploidinin oluşmasına neden olduğu bilinmektedir. Buna bağlı olarak, bu kontrol noktası ploidinin doğru aktarımı için gereklidir. Ancak bu mekanizmanın tam anlamıyla nasıl çalıştığı bu zamana kadar aydınlatılamamıştır. Bu çalışmada, Bud14 proteininin bu mekanizmada görev alan bir protein olduğunu keşfettik. *BUD14*'ün yokluğunun mitozdan çıkış mekanizması bozulmuş hücrelerde büyümeyi teşvik etmesi bu proteinin mitozdan çıkışı engelleyen bir protein olduğunu göstermektedir. Ayrıca, *BUD14*'ü eksik olan hücrelerde SPOC mekanizmasının çalışmadığını ve buna bağlı olarak mitotik iğ ipliklerinin yanlış hizalanması durumunda bu kültürlerin çoklu çekirdekli fenotipte hücrelere sahip olduğunu gösterdik. Bulgularımız, Bud14'ün bu görevinin formine bağlı aktin polimerizasyonu görevine bağlı olmadığını kanıtlamaktadır. Bud14'ün mitotik hücre döngüsünü engelleyici görevini yapması için Glc7 ile etkileşmesi gerektiğini gösterdik çünkü Glc7'nin bu etkileşime sahip olmayan versiyonunun (*glc7-12*) da SPOC mekanizmasının bozulmasına neden olduğunu gözlemledik. Deneysel bulgularımız ışığında, Bud14-Glc7 kompleksinin Bfa1-Bub2 kompleksinin metafaz ve anafazda Mil Pole Gövde (SPB)'ye olan lokalizasyonunu sınırladığını gösterdik. Ayrıca, Bud14'ün iğ ipliklerinin yanlış hizalanması sonucunda yavru hücre korteksinden düştüğünü ve hücre boyunca yayıldığını gözlemledik. Bud14-Glc7 kompleksinin SPOC kinaz olan Kin4 üzerinde bir etkisinin olmadığını, aksine bu iki yolağın iğ ipliği yönüne bağlı olarak hücre döngüsünü engellemek için birbirlerine paralel olarak çalıştığını modelledik.

Work presented in this thesis has been uploaded to bioRxiv and submitted to eLife.

Protein Phosphatase 1 in association with Bud14 inhibits mitotic exit in *Saccharomyces cerevisiae*. *bioRxiv*. (2020). doi: https://doi.org/10.1101/2020.08.30.273946

Protein Phosphatase 1 in association with Bud14 inhibits mitotic exit in *Saccharomyces cerevisiae*. *bioRxiv*. (2021). doi: https://doi.org/10.1101/2020.08.30.273946

ACKNOWLEDGEMENTS

First of all, I would like to thank The Scientific and Technological Research Council of Turkey (TUBITAK) for their support. This project was funded by TUBITAK BIDEB 117C041 awarded to Ayşe Koca Çaydaşı.

I would like to thank my advisor Dr. Ayşe Koca Çaydaşı. I feel so lucky to be under supervision of her. I learnt a lot from her. She not only broadened my scientific view, but also, she pushed me up when I encountered an obstacle in my project. She taught me lots of laboratory techniques in person that I will be using in my future career. I can truly say that I owe everything to her. Throughout this journey, I went through many challenges, and every time I was in a trouble, Ayşe was there to help and to welcome me. She was beyond an advisor for me; sometimes a friend who I can complain about things and sometimes a sister who I can freely talk and cry with. I wouldn't have all these scientific accomplishments including my master's degree, this thesis, my paper, and my PhD admission without her. I will be always there when she needs me. Always to remember and to be remembered.

I would like to thank the current and former members of our amazing Cell Cycle and Genome Stability Laboratory; Betül, Şeyma, Barış, Dilara, Cansu, İdil, Mukadder, Gülden and Mariam. We spent several hours together in the lab. This journey wouldn't be that amazing if you weren't there. We worked during nights and weekends to accomplish in this great field of science. What motivated me was not only the experiments and the results, but also existence of you. I feel and know we will be always connected by heart even though there are long distances between us. I have already missed to be together in the lab, and I fell I will always continue to miss that. Thank you so much for all these unforgettable memories.

I would like to thank my family. They were always with me. I felt and got their support at every moment of my life. They are not just a family for me, they are anything that I need when necessary; a friend, a mentor… They supported me both emotionally and economically throughout my life. I wouldn't be that successful without their existence. I would like to especially thank my elder sister Şehnaz. She is my first teacher. She taught me a lot at home. She motivated, directed, and prepared me for my educational life since my elementary school years. My family, you all are so special for me, and I know I am the luckiest person in this world to have you.

I would like to thank Tunahan. He always supported me. He helped me a lot during the experiments when he was a work and study student in our lab. It was both funny and informative to work with him. Apart from the lab life, he broadened my life view as well. Thank you so much for all those unique memories and stories that we have shared so far, and I know there will be several of them more in the following years. I am looking forward to starting a new journey in the US next year.

I would like to thank Koçtaşs; Tuğçe (or in short ATS), Cansu, İdil and Beste. The hardest part of the thesis has just begun. It is quite hard to hold my tears since I have started to think about all the memories, we had together, to write them down here. I have already missed you girls; and I am going to miss be with you a lot. Long nights spent together, had fun together, walked together in this road… I know we will be only apart in person; we are always connected by heart. I know and believe we will meet again soon. Cansu and İdil, I will never forget our lab songs, especially Galaksi (a friend of her sister) :). Also, İdil, sorry for all the jokes that we had done about İzmir :). Thank you so much for all these unforgettable amazing memories and stories that we have had so far, and I know there will be tons of them more in the following years.

I would like to thank Bahar. It has been years since we have met, and you are so special for me. I will never forget our daily tracking trips in the forest. We were the best motivation for each other during tough quarantine days. We suffered together while applying for PhD, writing our thesis, and here you go we did it! This fantastic friendship and journey will continue in the US. I deeply know that I am so lucky to have you, and your existence will make our PhD journey amazing.

I would like to thank Ezgi. I remember all the memories we had like they were just yesterday. Ezgi, you are the best storyteller I have ever met. I have missed to hear one from you. You are so special for me. Our journey and your fantastic friendship will continue in the US. I really look forward to meeting you in the Central Park as we decided years ago. Thank you so much for everything.

I would like to thank Aslı. She is one of the greatest supporters of me. She has been always with me at any cost. I know this is a life-long friendship, and I am so happy to have her in my life.

I would like to thank my beautiful mama, Çağla. She was with me in the hardest day of my life, and I will always owe to her. I really missed to spend time with her and Bahar. We have a lot of unforgettable memories. I thank her for always being a good friend of me.

I would like to thank Ceyda and Berfu. We started this amazing journey together. They were always with me to support me. I will never forget those memories we had together. We will always be connected by heart. I am so lucky to have you in my life.

I would like to thank Tais. She is one of the best gifts that this life gave to me. I really missed to talk with you for long hours. I will always remember those valuable memories we had together. I thank you for always being a good friend of me.

I would like to thank Demet, Selay, Yağmur, Yasemin, Mehtap, Melis, Ebru, İlayda, Vildan, Samira, Gökçe, Azra, Sema, Nazlı and Hüseyin for always being with me throughout this journey. I thank all of you for supporting me. I am so lucky to have you in my life.

TABLE OF CONTENTS

LIST OF TABLES

LIST OF FIGURES

ABBREVIATIONS

APC/C: Anaphase-Promoting Complex/Cyclosome

CDK: Cyclin Dependent Kinase

CKI: Cyclin Dependent Kinase Inhibitor

FEAR: Fourteen Early Anaphase Release

GAP: GTPase Activating Protein

GEF: Guanine Exchange Factor

MCC: Mitotic Checkpoint Complex

MEN: Mitotic Exit Network

MT: Microtubule

MTOC: Microtubule Organizing Center

SAC: Spindle Assembly Complex

SCF: Skp, Cullin, F-box Containing Complex

SIN: Septum Initiation Network

SPB: Spindle Pole Body

SPOC: Spindle POsition Checkpoint

Chapter 1: **INTRODUCTION**

1.1 *Budding Yeast as A Model Organism in Molecular Biology Studies*

Budding yeast, scientifically named as *Saccharomyces cerevisiae*, is also known as Baker's yeast. This organism is a single-celled eukaryotic species (Botstein & Fink, 1988). There is an extracellular matrix surrounding the cells of the budding yeast, and this matrix, called as the cell wall, is composed of a layered meshwork of β-glucans, chitin, and mannoproteins (Lesage & Bussey, 2006). Budding yeast is one of the widely used model organisms in molecular biology studies for years because of its advantageous genetic and physiological characteristics, which include ability to proliferate in haploid form, easiness of genetic manipulations and culture maintenance, a fully sequenced genome, and its conserved molecular biology with higher eukaryotic organisms. Additionally, one of the most important advantage of using budding yeast as model organism is its short culturing time. Budding yeast has a fast growth rate with a doubling time around 1.5 hours, that makes the cells easy to be tracked during the stages of cell cycle (Herskowitz, 1988).

The genome of S*accharomyces cerevisiae* has been completely sequenced in 1996, that makes budding yeast the first eukaryotic organism whose whole genome has been sequenced. It is composed of 12,068 kilobase genes with 5885 potential protein-encoding genes on 16 chromosomes (Goffeau et al., 1996). Budding yeast has a cell biology, that is quite like that of higher eukaryotes. This makes it useful for interpreting and understanding human DNA sequences and cell biology.

The availability of highly standardized and effective molecular biology methods for editing the genome of yeast cells, such as gene deletions and epitope tagging of proteins at both N and C termini, is another reason for which budding yeast has been commonly used in biological sciences as model organism for years (Duina, Miller, & Keeney, 2014). These gene editing techniques rely on homologous recombination in budding yeast. Homologous recombination is a cellular process in which genetic information is exchanged between two similar or identical molecules of nucleic acids. *RAD52* epistasis group proteins catalyzes this process in *Saccharomyces cerevisiae* (Eckert-Boulet, Rothstein, & Lisby, 2011). The rate of homologous recombination is higher in budding yeast compared to higher eukaryotes (Eckert-Boulet et al., 2011). PCR-based DNA

fragments can easily be exchanged with the genes in yeast chromosomal DNA with a high frequency due to the high recombination rate in budding yeast, and this enables scientists to edit the genome of budding yeast easily (Gardner & Jaspersen, 2014).

Another reason for budding yeast to be a suitable organism for genetic studies is that the cells of budding yeast can be obtained and maintained in a haploid stage. *Saccharomyces cerevisiae* has a life cycle composed of haploid and diploid stages (Botstein, Chervitz, & Cherry, 1997). In the haploid stage of the cycle, there is only one copy of each chromosome in cells. The haploid yeast can belong to one of the two different mating types which are MAT-a and MAT-α (Herskowitz, 1988). Under normal nutritional and environmental conditions, budding yeast cells secrete the mating factors, and this causes cells to synchronize at the G1 stage of the cell cycle and to form mating projections (Farley, Satterberg, Goldsmith, & Elion, 1999). In this case, opposing mating types are able to fuse together in order to give rise to a diploid cell having two copies of chromosomes. When the starvation is induced, diploid cells sporulate and undergo meiosis, giving rise to haploid cells (Figure 1.1) (Lee & Haber, 1998). It is easy to do targeted gene editing in haploid cells since only one copy of a given gene exists in the genome to be edited. Also, haploid yeast mating enables genetic complementation and backcross experiments. Most important of all, owing to this feature, several yeast mutants, including the temperature sensitive mutants, can be obtained by random mutagenesis, put into complementation groups, and easily scanned for phenotypes. Therefore, these features of budding yeast make it a quite useful tool to be used in genetic studies. Moreover, this feature of the budding yest cells is used for cell synchronization at the G1 stage.

In *Saccharomyces cerevisiae*, conditional temperature-sensitive (ts) mutations are commonly used to study the function of essential genes, which are highly conserved from budding yeast to humans (Hughes, 2002). Ts-mutations generally occur due to missense mutations destabilizing the protein or its protein-protein interactions at relatively high temperatures. Ts-alleles allow scientists to control the function of the genes by changing the growth temperature. At the permissive temperature, mutation is not functional, meaning that the phenotype of a ts-mutant is like wild-type strain. At the restrictive temperature, however, the activity of the ts-protein is drastically reduced or completely abolished, resulting in either a growing or a lethal phenotype. It has been known that ts-mutations in the genes controlling the cell cycle lead to cell cycle arrest at a specific stage,

and essentially, the master regulator of the cell cycle, the Cyclin Dependent Kinases (CDKs), were first discovered by a genetic screen using budding yeast ts-strains (Hartwell, Mortimer, Culotti, & Culotti, 1973).

Saccharomyces cerevisiae has been especially suitable and popular model organism to study cell cycle and its regulation. It would be much harder to do that in higher organisms, especially in propagated mammalian cell lines. There are a number of reasons why budding yeast has been a good choice to investigate cell cycle. First of all, propagated mammalian cell lines carry and accumulate mutations to make them grow indefinitely in petri dishes, and such mutations usually disrupt the control mechanisms of cell cycle (Carter & Shieh, 2015). Wild type budding yeast cultures, however, grow infinitely in the lab without requirement for additional mutations or accumulation of mutations. Secondly, one can roughly detect the phase of the cell cycle in budding yeast just by looking at the cellular morphology using a compound microscope. This enables scientists to determine and track the phase of the cell cycle a given cell experiences at a given time. The cells without a bud are in G1. Cells start budding when they enter cell cycle at the G1/S transition, thus cells with a small bud are in G1/S or S or G2 phases. The bud grows as cells progress in the cell cycle. Cells with a medium-to-large bud size are usually in the mitotic stage. The bud continues growing also when the cell cycle is arrested at a time after entry in the cell cycle. Combining cell morphology with a nuclear staining gives more time resolution, as one can also differentiate cells in anaphase/telophase then those in metaphase or earlier (Calvert, Lannigan, Pemberton, & Signaling, 2009). This feature of budding yeast is quite helpful for tracking cell synchronizations and progression through the cell cycle. Thirdly, one can easily synchronize the budding yeast at the desired phases upon addition of certain chemicals or induction/depletion/inactivation of certain genes. For example, commercial α-factor is widely used to keep the MAT-a type yeast cells at G1 phase in which the cells are have an unbudded, mononucleate structure (Udden & Finkelstein, 1978). As another example, Cdc20 depletion using inducible gene expression system is commonly used for the synchronization of cells in metaphase. Cdc20, a conserved activator of APC/C, promotes cleavage of Cohesin in metaphase, allowing for anaphase on set (see Section 1.4 for more information on anaphase onset) (Lim, Goh, & Surana, 1998; Uhlmann, Lottspeich, & Nasmyth, 1999). Cdc20 is degraded after mitotic exit. Therefore, promoter shut down of Cdc20 will lead to complete depletion of Cdc20 and cells will be arrested in metaphase.

Budding yeast is also a good choice of model organism to study asymmetric cell division as *Saccharomyces cerevisiae* divides asymmetrically (Mortimer & Johnston, 1959). In the asymmetric cell division, two new daughter cells with different characteristics and fates are produced because of the asymmetric inheritance of cellular components (Wang et al., 2009). During the cell cycle, budding yeast is polarized, giving rise to the formation of two cells having different fates and sizes. At the beginning of the cycle, mother cell is bigger than the daughter cell, which retains full lifespan (Mortimer & Johnston, 1959). In addition, transcription occurs differentially in mother and daughter cell during the cell cycle, giving district properties to the cells. To illustrate, mating type switching is restricted to the mother cell whereas the hydrolytic enzymes responsible for the destruction of cell wall can only be expressed in the daughter cells (Colman-Lerner, Chin, & Brent, 2001).Taken together, all the aforementioned advantages make budding yeast a very useful and powerful model organism for molecular biology and genetic studies. Therefore, for decades, it has been widely used as model system in biological studies aiming to enlighten molecular mysteries of complex cellular processes and human diseases.

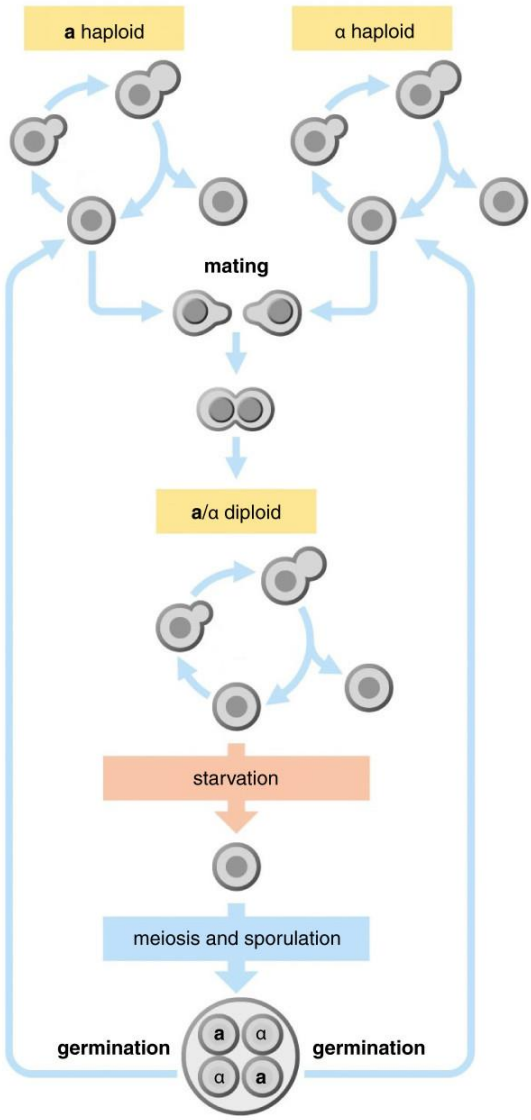

Figure 1. 1: The life cycle of the budding yeast. The haploid cells of opposing mating types mate only when the pheromones are recognized by the cell surface receptor of the opposite cell type. This initiates a signaling cascade, stimulating the fusion of the two cells, producing an a/α diploid cell. This newly produced diploid cell grows vegetatively when nutrients are available. However, in the presence of nutritional starvation, the cells undergo meiosis to produce four haploid spores, which is called sporulation. They can stay at the dormant state until the conditions improve. Haploid yeast of one mating type has an inactive version of opposing mating type gene found at a distant region. Mating type genes can be copied and inserted into a different location when it is desired to be active. This leads to mating type switching**,** which is advantageous for the yeast in the wild. HO endonuclease is the enzyme that is responsible for cutting the DNA at the region where active mating type gene is found (Nasmyth, 1993). In laboratory, mating type switching is unwanted because it causes a population of yeast with mixed mating type which can randomly give rise to diploid cells. Therefore laboratory yeast strains are usually held in the haploid state by the deletion of a the HO endonuclease (This figure is taken from Sun et al., 2011) (Sun & Heitman, 2011).

1.2 *Cell Cycle in Saccharomyces cerevisiae*

Cell division cycle is the process in which a cell gives rise to formation of two new daughter cells. The cell cycle is achieved through a highly reproducible temporal sequence of events which is common to almost all higher organisms. A typical cell cycle is composed of four stages: G1, S, G2 and M in order (Figure 1.2) (Leland H. Hartwell, Culotti, Pringle, & Reid, 1974).

Budding yeast is known to divide asymmetrically in which single cells divide to give rise to a mother and a daughter cell with different developmental fates (Amon, 1996). *Saccharomyces cerevisiae* cells divide by budding, - a process in which a smaller daughter cells pinches off the mother cell through polarized cell growth. In budding yeast, the new cycle starts only when a mother cell reaches to a certain size threshold at the G1 phase (Nurse, 1975). G1 is the phase where cells grow and prepare for the cell cycle (Hartwell et al., 1974). The budding process starts immediately during the transition from G1 to S phase. The budding site is determined by cortical landmarks from the previous division, and this site is called as bud emergence site (Casamayor & Snyder, 2002). After the emergence of bud, bud growth is concentrated at the tip which is defined as polarized cell growth (Casamayor & Snyder, 2002). As the cell cycle continues, the bud grows as connected to the mother cell. The budding process relates to the polarization of the yeast cells. During this process, the secretory vesicles and organelles are transported to the bud along with actin cables, which provides the polarized growth (Moseley & Goode, 2006). Polarization is assured by the presence of specific physiological and spatial polarization cues at the bud emergence site. Actin cables can only be formed in the mother-to-bud polarity axis by the action of these cues like bud scars and pheromone gradients (Slaughter, Smith, & Li, 2009).

At the S phase of the cell cycle, both chromosomes and the microtubule-organizing center known as Spindle Pole Body (SPB), yeast equivalent of the centrosome, are duplicated (Adams & Kilmartin, 1999). This phase lasts roughly for 25 minutes at the physiological temperature, and different origin of replications are fired at the same time to synthesize the whole chromosome (Donaldson et al., 1998).

G2 phase is defined as the time in between the termination of DNA synthesis and the onset of mitosis (Leland H. Hartwell et al., 1974). In budding yeast, this phase is either absent or quite short to be detected.

The last stage of the cell cycle is the M phase, also known as mitotic phase (mitosis). This stage aims to separate duplicated sister chromatids to mother and daughter cell equally. Mitosis mainly involves four stages, which are prophase, metaphase, anaphase, and telophase. In prophase, duplicated DNA condenses into sister chromatids. These two copies of chromosomes are held together by Cohesin ring, a multi-subunit protein complex mediating sister chromatid cohesion until metaphase-to-anaphase transition (Guacci, Koshland, & Strunnikov, 1997). Cohesion between sister chromatids is important to resist the pulling forces exerted by microtubules; therefore, cohesion ensures that sister chromatids attach to microtubules emanating from opposite spindle poles until the anaphase onset (Miyazaki & Orr-Weaver, 1994). In metaphase, condensed chromosomes align in the equatorial plate of the cell (Nicklas & Arana, 1992). In this stage, mitotic spindle which is made up of microtubules captures sister chromatids from a region called Kinetochore. This proteaceous region is built over the centromere of chromosomes to provide sites for microtubule attachment. At the anaphase onset, Cohesin ring is proteolytically cleaved from Scc1 subunit by the action of Esp1, a specific protease (Frank Uhlmann, Lottspelch, & Nasmyth, 1999). This allows the sister chromatids to be pulled away towards to opposite poles in the next stages of the mitosis (Mitchison & Salmon, 2001). In anaphase, mitotic spindle elongates, leading to proper chromosome segregation to opposite poles (Aaron F Straight, Marshall, Sedat, & Murray, 1997). For a daughter yeast cell to receive one copy of the duplicated genetic material, the cell needs to segregate its chromosomes along the polarity axis (mother-to-daughter direction), and this requires positioning of the mitotic spindle apparatus along this direction (Rhyu & Knoblich, 1995). In telophase, the last stage of M phase, condensed chromosomes decondense. Differently from the mammalian cells, budding yeast undergoes closed mitosis, a type of cell division that nuclear envelope never breaks down. Eukaryotic chromosomes are surrounded by a double membrane, which is called the nuclear envelope. This envelope can either remain intact or disassemble before the chromosomes segregate depending on the organism and cell type. If it disassembles, it is termed as open division whereas it is called as closed division if it does remain intact (Boettcher & Barral, 2013). Because nuclear envelope never disassembles at prophase in budding yeast, so it does not re-assemble in telophase as opposed to mammalian cells. At the end of the division, cells exit from mitosis followed by chromosome decondensation. In budding yeast, exit from mitosis is controlled by a signaling cascade called Mitotic Exit Network (MEN). Detailed molecular mechanism of MEN will be explained in following sections.

For exit from mitosis, Cyclin-Dependent Kinases (CDK) are inactivated, CDK substrates are dephosphorylated, and the mitotic spindle is broken apart (Zachariae & Nasmyth, 1999). The inactivation of CDKs is also essential for removing the block on the assembly of pre-replicative complex, which is mediated by high CDK activity, at the replication origins (Kaibuchi et al., 2001). At the last step of cell division, daughter cell is separated from the mother cell whom it had grown as attached during the cell cycle, and this physical separation is called as cytokinesis. Cytokinesis takes place by actomyosin ring contraction and septum deposition at the bud neck in budding yeast (McCollum & Gould, 2001). It is known that high CDK activity prevents cytokinesis, and the degradation of mitotic cyclins helps to determine the timing of cytokinesis (Echard & O'Farrell, 2003). Therefore, cytokinesis can only take place after the cells have exited from mitosis.

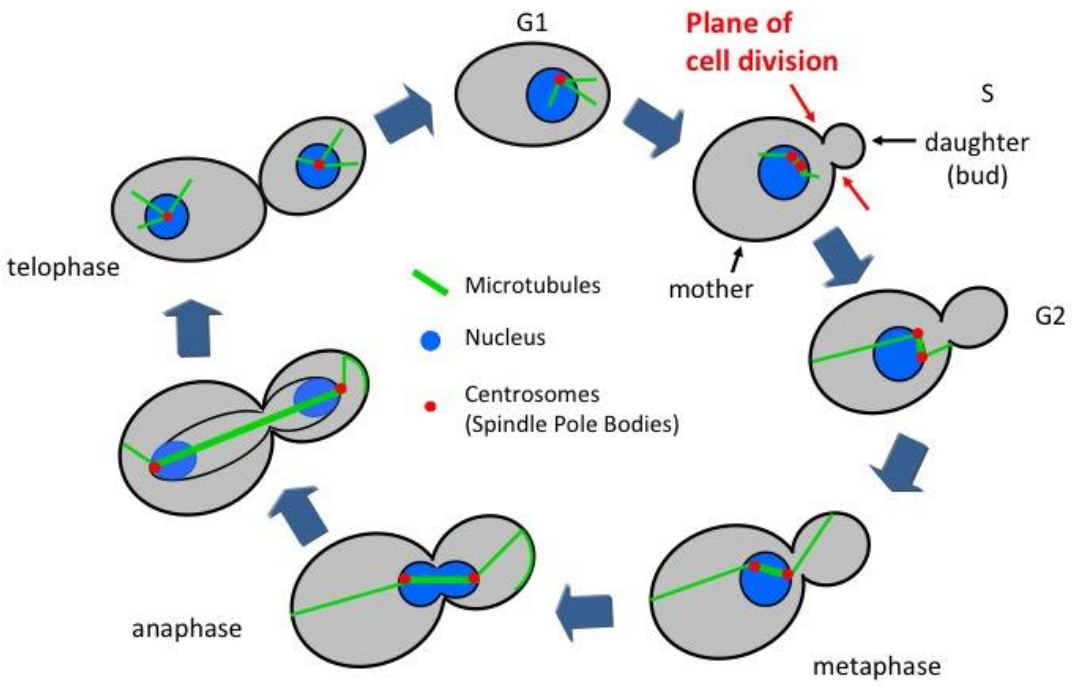

Figure 1. 2: The cell cycle of a budding yeast cell. It is composed of four phases: G1, S, G2 and M. It runs for around 90 minutes under optimal conditions.

The transitions of the cell cycle in eukaryotic organisms are controlled and triggered by cyclin-dependent kinases (CDKs) (L. Hartwell, 1973; Norbury & Nurse, 1992). The activity of CDKs needs to be tightly regulated by many mechanisms to ensure the correct timing and coordination of cell division (Morgan, 1995). CDKs are described as proline-directed serine/threonine protein kinases that control the progression of cell cycle (Malumbres, 2011). They have lots of target proteins, that function to initiate and regulate several events of the cell cycle, and these events characterize the different phases of cell cycle (Grana & Reddy, 1995). The activity of CDKs oscillates in a cell cycle dependent manner; therefore, the activity of CDK targets changes during cell cycle. There are different mechanisms regulating the activity of CDKs during the cell cycle; which are regulation of cyclin gene expression, post-translational modifications of CDKs in a phospho-dependent manner, proteasomal degradation of proteins, and the interaction of Cyclin/CDK complexes with protein inhibitors (Obaya & Sedivy, 2002). There is a complicated meshwork of proteins and enzymes involved in these mechanisms regulating the cyclic activity of CDKs. Among those, cyclins have a profound role by associating with CDKs transiently. Cyclins are a family of proteins that activate CDKs and provide substrate specificity to CDKs (Obaya & Sedivy, 2002). The levels of CDKs remain constant throughout the whole cell cycle. However, cyclin levels do change because of controlled degradation and periodical production; this is one of the regulations how the order and coordination of the cell cycle are controlled.

In budding yeast, there is only one cyclin-dependent protein kinase, encoded by *CDC28* gene, that drives the cell cycle. The timing of cell cycle commitment, bud initiation, DNA synthesis and chromosome segregation are controlled by the activity of Cdc28 (L. Hartwell, 1973; Mendenhall & Hodge, 1998). Cdc28 interacts with different cyclins in a cell cycle dependent manner, providing the order and coordination of the cell division (Figure 1.3). The G1-phase specific cyclins are Cln1, Cln2 and Cln3. They activate CDKs in late G1, and they are essential for the initial events of the cell cycle. For example, they are involved in spindle pole body duplication, budding, polarized growth, activation of G1 transcription and acquisition of pheromone resistance (Oehlen & Cross, 1994) . The levels of G1 specific cyclins fall in S phase. The S-phase cyclins are Clb5 and Clb6 (Küntzel, Schulz, & Ehbrecht, 1996). They are involved in DNA replication. The levels of S-cyclins remain high until mitosis. The M-phase cyclins are Clb1, Clb2, Clb3 and Clb4 (Fitch et al., 1992). M-phase cyclins are required for mitotic spindle assembly and

suppression of polarized bud growth (Bloom & Cross, 2007). In addition, mitotic cyclins inhibit mitotic exit and cell division until the cycle is completed. M-cyclin levels fall in mid-mitosis (B. Andrews & Measday, 1998).

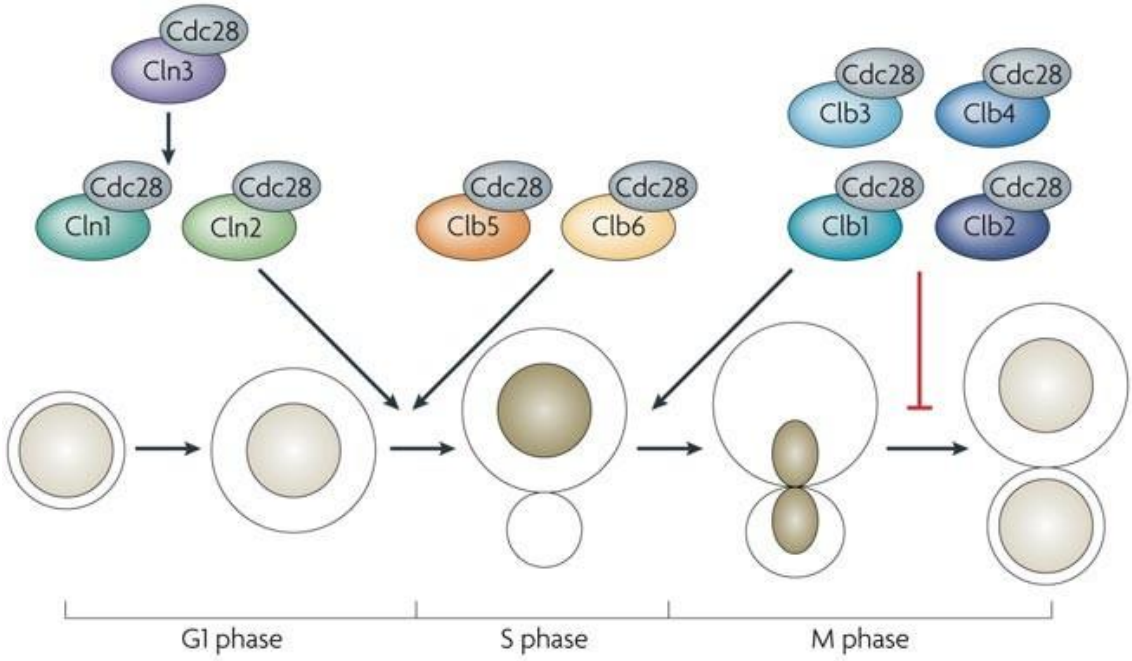

Figure 1. 3: Cyclins in the budding yeast cell cycle. There is a single CDK, Cdc28, in budding yeast. The levels of cyclins oscillate along the cell cycle and different cyclins function in different phases of cell division. The G1-phase specific cyclins are Cln1, Cln2 and Cln3. They promote bud emergence, spindle pole body duplication and activation of the B-type cyclins. The S-phase cyclins are Clb5, Clb6, promoting DNA replication. Finally, the M-phase cyclins which are Clb1, Clb2, Clb3 and Clb4 promote spindle formation and the initiation of mitotic phase. M-phase specific cyclins inhibit mitotic exit and cell division (This Figure is taken from Bloom et al., 2007) (Bloom & Cross, 2007).

As stated before, cyclic changes in the protein levels of cyclins lead to cyclic assembly and activation of cyclin-CDK complexes at specific stages of the cell division. Cells have evolved different mechanisms to control the activity of cyclin-CDK complexes in order to ensure the correct order and coordination of the cell cycle. These mechanisms are essential for preventing improper commitment of the upcoming events of the cell cycle. Activity of CDK Inhibitor Proteins (CKIs), regulated proteolysis and transcriptional regulation are included among these mechanisms controlling the cell cycle. CKIs bind to cyclin-CDK complexes, resulting in the inactivation of the complex. Upon this binding, there happens a structural rearrangement in CDK's active site. This mechanism is mainly

used by the cells to control the activities of G1/S- and S-cyclin-CDK complexes at the early steps of the cell cycle (Sherr & Roberts, 1999). Regulated proteolysis is another mechanism cells harbor to control the activity of cyclin-CDK complexes. In order cells to complete the cell cycle properly, S- and M-cyclin-CDK complexes should be inactivated by the action of anaphase promoting complex or cyclosome (APC/C) (Wäsch & Cross, 2002). APC/C is a E3 ubiquitin ligase, an enzyme responsible for catalyzing the ubiquitylation of proteins for destruction in proteosome. The S- and M-cyclins are one of the main targets of the APC/C. Upon activation of G1/S-CDK in late G1, APC/C is inactivated, leading to accumulation of cyclins in the next cycle (Hershko & Ciechanover, 1998; Fang, Yu, & Kirschner, 1999). The activity of APC/C changes along the cell cycle since its activating subunit changes. It has two activating subunits: Cdc20 that associates in mid-mitosis and Cdh1 that associates from late mitosis through early G1. These substrate specific activators are essential for the recognition of target proteins to be degraded (Rosella Visintin, Prinz, & Amon, 1997). As described, cell cycle control is mainly dependent on post-translational mechanisms including the regulation of ubiquitin-mediated proteolysis. However, transcriptional regulation is another important mechanism for the control of the cell cycle. To illustrate, cyclin levels are also controlled by the changes in the transcription of the cyclin genes in a cell cycle dependent manner (Breeden, 2000).

1.3 *Cell Cycle Regulation by Checkpoints*

The cell division need to be accurate and precise to prevent the transmission of any defects to the progeny. There are certain mechanisms to monitor the cell cycle. These mechanisms, called as checkpoints, can receive any kind of stimulus from the environment and monitor the progression of the cell cycle (Figure 1.4). They monitor the order, integrity, and the fidelity of the major events of the cell cycle. These include appropriate cell size, presence of damage on DNA, the replication and the integrity of chromosomes, proper mitotic spindle assembly as well as proper chromosome segregation at mitosis (Barnum & O'Connell, 2014). In other words, they are surveillance mechanisms that are essential for a proper division, and they have to be functioning appropriately to make the division precise and accurate. These checkpoints aim to block the cell cycle progression in the presence of any kind of error; therefore, cells can find a

time to correct these errors. If the error is not corrected, cells stay arrested at certain points of the cells cycle, eventually die.

The first checkpoint is G1/S Checkpoint, or Start, that monitors the proper growth of the cell and the morphogenesis (Morgan, 1995). Cells should double their content before cell division to ensure daughter cells are supplied with the proper amount of biological material while mother cells can maintain their size. This checkpoint in yeast mainly monitors the cell size and nutrition availability to decide whether cells start the cell cycle or not (Hartwell et al., 1974) Multicellular eukaryotes also monitor the presence of mitogens (Böhmer, Scharf, & Assoian, 1996). If the conditions are not suitable for entering a new cycle, cells enter a nonproliferating state called quiescent state, or G0 (Cheung & Rando, 2008). Failure of this checkpoint might lead to mutations, fragmentation of chromosomes, and genetic instability, which are all known to be related with the cancer development (Tvegård et al., 2007). If the conditions are suitable, the formation of G1/S- and S-cyclin-CDK complexes are stimulated; therefore, cells are committed to enter the S phase. G1/S checkpoint regulates the synthesis of Cln2-Cdk1 complex (Cross, 1995). Transcription factor SBF, a heterodimer consisting of Swi4 and Swi6, controls the synthesis of Cln2. SBF is inactive in the bound state to Whi5. As the cells grow, the amount of Cln3-Cdk1 complex increases. It is known that Cln3-Cdk1 phosphorylates Whi5, and when Whi5 is phosphorylated, it dissociates from SBF, activating it (De Bruin, McDonald, Kalashnikova, Yates, & Wittenberg, 2004). Therefore, the transcription of G1/S- and S-Cyclins (Cln1 and Cln2) are promoted by SBF. This is important for the transition from G1 through S phase of the cell cycle (Costanzo et al., 2004). Recently, a new level of control has been found that the concentration of Cln3 is proportional to cell size, meaning its total concentration does not change during G1 (Schmoller, Turner, Kõivomägi, & Skotheim, 2015). Instead, Whi5 is diluted by the growth of cells, resulting in decreased Whi5 activity; therefore, proliferation is controlled by cell size (Schmoller et al., 2015).

The second checkpoint is DNA Damage Checkpoint in which damage on DNA is monitored to prevent the transmission of DNA damage to the progeny. DNA damage causes a cell cycle arrest, allowing the repair pathways to correct the damage before the upcoming cell cycle phases commence. The source of the DNA damage might either be intrinsic like metabolism, oncogene overexpression and replication errors, or extrinsic such as sunlight, ionizing radiation and carcinogens. Depending on the type of the lesion

on DNA, different repair mechanisms are activated, aiming to keep CDKs inactive until the lesion is repaired or removed. Protein kinases have a significant function in the DNA damage response in eukaryotes. They both sense the DNA damage and regulate the cellular processes to respond the damage. In *Saccharomyces cerevisiae,* DNA damage checkpoint signaling kinases are Tel1 (ATM homolog) and Mec1 (ATR homolog). These kinases are recruited to damaged DNA where they are activated to initiate the downstream signaling cascade. While Mec1 is recruited to RPA-coated ssDNA, Tel1 is recruited to DNA ends formed by double-strand breaks (Zhou & Elledge, 2000). They phosphorylate downstream checkpoint kinases, Rad53 and Chk1, that phosphorylate target proteins to mediate the cellular responses to DNA damage, including cell cycle arrest, DNA repair, dNTP regulation, replication for protection and inhibition of origin firing. Rad53 is important for mediating all the damage-related responses in budding yeast (Zhaoxia, Hsiao, David, & Stern, 1997). Rad53 exerts its function through regulation of the Polo kinase Cdc5 (Sanchez et al., 1999). DNA replication errors leads to inhibition of the replication origin firing, eventually causing cell cycle arrest at S phase. The fact that the checkpoint signaling kinases Mec1 and Tel1 phosphorylate Rad9 and Mrc1, adaptor proteins respectively, activates effector kinases Chk1 and Rad53. Activated effector kinases act on transcription factors that regulate the transcription of genes necessary for G1/S- and S- phases (Iliakis, Wang, Guan, & Wang, 2003). Also, activated effector kinases target Swi4/Swi6, primase and Pds1 to inhibit the progression of cell cycle (Longhese, Foiani, Muzi-Falconi, Lucchini, & Plevani, 1998).The replication origins are the specific sites where DNA replication starts. Certain proteins play a role in ensuring that the origins fire only once per division. CDK-dependent phosphorylation of Cdt1 and Cdc6 controls the replication origin firing in budding yeast. This phosphorylation allows the initiation of replication. Also, it causes degradation of these proteins to prevent refiring of the origin (Piatti, Böhm, Cocker, Diffley, & Nasmyth, 1996). In the presence of a block on the template DNA, the replisome stays associated with it until the block is removed; therefore, replication resumes.

The third checkpoint is the Spindle Assembly Checkpoint (SAC) that monitors the proper attachment of the mitotic spindle to kinetochores. For the proper segregation of the chromosomes, mitotic spindle needs to attach to kinetochores as bi-oriented, which is called amphitelic attachment. In this type of attachment, each kinetochore is captured by microtubules elongated from a single spindle pole body, thus the two kinetochores of a

chromosome will be attached to opposite poles. This checkpoint keeps the cells at metaphase until all the chromosomes are attached to the mitotic spindle properly (Hoyt, Totis, & Roberts, 1991). SAC targets APC/C; therefore, keeps the cells at metaphase-to-anaphase transition. APC/C is a ubiquitin ligase that targets Securin to proteosome for destruction a protein that keeps. Securin is responsible for keeping Separase inactive until metaphase-to-anaphase transition. At anaphase onset, Separase, activated by the ubiquitin-dependent degradation of Securin, can cleave Cohesin subunit Scc1 to promote sister chromatid separation (Uhlmann et al., 1999). Mad2 has two distinct conformations; open conformation (O-Mad2) when it is not bound, and closed conformation (C-Mad2) when it is bound to Mad1 (De Antoni et al., 2005). When the cell enter mitosis, the Mad1-C-Mad2 complex, called core complex, is recruited to unattached kinetochores, which is catalyzed by tensionless kinetochores. Cytosolic O-Mad2 can then be recruited to core complex found on kinetochores (Shah et al., 2004). This O-Mad2 is able to capture Cdc20, forming a C-Mad2-Cdc20 complex which is the first step in the formation of mitotic checkpoint complex (MCC) which is composed of BubR1, Bub3, Mad2 and Cdc20 (De Antoni et al., 2005; Sudakin, Chan, & Yen, 2001). Therefore, SAC sequesters Cdc20 away from APC/C, inhibiting its action on Pds1; therefore, this checkpoint blocks the metaphase-to-anaphase transition. To sum up, SAC prevents chromosome mis-segregation during mitosis by monitoring the proper kinetochore-microtubule attachment. Defects in this checkpoint are likely to result in aneuploidy and genomic instability, promoting tumorigenesis (Malmanche, Maia, & Sunkel, 2006).

The last checkpoint is the Spindle Position Checkpoint (SPOC) in which proper alignment of the mitotic spindle in the mother-to-daughter polarity axis is monitored (Pereira, Höfken, Grindlay, Manson, & Schiebel, 2000). To assure segregation of a copy of the genomic DNA to daughter cells, most of the cell types build a cleavage furrow perpendicular to the mitotic spindle which pulls the chromosomes towards the spindle poles. However, in budding yeast the site of cleavage furrow is already determined at the G1/S transition concomitant with the emergence of the bud (Palmer, Sullivan, Huffaker, & Koshland, 1992). Since the site where cytokinesis is going to take place is determined before the alignment of the mitotic spindle, it is crucial that the mitotic spindle is aligned in the mother-to-daughter polarity axis. This alignment is achieved through interactions of astral microtubules with polarized actin cables and cortical proteins (Marisa Segal & Bloom, 2001). SPOC is responsible for monitoring the correct orientation of the mitotic

spindle in *Saccharomyces cerevisiae*. In the presence of spindle misalignment, this checkpoint inhibits cell cycle progression by delaying mitotic exit and cytokinesis. Therefore, SPOC provides the time required for cells to correct the alignment defects before they exit from mitosis (Pereira et al., 2000). Functionality of SPOC is essential for the cells which are defective in the spindle positioning pathways and/or having disrupted microtubule function, to maintain the accuracy of chromosome segregation. If this checkpoint is not working properly in a cell, misaligned cells continue cell cycle and exit from mitosis, giving rise to formation of a population of enucleated or multinucleated cells (Caydasi et al., 2017). SPOC works by inhibiting the Mitotic Exit Network (MEN) - the essential pathway for mitotic exit. The molecular mechanisms of SPOC and MEN will be explained in detail in following sections.

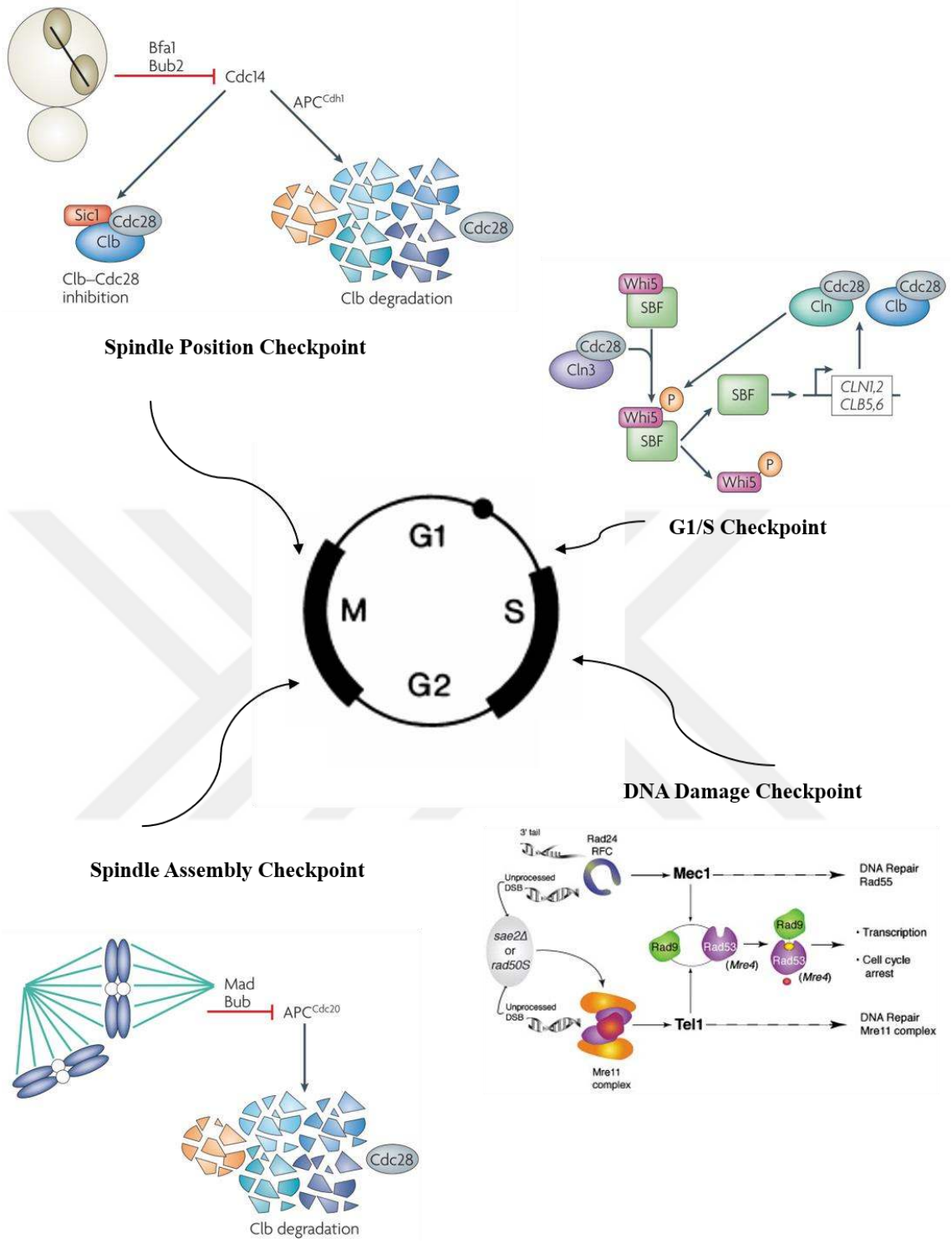

Figure 1. 4: Checkpoints in the budding yeast cell cycle. There are four checkpoints in the cell cycle of budding yeast: G1/S checkpoint, DNA Damage checkpoint, Spindle Assembly Checkpoint (SAC) and Spindle POsition Checkpoint (SPOC). The main effectors involved in these pathways and the conditions causing checkpoint activation are shown. Cell cycle is inhibited upon the activation of checkpoint. Curved arrows indicate the point where checkpoint activation takes place (This figure is adapted from Usui et al., 2001 and Bloom et al., 2007) (Usui, Ogawa, & Petrini, 2001; Bloom & Cross, 2007).

1.4 *Spindle Pole Body Function and Structure*

Spindle Pole Body (SPB), also known as duplication plaque of fungi, is the functional equivalent of centrosomes in higher eukaryotes. SPBs function as Microtubule Organizing Centers (MTOCs) in the budding yeast. MTOCs serve as sites in which microtubules are polymerized from α/β tubulin dimers tubulin subunits (Rout & Kilmartin, 1990). This provides the microtubule polarity, meaning that the minus-end of microtubules is found at SPBs whereas the plus-end grows through the cytoplasm and nucleoplasm. It is the polarity of microtubules providing the directional movement of cellular vesicles travelling on the motor proteins along with the microtubules (Byers, Shriver, & Goetsch, 1978).

SPBs are large, proteinaceous, multi-layered structures which are embedded in the nuclear envelope, remaining intact during the mitosis in budding yeast (Figure 1.5). Since they face both cytoplasm and nucleoplasm, SPBs are responsible for organizing two types of microtubules; the nuclear one which is essential for chromosome segregation and the cytoplasmic one which is required for the positioning of nucleus (Robinow & Marak, 1966). SPBs have two most visible, structurally distinct layers, also called plaques, which are the outer plaque and central plaque (Moens & Rapport, 1971). Outer plaque, which is stained lightly under transmission electron microscopy, is found above the nuclear membrane, facing the cytoplasm. It is the site in which cytoplasmic microtubules are attached. On the other hand, central plaque, which is stained densely, is found in the plane of the nuclear membrane. There is an electron-dense area on the nuclear envelope, which is called as the half-bridge where one side of the central plaque is associated with. the half-bridge has a multi-layered structure that is composed of two continuous layers and an additional layer which is found on the cytoplasmic side of the half-bridge (Figure 1.5) (Jaspersen & Winey, 2004). The assembly of new SPB occurs in the half-bridge since the darkly staining material accumulates on the distal, or cytoplasmic, tip of it during G1 phase (Byers & Goetsch, 1974; Adams & Kilmartin, 1999). A third layer, called inner plaque, had been identified with the negative staining of mitotic spindles (King, Hyams, & Luba, 1982). Inner plaque is located within the nucleus, facing the nucleoplasm. It serves as a site where nuclear microtubules nucleate, forming intranuclear spindle that is responsible for mediating chromosome segregation.

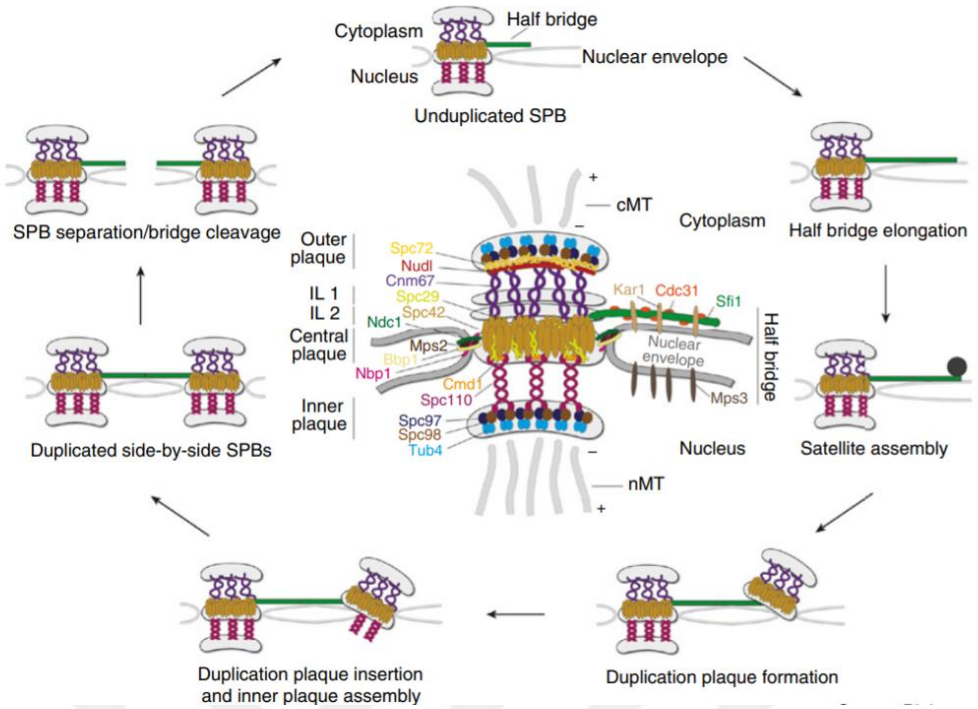

Figure 1. 5: The structure and duplication cycle of SPB in the budding yeast. It represents the SPB proteins and their localization. The surrounding scheme shows the steps of SPB duplication (This figure is taken from Seybold et al., 2013) (Seybold & Schiebel, 2013).

The central core of SPB is mainly composed of Spc42, which is an essential coiled-coil protein. It has a molecular weight of 42-kDa, and localizes to electron-dense central plaque (Donaldson & Kilmartin, 1996). Roughly a thousand of Spc42 molecules come together and form the hexagonal lattice (Bullitt, Rout, Kilmartin, & Akey, 1997). It has been found that overexpression of Spc42 gives rise to lateral expansion of the hexagonal lattice through the plane of membrane, forming a structure called as superplaque (Donaldson & Kilmartin, 1996). Spc110 and Spc29 are two other coiled-coil proteins localizing to the nuclear part of the SPB. They associate with the N-terminus of Spc42 (Adams & Kilmartin, 1999). The C-terminus of Spc110 faces towards to the central plaque where it binds to Spc29 and Cmd1 (Stirling, Welch, & Stark, 1994). Spc29 binds both Spc110 and Spc42, indicating that it acts as a linker, bridging inner and central plaques. On the other hand, the N-terminus of Spc110 is located in the inner plaque, and it binds to Spc98, a γ -tubulin binding protein essential for microtubule nucleation (Knop & Schiebel, 1997). The C-terminus of Spc42 localizes towards to the cytoplasm, and it binds to the C-terminus of Cnm67 (Adams & Kilmartin, 1999). Cnm67, which is also a

coiled-coil protein, acts as a spacer between IL1 (intermediate layer 1) and IL2 (intermediate layer 2) (Schaerer, Morgan, Winey, & Philippsen, 2001). Nud1, a scaffold protein required for exiting from mitosis, interacts with the N-terminus of Cnm67. Spc72, which is a non-essential (in some backgrounds) coiled-coil protein, localizes in the outer layer of SPB (Wigge et al., 1998). Whereas the C-terminus of Spc72 binds to the C-terminus of Nud1, the N-terminus interacts with the elements of the γ -tubulin complex, facilitating the nucleation of microtubules (Knop & Schiebel, 1998).

The duplication of SPBs occurs per cell cycle conservatively, meaning that a daughter SPB is synthesized next to the mother SPB. Preferentially, the older SPB migrates into the daughter cell during cell division. Cytoplasmic microtubules, which are essential for the positioning of nucleus and movement into the bud, are nucleated first; that might be the reason for which the old SPB moves into the daughter cell (Pereira, Tanaka, Nasmyth, & Schiebel, 2001). The duplication of SPB is composed of multiple steps, starting at early G1. In the first step, elongation of the half-bridge takes place, and deposition of the amorphous satellite material occurs on the distal cytoplasmic tip of the half-bridge (Byers & Goetsch, 1974). The key effectors involved in the first step are Cdc31, Kar1, Mps3, and Sfi1 (Jaspersen, Giddings, & Winey, 2002). They all localize to the SPB half-bridge along the cell division (Biggins & Rose, 1994). In the next step, the satellite expands trough the duplication plaque. In addition, self-assembly of the core plaque component Spc42 takes place in this step, which is controlled by the phosphorylation (Adams & Kilmartin, 1999). Elongation of the half-bridge also occurs in this step. It involves that the nuclear and cytoplasmic faces of the half-bridge fuse, forming a complete bridge. In the last step of SPB duplication, the duplication plaque is inserted into the nuclear envelope, and the nuclear components of SPB are assembled (Byers & Goetsch, 1974). Eventually, the duplicated SPBs become connected to each other with the complete bridge. After the insertion process is completed, Spc110, Cmd1 and γ -tubulin complex assemble on the newly synthesized SPB (Kilmartin & Goh, 1996). Concomitant with the cell cycle, the SPB duplication takes place. The activity of budding yeast CDK, Cdc28, with mitotic cyclins (Clb1-4) and the activity of SCF, a ubiquitin ligase, are required for the cleavage of the bridge during the SPB separation followed by its movement to the bud (Fitch et al., 1992). In addition, Kip1 and Cin8, microtubule motor proteins, are involved in this movement (Roof, Meluh, & Rose, 1992).

As described before, SPBs are mainly responsible for microtubule nucleation. However, it has been later detected that SPBs are also crucially involved in the regulation of late events of mitotic cell cycle. They serve as scaffold protein for the assembly of signaling cascades such as the mitotic exit network (MEN) in *Saccharomyces cerevisiae* and the septum initiation network (SIN) in *S. pombe*. The components of MEN are known to be found on the SPB during the cell cycle (McCollum & Gould, 2001); therein, SPB serves as a signaling platform for MEN proteins, that increases the concentration of them in a local area, enhancing the interactions among the components. It is found that although the MEN components are available and functional, the mislocalization resulted from *nud1* mutation leads to inhibition of mitotic exit in budding yeast (Ulrike Gruneberg, Campbell, Simpson, Grindlay, & Schiebel, 2000). In addition to the components of MEN, SPOC components as well as the proteins involved in the spindle positioning signaling cascades, which are Dyn1 and Kar9, localize to the SPB (Yeh, Skibbens, Cheng, Salmon, & Bloom, 1995; Miller & Rose, 1998). The regulation of MEN signaling cascade by the localization of SPBs is dual.

1.5 *Spindle Positioning by Redundant Pathways in Saccharomyces cerevisiae*

Correct positioning of the spindle is essential for asymmetric cell division. As explained before, in budding yeast, the site of cytokinesis is determined before formation of the mitotic spindle, so it is essential that the spindle is positioned in the direction of mother-to-bud polarity axis to ensure accurate ploidy (Palmer et al., 1992). In *Saccharomyces cerevisiae*, there are two partially redundant pathways for spindle positioning: the early and late pathways (Figure 1.6). Deletion of genes in any of these pathways is not lethal while double deletion causes synthetic lethality (Rita K Miller et al., 1998).

The early pathway depends on Kar9 which is the homolog of mammalian Adenomatous Polyposis Coli (APC) (Adames & Cooper, 2000; Beach, Thibodeaux, Maddox, Yeh, & Bloom, 2000). It is defined as a both microtubule and actin associated protein. It connects the astral microtubules and the actin cables, facilitating the correct positioning of the mitotic spindle along actin cables. In this pathway, Bim1, which is a plus-end directed microtubule motor protein, binds to Kar9, which acts as adaptor protein to bind Myo2 (myosin V) (Korinek, Copeland, Chaudhuri, & Chant, 2000; Yin, Pruyne, Huffaker, & Bretscher, 2000). Myosin V, which is a motor protein having double heads, localizes to

the polarized actin cables. It is responsible for the transportation of the plus-end of microtubules toward the bud (Hwang, Kusch, Barral, & Huffaker, 2003).

Kip3 is found in the kinesin-8 family, localizing to the midzone (Gupta, Carvalho, Roof, & Pellman, 2006) It is responsible for the control of microtubule length. Kip3 follows the plus-end of growing spindle until the bud cortex where it turns into a plus-end depolymerase, shortening the astral microtubules (Figure 1.6.1); otherwise, growing astral microtubules could cause the spindle to be pushed back to the mother cell. In other words, Kip3 is needed for disassembly of the mitotic spindle upon exit from mitosis (Woodruff, Drubin, & Barnes, 2010; Gupta et al. 2006). It scales the length of anaphase spindle with the length of cell. In cells with deleted KIP3, mitotic spindle hyper-elongate exceeding the length of cell (Rizk, DiScipio, Proudfoot, & Gupta, 2014). It has been recently discovered that the activity of Kip3 requires Bud6, Bim1 and cytoplasmic dynein (Ten Hoopen et al., 2012).

Kar9 is known to localize asymmetrically at metaphase. It preferentially accumulates on the daughter spindle pole as well as on the plus-ends of the astral microtubules growing from the daughter spindle pole body (Liakopoulos, Kusch, Grava, Vogel, & Barral, 2003). The asymmetry in Kar9 localization is achieved by the cortical pulling force of Bim1-Kar9-Myo2 complex. Clb4-Cdc28 complex phosphorylates Kar9, that causes the loading of Kar9 to the cytoplasmic microtubules where it is transported to the bud in a myosin-dependent manner (Liakopoulos et al., 2003). Mutations on the Cdc28 phosphorylation consensus site of Kar9 are found to disrupt the asymmetrical localization, targeting both SPBs to the daughter cell (Liakopoulos et al., 2003; Paoletti & Bornens, 2003).

The late pathway is dependent on Dyn1 which is a minus-end directed microtubule motor protein (Li, Yeh, Hays, & Bloom, 1993). This pathway is activated at the metaphase-to-anaphase transition by the removal of She1, which is the dynein inhibitor in budding yeast (Woodruff, Drubin, & Barnes, 2009). Dyn1 localizes to the plus-end of the growing mitotic spindle. Bik1, a plus-end targeted protein, is responsible for the recruitment of Dyn1 to the microtubules (Sheeman et al., 2003). Kip2, a plus-end directed kinesin, transports Bik1 as cargo. Thus, the Kip2/Bik1 complex transports the cytoplasmic dynein (Dyn1) to the plus ends of the cytoplasmic microtubules, that reach to the cortex of the daughter cell (Carvalho, Gupta, Hoyt, & Pellman, 2004). Then, Num1, which is a cortical protein distributed through the cell, anchors the dynein tail to the cortex, stabilizing the

dynein tail at the cortex. Therein, free motor domains of the cortex anchored dynein capture the microtubules and start pulling them (Adames & Cooper, 2000). The SPB localization of cytoplasmic dynein on the microtubules is also asymmetric. It preferentially localizes to the plus-end of the growing microtubules as well as daughter SPB at metaphase. The activity of certain kinases such as Elm1, Hsl1 and Gin4 localized at the bud neck provides the asymmetry in the localization of cytoplasmic dynein (Grava, Schaerer, Faty, Philippsen, & Barral, 2006). This asymmetry is cleared on the plus-ends at anaphase, preventing the movement of both poles to the bud during cell cycle (Grava, Schaerer, Faty, Philippsen, & Barral, 2006; McNally, 2013).

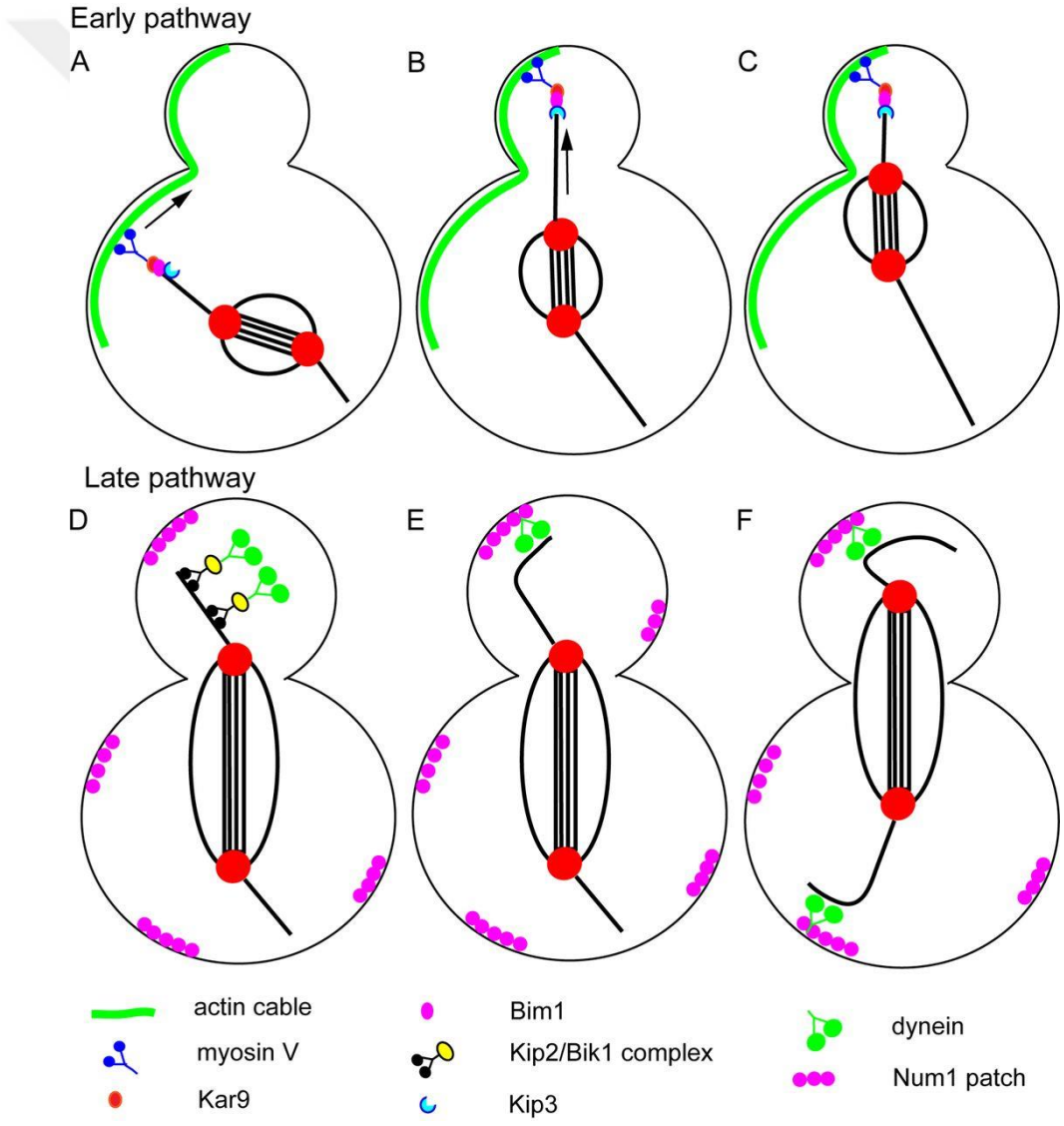

Figure 1.6. 1: Spindle positioning by redundant pathways in Saccharomyces cerevisiae. The pathways and their molecular compositions are represented (This figure is taken from McNally, 2013) (McNally, 2013).

Cyclin-CDK complexes are involved in the regulation of the mitotic spindle orientation (Figure 1.6.2) (Segal, Clarke, & Reed, 1998). For example, Kar9 asymmetry on the plus-end of microtubules is regulated by phosphorylation performed by the activity of certain cyclin-CDK complexes. This phosphorylation restricts Kar9 to the daughter SPB, which is inhibited by the mutations at the Cdc28 consensus phosphorylation sites in Kar9 (Liakopoulos et al., 2003). In addition, Kar9 physically interacts with Clb5, and this may be suggestive of the fact that Kar9 phosphorylation by Clb5 entraps it at daughter SPB (Moore, D'Silva, & Miller, 2006). Moreover, Clb1- and Clb2-Cdc28 complexes are essential for the asymmetric localization of cytoplasmic dynein at metaphase.

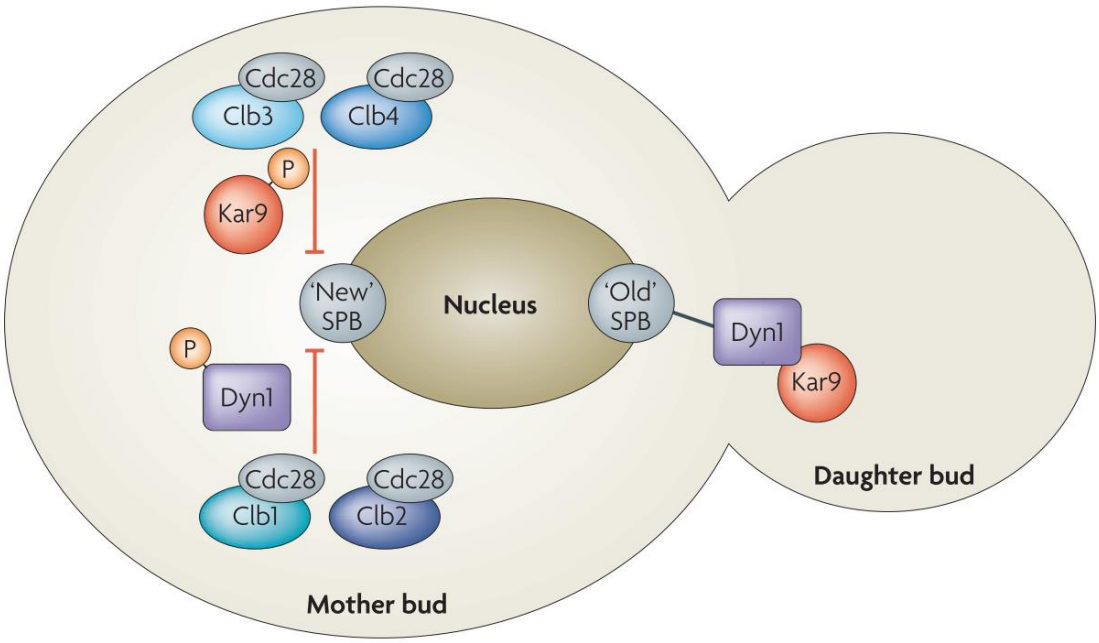

Figure 1.6. 2: Regulation of the mitotic spindle formation by cyclin-CDK complexes. Kar9 is phosphorylated by Clb3- and Clb4-Cdc28 complexes, whereas Dyn1 is phosphorylated by Clb1- and Clb2-Cdc28 complexes. These phosphorylation events prevent their localization to mother SPB until anaphase place (This figure is taken from Bloom et al., 2007) (Bloom & Cross, 2007).

1.6 *Mitotic Exit in Saccharomyces cerevisiae*

The late events of mitosis occur in a rapid and correct fashion. These events are mainly controlled by two molecular processes. First, the mitotic cyclin-CDK complexes need to be inactivated. Second, cyclin-CDK substrates are dephosphorylated by the action of phosphatases. It has been known that APC/Cdc20 complex is important to initiate the

destruction of cyclin-CDK complexes as well as mitotic spindle elongation. However, APC/Cdc20 is not enough for complete M-cyclin degradation, thus for M-to-G1 transition, in *Saccharomyces cerevisiae* (Jaspersen, Charles, Tinker-Kulberg, & Morgan, 1998). Cdh1, another substrate specificity subunit of APC, replaces Cdc20 and targets M-cyclin (Clb2) for full destruction of Clb2 (Pfleger & Kirschner, 2000; Visintin, Prinz, & Amon, 1997)(Qiao, Zhang, Gamper, Fujita, & Wan, 2010). APC/Cdh1 also mediates the destruction of certain proteins involved in cytokinesis and SPB duplication including Ilp1 during late mitosis (Taylor & Peters, 2008).

Budding yeast cells need the activity of the phosphatase, Cdc14, for exiting mitosis (Visintin et al., 1998). Cdc14 dephosphorylates phosphoserines or phosphothreonines followed by a proline. This is the minimum consensus sequence of CDK phosphorylation site; therefore, Cdc14 counteracts the phosphorylation status of M-cyclin-CDK substrates. Three main targets of Cdc14 are key for downregulation of M/CDK activity and hence for mitotic exit: Cdc14 dephosphorylates Cdh1, promoting APC/C association, which results in degradation of M-Cyclin-CDK complexes in proteosome (Visintin et al., 1998). It also dephosphorylates Sic1, a CKI, stabilizing it to ensure the inactivation of S-Cyclin-CDKs (Visintin et al., 1998). Another main target of Cdc14 is Swi5, a transcription factor of *SIC1*. Dephosphorylation of Swi5 by the activity of Cdc14 removes the CDK-dependent block on importing into the nucleus where it can now activate the expression of *SIC1* (Visintin et al., 1998).

Cdc14 is entrapped in the nucleolus as inactive until metaphase-to-anaphase transition (Stegmeier & Amon, 2004). The release of Cdc14 is controlled by two distinct mechanisms. cdc Fourteen Early Anaphase Release (FEAR) pathway controls the early stages of Cdc14 release where only a small amount is released into the cytoplasm. Mitotic Exit Network (MEN), afterwards, triggers the sustained release of Cdc14. In nucleolus, Cdc14 is bound to Net1, a protein involved in silencing rDNA repeats (Straight et al., 1999). The N-terminal region of Net1 binds to Cdc14. This binding not only anchors Cdc14 in the nucleolus but also inhibits the activity of Cdc14 (Traverso et al., 2001). Fob1 together with its binding partner Spo12 is responsible for keeping Net1-Cdc14 complex in the nucleolus (Toyn & Johnston, 1993). Fob1 interacts with a silencing protein, Sir2, to anchor Net1-Cdc14 complex to rDNA repeats. They all together form the complex called the regulator of nucleolar silencing and telophase (RENT) (Wenying Shou et al., 1999). FEAR-dependent release of Cdc14 is controlled by a dynamic balance between

phosphorylation and dephosphorylation events. Until the metaphase-to-anaphase transition, Net1 is kept as dephosphorylated, maintained by the activity of PP2A/Cdc55 complex (Wang & Burke, 1997). However, M-cyclin-CDKs, then, phosphorylate Net1 and other RENT components, causing partial release of Cdc14 from the nucleolus during anaphase (Azzam et al., 2004). FEAR-released Cdc14 is important to prime the activity of mitotic exit network (MEN). Thus, the efficiency of MEN is increased by FEAR-released Cdc14 (Rock & Amon, 2009). It is also important for the assembly of the spindle midzone by dephosphorylating Ase1, a spindle midzone bundling protein (Khmelinskii, Lawrence, Roostalu, & Schiebel, 2007). Also, Slk19-Esp1 is shown to activate FEAR pathway for early Cdc14 release (Stegmeier, Visintin, & Amon, 2002). Esp1 activated Cdc14 is required for the dephosphorylation and relocalization of Sli15, modulating the assembly of the spindle midzone through Sli15-Ipl1 complex (Pereira & Schiebel, 2003).

Full release of Cdc14 is controlled by an essential signaling pathway called Mitotic Exit Network (MEN) in budding yeast (Figure 1.7). In anaphase, MEN triggers full and robust release of Cdc14 from the nucleolus into the cytoplasm, that promotes exiting from mitosis. MEN is a GTPase driven signaling cascade (Jaspersen et al., 1998). The core pathway is composed of Tem1, a GTP-binding protein of Ras superfamily, Cdc15, a protein kinase which is the homolog of mammalian sterile-20-related kinase, and Dbf2, a protein kinase which is the homolog of nuclear Dbf2-related kinase, together with its regulatory protein Mob1 (Shirayama, Matsui, & Toh-E, 1994; Luca & Winey, 1998; Shou et al., 1999; Bardin, Boselli, & Amon, 2003). These main players of MEN regulating exit from mitosis initially localize to daughter spindle pole body, creating an asymmetry which is required for the recognition of spindle misalignment (Cenamor, Jiménez, Cid, Nombela, & Sánchez, 1999; Visintin & Amon, 2001). They associate with the centriolin-related SPB scaffold protein, Nud1, at the SPB, and this localization is critical for the activation of MEN (Satoshi Yoshida, Asakawa, & Toh-e, 2002). Cdc15 functions at the upstream of Dbf2-Mob1 complex in the MEN. It phosphorylates the C-terminus hydrophobic motif (HM) site of Dbf2, enhancing its enzymatic activity, a critical step in the MEN activation. The C-terminus of Cdc15 contains a short segment that is important for Tem1 binding (Asakawa, Yoshida, Otake, & Toh-e, 2001).

It has been known that the localization and the nucleotide status of Tem1 is crucial for the regulation of MEN. The activity of Tem1 is controlled by a bipartite GTPase Activating Complex (GAP) consisting of Bfa1 and Bub2 proteins, that inactivates Tem1

by converting it to GDP-bound form (Bardin, Visintin, & Amon, 2000). It is also suggested that Tem1 itself can hydrolyze GTP to GDP, and Bfa1 may function to inhibit GDP exchange (Geymonat et al., 2002). Therefore, the activity of Bfa1-Bub2 complex is important for controlling MEN. This complex localizes to the daughter SPB, and recruits Tem1 (Pereira et al., 2000).

Cdc5, a polo-like kinase, is an essential kinase that positively regulates the mitotic cell cycle in budding yeast. It inactivates Bfa1-Bub2 complex by phosphorylating it (Wang, Hu, & Elledge, 2000). Therefore, the GAP activity of Bfa1-Bub2 complex towards Tem1 is inhibited. This phosphorylation event is dependent on the positioning of the mitotic spindle. In the cells having correctly positioned mitotic spindle, Cdc5 phosphorylates Bfa1, inhibiting its activity. However, in the presence of spindle misalignment, Kin4, a serine/threonine kinase involved in SPOC, phosphorylates Bfa1 (Maekawa, Priest, Lechner, Pereira, & Schiebel, 2007). In this status, Bfa1 can no longer be phosphorylated by Cdc5; therefore, Bfa1-Bub2 complex is active and stimulates GTP hydrolysis that prevents the activity of Tem1, eventually MEN is inhibited (Figure 1.7).

Ras family small GTPases are highly conserved signal transducers modulating cellular proliferation, survival, and differentiation. Tem1 switches between GDP (inactive) and GTP (active) bound states. Conversion to the active form is promoted by a guanyl nucleotide exchange factor (GEF) and counteracted by GTP hydrolysis stimulated by a GAP. Tem1 activation is ensured by Lte1, which acts as a GEF factor (GEF) (Bardin et al., 2000). However, no GEF activity of Lte1 on Tem1 was detected *in vitro* (Geymonat et al., 2009). Instead, it was shown that Lte1 plays roles in the SPB localization of Bfa1 and Kin4 (Geymonat et al., 2009; Bertazzi, Kurtulmus, & Pereira, 2011) . Lte1 localize to the bud cortex and becomes essential at colder temperatures (lower than 16 ^{o}C) (Shirayama et al., 1994). It has been shown that Lte1 is important for removal of Bfa1 from mSPB at cold temperatures (Geymonat et al., 2009) . It was also shown that Lte1 inhibits the SPB localization and activity of Kin4 in the daughter cell (Falk, Chan, & Amon, 2011; Bertazzi et al., 2011). The function of GEF domain of Lte1 in mitotic exit is unclear (Geymonat et al., 2009).

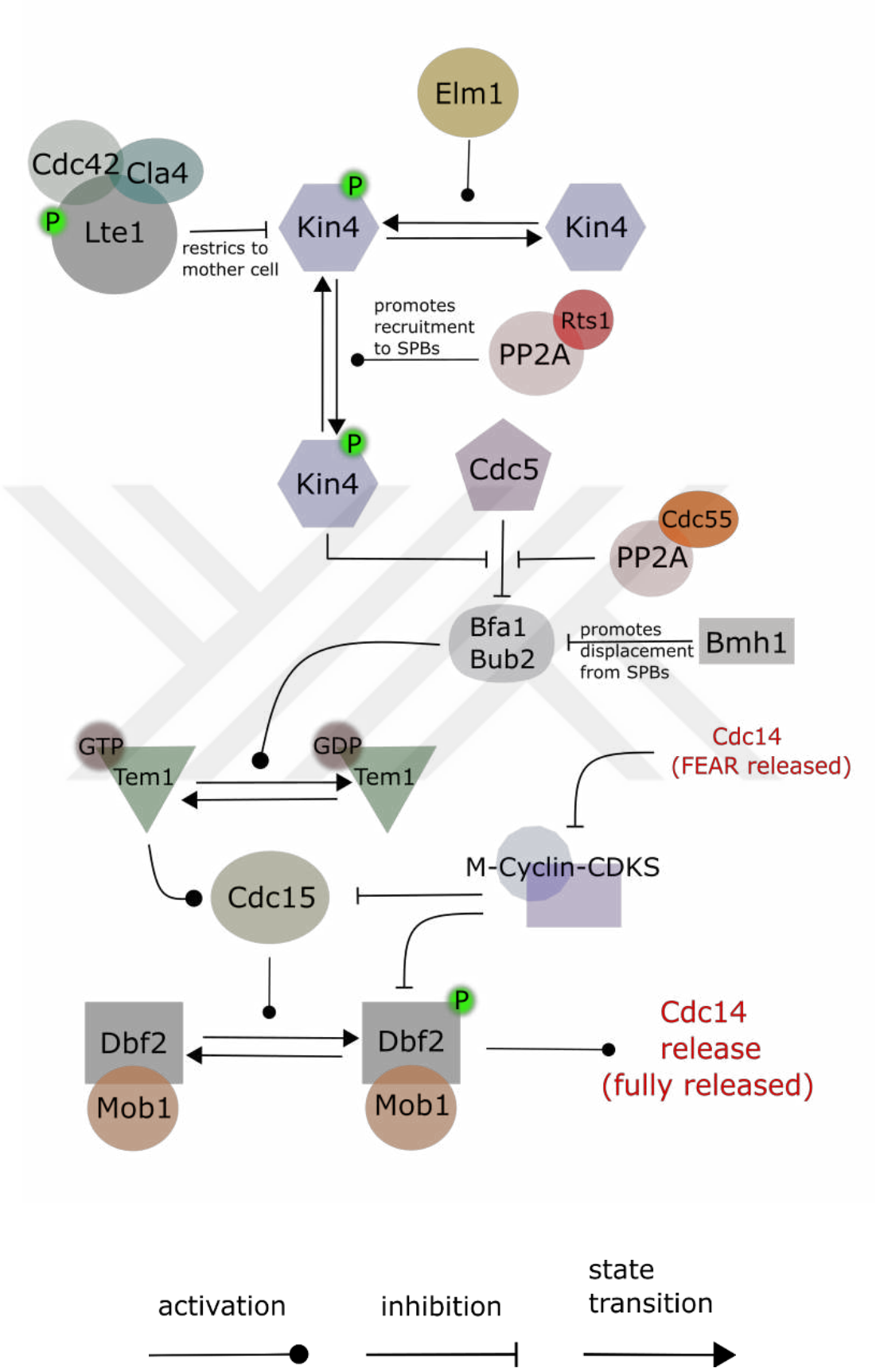

Figure 1. 7: The whole signaling cascade controlling the exit from mitosis in budding yeast. SPOC inhibits cell cycle progression in the presence of spindle misalignment, activating Bfa1. MEN triggers the full release of Cdc14. See the text for details.

1.7 *Spindle Position Checkpoint in Saccharomyces cerevisiae*

The maintenance of the correct ploidy from one generation to the next is essential. Genetic material should be partitioned equally in between the mother and daughter cells during mitosis. To ensure the faithful segregation, first all the kinetochores should be captured by the mitotic spindle in a bi-oriented manner, which is controlled by SAC. Secondly, the mitotic spindle should align with respect to mother-bud axis at anaphase onset to deliver one set of the chromosomes to the daughter cell. Therefore, the accurate alignment of the mitotic spindle in the mother-to-daughter polarity axis is crucial for maintaining the correct ploidy in budding yeast. Spindle Position Checkpoint (SPOC) is a surveillance mechanism that monitors the orientation of the mitotic spindle in budding yeast. In the presence of spindle misalignment, SPOC inhibits cell cycle progression of cells through inhibition of the MEN (Figure 1.8) (Caydasi, Ibrahim, & Pereira, 2010). Therefore, it provides time for the cells to correct their spindle orientation before the mitotic exit takes place (Yeh et al., 1995; Bardin et al., 2000).

SPOC keeps the cells at anaphase until one of the SPBs is delivered into the daughter cell (Adames & Cooper, 2000). It controls MEN through the inactivation of Tem1 GTPase by Bfa1-Bub2 complex (Geymonat et al., 2002). The activity of Bfa1-Bub2 complex is strongly dependent on the phosphorylation of Bfa1. As described before, Bfa1 is phosphorylated by Cdc5 in the cells with normally aligned spindle (Figure 1.8) (Geymonat, Spanos, Walker, Johnston, & Sedgwick, 2003). However, Kin4 phosphorylates Bfa1 on residues S150 and S180 in the presence of spindle misalignment, that prevents Cdc5 phosphorylation from turning off Bfa1-Bub2 complex (Hu et al., 2001; Maekawa et al., 2007). Asymmetric SPB localization of Bfa1 changes into symmetric upon phosphorylation by Kin4 in response to spindle misalignment. This phosphorylation causes a reduction in the SPB localized Bfa1 levels, redistributing it through the cytoplasm; therefore, changing the asymmetric localization of Bfa1 (Maekawa et al., 2007; Caydasi & Pereira, 2009). Kin4 phosphorylation creates a docking site on Bfa1 where 14-3-3 family protein Bmh1 can bind. Recruitment of Bmh1 onto Bfa1 causes the displacement of it from the SPBs, providing the symmetric Bfa1 localization upon spindle mispositioning (Caydasi, Micoogullari, Kurtulmus, Palani, & Pereira, 2014).

Kin4 localizes to the mother cell cortex, the bud neck and mother SPB where it inhibits mitotic exit by increasing the turnover rate of Bfa1 (Bardin et al., 2000; D'Aquino et al., 2005; Caydasi & Pereira, 2009). Notably, Kin4 cannot localize to daughter SPB, meaning its localization to mother SPB is restricted. The mother cell specific SPB localization of Kin4 is regulated by Lte1, a daughter localized effector of MEN. It prevents permanent loading of Kin4 on the daughter SPB (Bertazzi et al., 2011). The Rho GTPase Cdc42 with its effector Cla4, a protein kinase, control the localization of Lte1 to the bud cortex (Seshan, Bardin, & Amon, 2002). Phosphorylation of Lte1 by Cla4 stimulates its interaction with Cdc42, and this interaction stabilizes Lte1 at the bud cortex (Seshan & Amon, 2005). Hence, the asymmetric localization of Kin4 and Lte1 regulates the Tem1 activity through regulating the activity of Bfa1-Bub2 complex (Figure 1.8) (Falk et al., 2011).

The activity of Kin4 is controlled by different mechanism. The kinase activity of Kin4 is regulated by Elm1, an important effector for SPOC, and its activity requires localization to the bud neck (Moore, Chudalayandi, Heil-Chapdelaine, & Cooper, 2010; Caydasi et al., 2010). It phosphorylates Kin4 from a threonine residue found on the activation loop, called T-loop, and this phosphorylation catalytically activates Kin4 (Caydasi et al., 2010). On the other hand, localization of Kin4 is regulated by protein phosphatase PP2A together with its regulatory subunit Rts1. PP2A-Rts1 promotes localization of Kin4 to mSPB and mother cell cortex through dephosphorylation of Kin4 and this dephosphorylation is required for the functionality of Kin4 (Chan & Amon, 2009). Kin4 is kept dephosphorylated by the activity of PP2A during S phase and mitosis. (Chan & Amon, 2009).

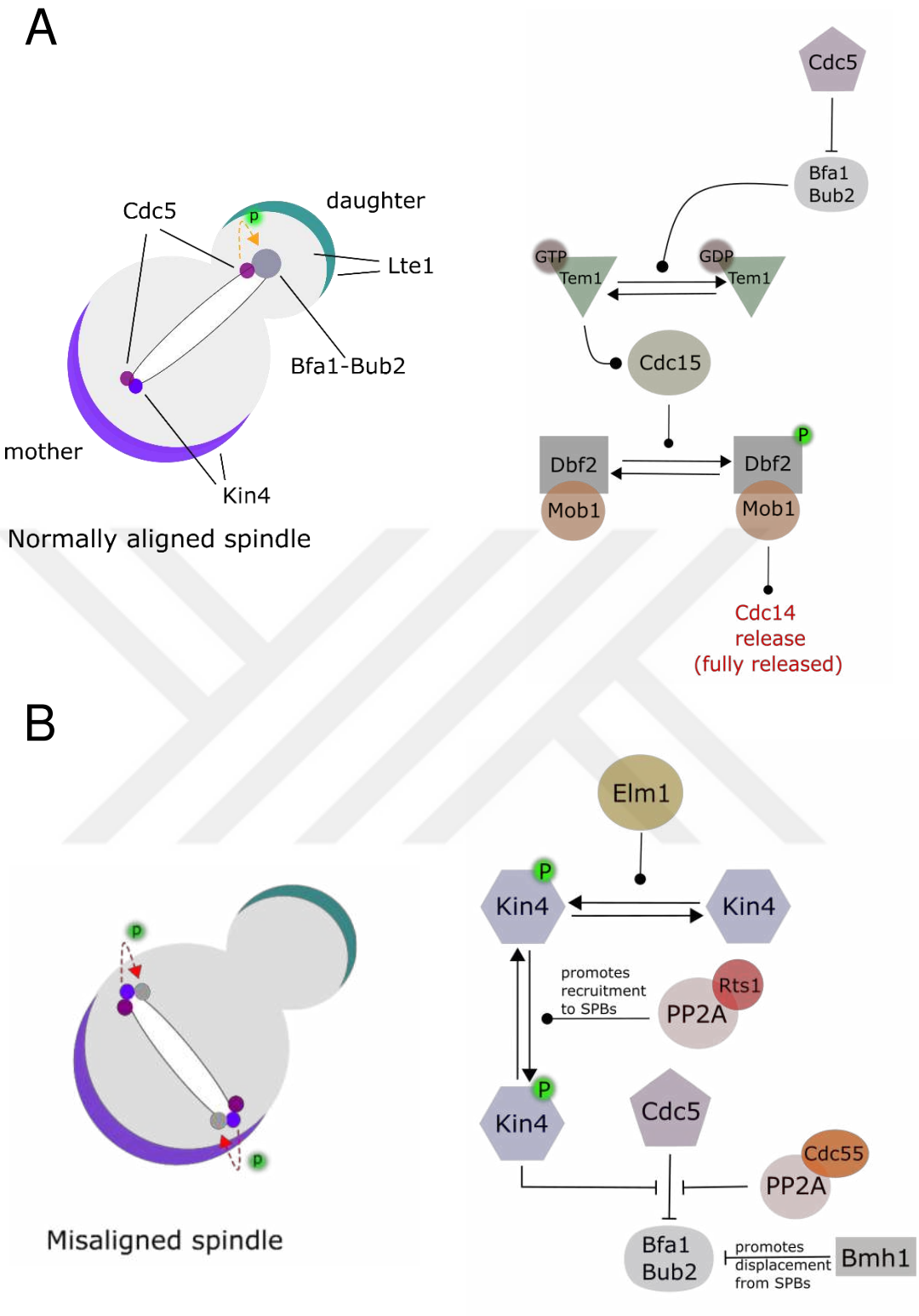

Figure 1. 8: The activation of MEN is coupled to the spindle positioning. A. Cdc5 phosphorylates Bfa1 (orange dashed arrow), inhibiting its GAP activity on Tem1, stimulating mitotic exit. **B.** In the presence of spindle misalignment, Kin4 phosphorylates Bfa1 (red dashed arrow), antagonizing the inactivation of Bfa1-Bub2 by Cdc5. This inhibits MEN.

Chapter 2: **MATERIAL AND METHODS**

2.1 ***Saccharomyces cerevisiae Methods***

The name and description of all media, buffer and reagent compositions are listed in Table 7.4.

2.1.1 Yeast Strains and Growth Media

The yeast strains used for this study are isogenic with S288C and are listed in Table 7.3. The yeast strains were grown in respective selective medium containing D-(+)-Glucose (BioFroxx, #1191GR500) as the sole carbon source, if there is not going to be induction with D-(+)-Galactose. YPAD medium was the medium used for general growth of yeast cultures. For the induction from pGal1 promoter, 2 % D-Raffinose (AFG Bioscience #379827) containing medium with 3 % D-(+)-Galactose (AFG Bioscience #307688) was used instead of 2% D-(+)-Glucose (BioFroxx, #1191GR500). For the preparation of agar plates of these media, 20 g Agar (Carl Roth, #5210.2) was added into the medium to make 1 liter of agar plate. All the growth media and plates were autoclaved for sterilization, unless otherwise stated.

2.1.2 Yeast Growth

Yeast strains were grown at 30 °C and in rich medium unless otherwise stated. Plasmid containing strains were grown in synthetic complete (SC) media lacking the respective selective auxotrophic nutrients. The temperature MEN-*temperature sensitive* (MEN-*ts*) mutant cells and *kar9*Δ cells were maintained at 23 °C and shifted to the respective restrictive or/and semi-permissive temperatures for investigating the phenotype.

To perform the experiments, firstly the yeast cultures were obtained in the stationary phase. To do so, yeast cells were grown on the respective agar plate. Next, they were taken from agar plates and inoculated in proper growth medium. They were cultivated at the proper temperature until the cultures reach the stationary phase, which is the value that optical density value at 600 nm (OD600) is approximately greater than 5.0. This generally corresponds to overnight incubation of the cultures, taking 12-18 hours at the physiological temperature which is 30 °C for budding yeast. Afterwards, stationary phase

cultures were diluted to OD600 value of 0.1-0.2 in a fresh medium. Spectrophotometric measurements were performed in a spectrophotometer (PG Instruments, T60 Visible Spectrophotometer). Finally, the experiments were carried out only after these freshly diluted cultures reach to OD600 value of 0.8-1.0 (~2.5 cell divisions after dilution of the stationary culture), which corresponds to the logarithmically growing yeast culture.

2.1.3 Yeast Competent Cell Preparation and Transformation

In order to make the yeast cells competent, we used chemical method. Firstly, cells were inoculated the day before in 10 mL of appropriate medium and incubated at 30 °C or 23 °C for temperature sensitive mutants. Then, the culture was diluted to OD600 value of around 0.15 in 50 mL of fresh media. Next, the culture was incubated until the OD600 reaches 1.0 which makes approximately $2x10^7$ cells/mL. The culture reached log phase was centrifuged at 3200 rpm for 2 minutes at room temperature. Supernatant was discarded and then 45 mL sterile double-distilled water was added to re-suspend the cells. It was centrifuged at 3200 rpm for 2 minutes at room temperature. Supernatant was discarded and cells were re-suspended in 15-25 mL LiSORB. Centrifuged as before and then supernatant was discarded to remove excess LiSORB. The remaining pellet was centrifuged once more to get rid of all the liquid remaining. Afterwards, the cells were resuspended in 300 µL LiSORB and 50 µL denatured Salmon Sperm. The denaturation of the salmon sperm was achieved by boiling it at 95 °C for 5 minutes followed by direct incubation on ice for 5 minutes. The amount of LiSORB and Salmon Sperm can be scaled according to the cell amount. Finally, the competent cells were aliquoted as 100 µL per microcentrifuge tube, and they can either be used for transformation process directly or be stored at -80 °C for a while.

Competent yeast cells are able to get foreign PCR products and plasmids inside the cell. PCR products are integrated into the genome by homologous recombination whereas the plasmids can either be internalized as circular or be integrated into the genome if cut by appropriate restriction enzymes. In order to transform the compentent cells with these foreign DNA pieces, firstly certain amount of PCR product (generally 5 µL) or plasmid (generally 3 µL for integration plasmids; 1 µL for circular plasmids) were added onto 50 µL competent cells and incubated at room temperature for 15-20 minutes. Then, 300 µL LiPEG was added onto the mixture and vortexed well followed by 20 minutes of incubation at room temperature. After that, 35 µL of DMSO (Fisher Scientific #BP231-

1) was added into the mix and vortexed followed by straightaway incubation in the 42 °C water bath for 15 min. The incubation time was 12 minutes for the transformation of temperature-sensitive mutants. After the incubation, cells were centrifuged at 3200 rpm for 2 min at room temperature, and the supernatant was discarded by aspiration. Then, the cell pellet was resuspended in 200 µL 1X sterile PBS and directly plated out onto auxotrophic selective agar plate. However, if the selection marker is antibiotic resistance, then the cells were recovered in non-selective medium overnight before plating out onto respective agar plate containing respective antibiotic.

2.1.4 Yeast Growth Comparison: Drop Test

Yeast cultures were grown in the appropriate growth conditions for 24-48 hours. OD600 value of all the yeast cultures, then, was adjusted to 1.0 using 1X sterile PBS. The cultures were serially diluted 10-fold using sterile 1X PBS. 10 µl of each serial dilutions were spotted on the appropriate agar plates. The plates were incubated at the appropriate temperatures for 1-3 days.

2.2 ***PCR-based Methods***

Cassette PCR-based genome editing tool was used for gene deletions and tagging at N- or/and C- terminus of the proteins. This method is based on homologous recombination (Janke et al., 2004; Michael Knop et al., 1999). Gene deletions were also confirmed by using PCR. Chromosomal DNA isolation or Yeast Colony PCR using Sarkosyl were used to isolate yeast chromosomal DNA from the cells. Furthermore, mutations were introduced using PCR-based site-directed mutagenesis.

2.2.1 Cassette PCR

All the PCR-based cassette constructs were produced as described in (Michael Knop et al., 1999) using Biometra TAdvanced Twin Analytik Jena PCR machine. For constructing 50 µL cassette PCR reaction, 5 µL from 20 ng/µL plasmid template, 3.2 µL from forward -S1 or -S3 primers (10 µM), 3.2 µL from reverse -S2 or -S4 primers (10 µM), 0,6 µL from the polymerase enzyme mix composed of (2X µL Taq DNA Polymerase (5U/ µL, NEB #M0273L) + 1X µL Vent (2U/µL, NEB #M0254S), 8.75 µL from 2 mM dNTPs mix (NEB #N0446S), 5 µL from 10X PCR Buffer and 24.25 µL double distilled water (ddH_2O) were mixed. S1/S2 primer combination was used for gene deletion, and S2/S3

primer combination was used for C-terminal tagging whereas S1/S4 was for N-terminal tagging. (Table 7.3)

The PCR cycle conditions were set as following: Step1 (initial denaturation): 2 min at 95 ºC, Step 2 (denaturation): 30 sec. at 95 ºC, Step3 (annealing): 30 sec at 52 ºC, Step 4 (elongation): X min at 68 ºC, (X corresponds to the time required to synthesize the PCR product. It is calculated as 1 minute per 1000 bp of the expected product size). Steps from 2 to 4 were repeated for 9 times. Step 5 (denaturation): 30 sec at 95 ºC, Step 6 (annealing): 30 sec at 52 ºC, Step 7 (elongation): X min with an increment of 20 sec per step at 68 ºC. Steps from 5 to 7 were repeated 19 times. The reaction was finally held at 4 ºC. The PCR constructs and amounts were analyzed on 0.8 % agarose gel prepared in 1X TAE buffer.

2.2.2 Yeast Colony PCR

In order to isolate chromosomal DNA directly from solid culture, colony PCR with Sarkosyl was used. Firstly, a small amount of yeast cells was taken from the appropriate plate. Efficiency of the isolation increases if the cells are fresh, which is a day after from streaking onto the plate. Then, the cells were resuspended in 50 µL of 0.01% Sarkosyl in 0.02 N NaOH, and vortexed well. The mixture was boiled at 95 ºC for 15 minutes followed by direct incubation at -80 ºC for a couple of minutes to ease the cell lysis.

For constructing 25 µL PCR reaction using chromosomal DNA, 1.25 µL from 10 µM gene-specific forward primer, 1.25 µL from 10 µM gene-specific reverse primer (Table 7.3), 2.5 µL from 10X PCR buffer, 2.5 µL from 2 mM from dNTP mixture, 0.2 µL from 5U/µL Taq DNA polymerase, 16.3 µL from double-distilled water and 1 µL from chromosomal DNA were mixed.

The PCR cycle conditions were set as following: Step1 (initial denaturation): 5 min at 95 ºC, Step 2 (denaturation): 30 sec at 95 ºC, Step3 (annealing): 30 sec at 54 ºC, Step 4 (elongation): X min at 68 ºC, (X corresponds to the time required to synthesize the PCR product. It is calculated as 1 minute per 1000 bp of the expected product size). Steps from 2 to 4 were repeated for 35 times. Step 5 (final extension): 3 minutes at 68 ºC. The reaction was finally held at 4 ºC. The gene deletions with proper WT controls were analyzed on 0.8 % agarose gel prepared in 1X TAE buffer.

2.2.3 Yeast Chromosomal DNA Isolation

In order to isolate chromosomal DNA directly from liquid culture, first of all, cells were inoculated the day before in 5-10 ml of appropriate medium and incubated at 30 °C or 23 °C for temperature sensitive mutants. 1.5-3 ml of the overnight culture was centrifuged at 14800 rpm for 1 minutes, and the supernatant was discarded. Then, 300 µL 6 % SET was added, and vortexed well to resuspend the cells. The cells were incubated at 65 °C for 15 minutes. Then, the cells were transferred to ice and 150 µL 3M P3 buffer was added. Next, the mixture was mixed by inverting several times followed by incubation on ice for 15 minutes. After that, the mixture was centrifuged at 14800 rpm for 10 minutes at room temperature. The supernatant was transferred to a new microcentrifuge tube containing 500 µL isopropanol, mixed by invert rotation vigorously, and spined at full speed for 1 minute. Then, the supernatant was discarded, and the pellet was rinsed with 200 µL cold 70 % ethanol. Next, the liquid was removed by inverting the tubes and then they were left to air-dry until all the remaining liquid evaporates. After that, DNA pellets were resuspended in 30 µL ddH_2O pre-heated to 65 °C, and 1 µL 1 mg/mL RNase A was added. Finally, the pellets were incubated at 37 °C for 15-20 minutes.

The PCR reactions and cycle conditions were set as described before.

2.2.4 Site-Directed Mutagenesis

To introduce a desired point mutation into plasmids, site-directed mutagenesis PCR was used. For constructing 50 µL mutagenesis PCR reaction, 5 µL from 5 ng/µL plasmid template, 1.5 µL from forward primer (10 µM), 1.5 µL from reverse primer (10 µM) (Table 6.3), 1.5 µL from Turbo PFU DNA Polymerase (Agilent #600250), 4 µL from 2 mM dNTPs mix (NEB #N0446S), 5 µL from 10X PFU Turbo Buffer and 31.5 µL double distilled water (ddH2O) were mixed. As control 5 µL from 5 ng/µL plasmid template, 5 µL from 10X Turbo PFU Buffer and 40 µL double distilled water (ddH2O) were mixed.

The PCR cycle conditions were set as following: Step1 (initial denaturation): 30 sec at 95 ºC, Step 2 (denaturation): 30 sec. at 95 ºC, Step3 (annealing): 1 min at 54 ºC, Step 4 (elongation): X min at 68 ºC, (X corresponds to the time required to synthesize the PCR product. It is calculated as 2 minutes per 1 kb of the expected vector size). Steps from 2 to 4 were repeated for 16 times. The reaction was finally held at 4 ºC.

After the plasmid was produced through PCR-based mutagenesis, the plasmid was treated with 2 µL of DpnI restriction enzyme (Thermo Fisher Scientific #ER1705) overnight at 37 ºC. Then, the plasmid was transformed into *E. coli DH5α* competent cells for amplification of the plasmid. Next, amplified plasmid was isolated from these cells and sent to sequencing to confirm the mutation.

2.2.5 Manual Plasmid DNA Isolation from E. coli (MiniPrep)

A single colony of *E. coli*, transformed with the plasmid of interest, was inoculated into 3 mL TY medium with appropriate selective antibiotics, and the cultures were grown at 37 °C overnight (12-18 hours) with proper shaking and aeration. Then, 2 mL of the cultures was harvested at 6000 rpm for 5 minutes at RT. The supernatant was discarded. Remaining pellet part, afterwards, was resuspended with 300 µL of P1 buffer by vortexing. Next, 300 µL of P2 buffer was added into the cell suspension and invert-rotated several times to mix. Then, 300 µL of cold P3 was immediately added, and invert-rotated several times to mix well. The mixture was centrifuged at full speed (13000-14000 rpm) for 10 minutes at RT. Then, the supernatant was transferred into a new microcentrifuge tube containing 600 µL Isopropanol (ACS #0312.2500) and mixed well by invert-rotation. The mixture was centrifuged at full speed for 20 minutes at RT. The supernatant was decanted, and the pellet was washed with 800 µL of 70 % Ethanol, and then centrifuged at full speed for 5 minutes at RT. Then, the supernatant was removed, and the pellet was centrifuged once more to get rid of all the remaining Ethanol. The pellet was air dried by leaving the tubes open, and finally resuspended using 30 µL of pre-heated ddH2O at 65 °C.

2.3 ***Biochemical Methods***

2.3.1 Total Cell Protein Extraction using TCA

2 mL of logarithmically growing yeast culture with known OD600 was harvested at 14000 rpm for 2 minutes. The supernatant was removed, and the pellet was resuspended in 800 µL cold ddH2O on ice. Then, 150 µL of 1.85M NaOH (Merck, #106498) was immediately added into the suspension, vortexed and incubated on ice for 5 minutes. Next, 150 µL of 55 % (w/w) TCA (Trichloroacetic acid, Merck #100807) was added into the suspension, and vortexed well followed by incubation on ice for 10 minutes. Then,

the suspension was centrifuged at 14000 rpm for 20 minutes at 4 °C. The supernatant was removed, and the pellet was centrifuged once more for 1 minute to get rid of all the remaining liquid. Afterwards, the supernatant was aspirated, and the pellet was resuspended in HU-DTT. 150 µL of HU-DTT was used for 1 mL 1 OD600 abundant protein of interests whereas 75 µL of HU-DTT was used for 1 mL 1 OD600 less abundant protein of interests, or larger proteins. The amount of HU-DTT to be added was easily scaled according to the OD600 value as well as the volume of the culture to be pelleted. After the addition of HU-DTT, the pellet was vortexed well. When the suspension turned into a yellowish color, 2 µL of 2M Tris-HCI was added to neutralize the pH. For SDS-PAGE loading, the samples were boiled up at 65 °C for 15 minutes, and then centrifuged at 14000 rpm for 2 minutes at room temperature before loading. 15 µL of the samples was loaded per lane.

2.3.2 Native Protein Isolation and anti-TAP Immunoprecipitation

Protein of interest was tagged with TAP-tag (CBP-TEV-4ProA) using PCR-based homologous recombination. For cell harvesting, yeast cells were, first of all, grown in an appropriate medium. Logarithmically growing cells were pelleted at 3200 rpm for 10 minutes at 4 °C to get rid of the medium. Then, the pellet was washed with 1X cold PBS containing 4mM Benzamidine and 2mM PMSF, and transferred to 2 mL lysis tubes (Sarstedt, #72.693) as 100 OD600 per tube, and centrifuged at 14000 rpm for 2 minutes at 4 °C. The cell pellets, afterwards, were frozen and stored at -80 °C.

For protein isolation, cells were lysed in the lysis buffer (25mM HEPES-HCI pH:7.5, 400mM NaCl, 33mM EGTA, 1mM EDTA, 0.1% NP-40, 2mM PMSF, 4mM Benzamidine, 1mM DTT and Complete Protease Inhibitor Cocktail (Sigma, #11873580001) with glass beads (Sigma, #G8772) by using a cell homogenizer (SpeedMill Plus AnalytikJena) to obtain a cell lysate. 350 µL 1X lysis buffer was used per 100 OD600 cell pellet. Then, the lysate was clarified at 10000 rpm for 20 minutes at 4 °C. The supernatant was transferred into a new tube, and the pellet was discarded. Next, the protein concentration of the total extract samples was measured by using 1X Bradford Reagent (BioRad, #500-0006) to have an equal concentration of proteins per sample in the same volume (approximately 1 OD595 in the obtained volume).

For anti-TAP immunoprecipitation, IgG-Sepharose (GE Healthcare, # 17-0969-01) beads were first washed with 1 mL of 1X TAP Washing Buffer (25mM HEPES-HCI pH:8.0,

150mM NaCl, 0.1% NP-40) at 1000 rpm for 1 minute for 4-5 times. Then, the total extract was incubated with the washed beads for 3 hours at 4 °C with proper rotation. After the incubation, the beads were washed with 1X TAP Washing Buffer at 1000 rpm for 1 minute at 4 °C for 6-7 times. Then, the beads were incubated with TEV protease (BioVision, #7847) in 1X TEV Cleavage Buffer (50mM Tris-HCI pH:8.0, 0.1M NaCI, 5mM DTT) at 34 °C with gentle shaking. Afterwards, the elute was incubated with pre-washed Calmodulin Affinity Resin (Agilent #214303) in Calmodulin Binding Buffer (10mM β-mercaptoethanol, 25mM HEPES-HCI pH:8.0, 150mM NaCI, 1mM Magnesium acetate, 1mM Imidazole pH:8.0, 2mM Calcium chloride, 0.1% NP-40) for 1 hour at 4 °C with proper rotation. The beads were then washed with 1X Calmodulin Washing Buffer (20 mM Tris-HCl pH:8.0, 0.1% NP-40, 2mM Calcium chloride) at 1000 rpm for 1 minute at 4 °C for 6-7 times. Next, the beads were eluted with 720 µL of 1X Calmodulin Elution Buffer (20 mM Tris-HCI pH:8.0, 50mM NaCI, 5mM EGTA) at 23 °C for 25 minutes. The elute was stored at -20 °C before using.

For LC-MS/MS analysis, the samples were first concentrated using a vacuum concentrator (Thermo Scientific Savant SPD1010 SpeedVac). Then, the samples were denatured using HU-DTT in the equal volume and boiled at 65 °C for 15 minutes. Afterwards, the samples were loaded into SDS-PAGE to separate proteins according to their molecular weight, and the gel was incubated with Colloidal Coomassie Brilliant Blue overnight for staining. The gel was then destained with ddH2O and sent to the MS facility for LC-MS/MS analysis.

2.3.3 SDS-PAGE

Separation of proteins was performed using Sodium Dodecyl Sulphate (SDS)-Polyacrylamide Gel Electrophoresis (PAGE) method. SDS-PAGE gels were prepared by using Mini-Protean II gel system. The resolving gel was prepared by using the stock solutions of 1.5M Tris-HCl pH: 8.8, 10% (w/v) SDS, 6-15% polyacrylamide mixture (30%: 0.8% (w/v) Acrylamide:Bisacrylamide, Carl Roth, #3029.1), and polymerized using 10% (w/v) Ammonium persulfate (APS, Sigma #A3678) and TEMED (Sigma, #T7024). The stacking gel was prepared by using the stock solutions of 0.5M Tris-HCl pH: 6.8, 10% (w/v) SDS, 4% polyacrylamide mixture. Polymerization of the gels was obtained with 10% APS and TEMED.

The samples were loaded to the gels and the running (electrophoresis) was performed at 20 mA constant (20 mA per gel in a running tank) in 1X Laemmli Running buffer.

2.3.4 Western Blotting

After the protein samples were resolved by SDS-PAGE, they were transferred to a nitrocellulose membrane (Merck, GE10600002) in 1X Blotting Buffer for 2 hours at 0.1 A constant using Bio-Rad Mini-Trans-Blot transfer apparatus. After transfer was completed, the membrane was stained with Ponceau S visualizing the proteins on it to be sure the transfer was successful. Then, the lanes were marked, and the Ponceau S was destained using 1X PBS-T (0.02% Tween-20). The membrane was blocked using 5% non-fat dried milk (AppliChem, # A0830) prepared with 1X PBS-T for 1 hour at RT or overnight at 4°C with gentle shaking. The membrane was then incubated with 3 mL of primary antibody diluted in 1X PBS-T supplemented with 3% non-fat dried milk for 1 hour at RT or overnight at 4°C with gentle shaking. After the incubation, the membrane was washed 3 times with 1X PBS-T for 5 minutes each, and then incubated with 3 mL of respective secondary antibody diluted in 3% non-fat dried milk prepared with 1X PBS-T for 1 hour at RT. Secondary antibodies were Goat-anti-rabbit (Advansta #R-05062-500) or Goat-anti-mouse (Advansta #R-05071-500) conjugated with Horse Radish Peroxidase (HRP). Secondary antibodies were diluted 1:10000. After the incubation, the membrane was washed 3 times with 1X PBS-T for 5 minutes each. The membrane was developed, and the proteins on the membrane were visualized by exposing on X-ray films (Carestream Medical X-ray Green/MXG Film, #8116428) using home-made enhanced chemiluminescence (ECL).

2.4 ***Microscopy-based Methods***

All fluorescence microscopy methods were carried out using Carl ZEISS Axio Observer 7 motorized inverted epifluorescence microscope equipped with Colibri 7 LED light source, Axiocam 702 Monochrome camera, 100X and 63X Plan Apochromat immersion oil objective lenses, Filter sets 95 (GFP/Cherry), 20 (Rhodamin), FITC and DAPI, and an XL incubation and climate chamber. For analysis of DAPI, Tubulin-GFP, Bud14-GFP analysis 63X objective was used. For analysis of Bfa1-GFP, Bub2-GFP, Tem1-GFP and Mob1-GFP 100X objective was used.

2.4.1 Live-cell Imaging

For time-lapse experiments, cells were first attached to the glass center of glass bottom petri dishes (WVR 10810-054 Matsunami) covered 150 µL of 6% Concanavalin A (*Canavalia ensiformis* Jack Bean, type IV Sigma C2010-G) for 10 minutes at RT. Concanavalin A was taken back, and the excess was washed out using sterile ddH2O for 5 times. 150 µl of culture was pipetted on the dish followed by a 30 min incubation at 30 °C. Cells were then aspirated gently, and the dish was washed with pre-heated sterile medium for 5 times to remove the cells that were not attached on the dish. 3 mL of media was used to fill the dish after the final wash. The dish was then placed on the microscopy stage in the pre-heated chamber and left for 30 minutes in advance the start of the experiment.

2.4.2 Fixed-cell Imaging

For end-point analysis of the samples, 2 µl of culture were sandwiched between the coverslip and microscopy slide to prepare wet mount samples. Cells were either fixed using 70% Ethanol and stained with DAPI or analyzed live. For the Ethanol fixation, 700 µl of 100% Ethanol was mixed with 300 µl of the culture 300 µl culture followed by invert rotation. Fixed samples were stored at dark 4 °C until visualization. Prior to the staining, cell suspension was centrifuged at 3200 rpm for 2 minutes to get rid of Ethanol, and then the supernatant was aspirated. Afterwards, the pellet was resuspended in 10 µl of 1 mg/mL DAPI in 1X PBS (1:10000).

2.4.3 Image Analysis

All microcopy-based image analysis were performed using Image J. Graphs were plotted, and statistical results were computed by using Prism 8.0.1 (GraphPad, La Jolla, CA). Two-tailed t-test was used to find the statistical significance of the signal intensity measurements in a pair-wise manner. Chi-square test were applied for comparison of Bud14-GFP cortex localization. $p < 0.05$ or > 0.05 (ns) as indicated.

2.4.4 Quantifications of The Localization Based Fluorescence Signals

For signal intensity quantification of Bfa1-GFP, Bub2-GFP, Tem1-GFP, and Mob1-GFP, we took still images of live cells bearing SPC42-eqFP and mCherry-TUB1 as a mitotic marker. Each still image consisted of 13 z-stacks of 0.3 µm thickness. Z-stacks of the images were sum-projected, and mean fluorescence intensities were measured using Image J (NIH) software. To do so, a 0.577 µm2 (42 pixels) rectangle region was selected around the spindle pole body under inspection (ROI, region of interest) and the mean fluorescence intensity of the GFP signal was measured. An area outside the respective cell was measured to determine the background fluorescence intensity. The correction was done by subtracting the mean fluorescence intensity of the background from the mean fluorescence intensity of the ROI.

2.5 ***SPOC Functionality Assay***

For analyzing the functionality of SPOC, *kar9*Δ cells were first grown at 23 °C until the log-phase. After reaching the log-phase, the culture was shifted to 30 °C for 3-5 h. On the other hand, *dyn1*Δ cells were first grown at 30 °C until the log-phase. After reaching the log-phase, the culture was shifted to 18 °C overnight. After the temperature shift, cells were fixed using 70% Ethanol, and resuspended with 1 µg/ml DAPI in 1X PBS. Then, the cells were analyzed under fluorescence microscopy. Cells having normal and misaligned nuclei phenotypes, as well as cells with SPOC-deficient phenotypes including multinucleated cells were counted. SPOC functionality was assessed by calculating the SPOC deficiency index of the cell populations. SPOC deficiency index shows the ratio of cells with SPOC deficient phenotypes to cells with misaligned spindles. It was calculated using the following formula: SPOC deficiency index = (% SPOC deficient phenotypes) / (% misaligned spindle) X 10. For analyzing the functionality of SPOC in living cells, the duration of anaphase in normally aligned and misaligned cells were calculated. Anaphase duration was calculated by subtracting the time-point of metaphase-to-anaphase transition from the time-point of spindle breakdown.

2.6 *GLC7 Functionality Assay*

For the analysis of *GLC7* functionality, *GLC7* and *glc7-12* cells were grown at 23 °C until the log-phase. After reaching the log-phase, the culture was shifted to 30 °C, 33 °C, 35 °C and 37 °C for 4 hours for end-point analysis. After the temperature shift, cells were fixed using 70% Ethanol, and then resuspended in with 1 µg/ml DAPI in 1X PBS prior to microscopic visualization. Then, the cells were analyzed under fluorescence microscopy. All the cells were counted and categorized accordingly. For analyzing the functionality of *GLC7* by growth assay, the cultures were grown at 23 °C for 24-48 hours. OD600 value of all the yeast cultures, then, was adjusted to 1.0 using 1X sterile PBS. The cultures were serially diluted 10-fold using sterile 1X PBS. 7.5 µl of each serial dilutions were spotted on the appropriate agar plates (YPD and YPD containing 0.01M HU). The plates were incubated at the appropriate temperatures for 1-3 days.

Chapter 3: **AIM OF THE THESIS**

Lte1 is a mitotic exit activator which turns into being essential for mitotic exit at colder temperatures (<16 °C) (Shirayama et al., 1994). The viability of *lte1*Δ cells depend on the presence of the FEAR network to exit mitosis at the physiological temperatures (i.e., 30 °C). It has been shown that deletion of FEAR network components like *SPO12* or *SLK19* in *lte1*Δ cells results in synthetic lethality due to failure of mitotic exit (Stegmeier et al., 2002). This synthetic lethality of double mutants can be reverted in the absence of the known mitotic exit inhibitors *BFA1*, *BUB2* and *KIN4* (D'Aquino et al., 2005). Previously, it was shown in our lab that deletion of *BUD14* also rescues the synthetic lethality of *lte1*Δ*spo12*Δ double mutants (Kocakaplan D., 2020 Figure 3.1A). In addition, cold sensitivity of *lte1Δ* cells was also rescued by *BUD14* deletion (Kocakaplan D., 2020, Figure 3.1B).

These data suggest that Bud14 is a novel inhibitor of mitotic exit. In this thesis, we aim to characterize the molecular function of Bud14 in inhibiting exit from mitosis.

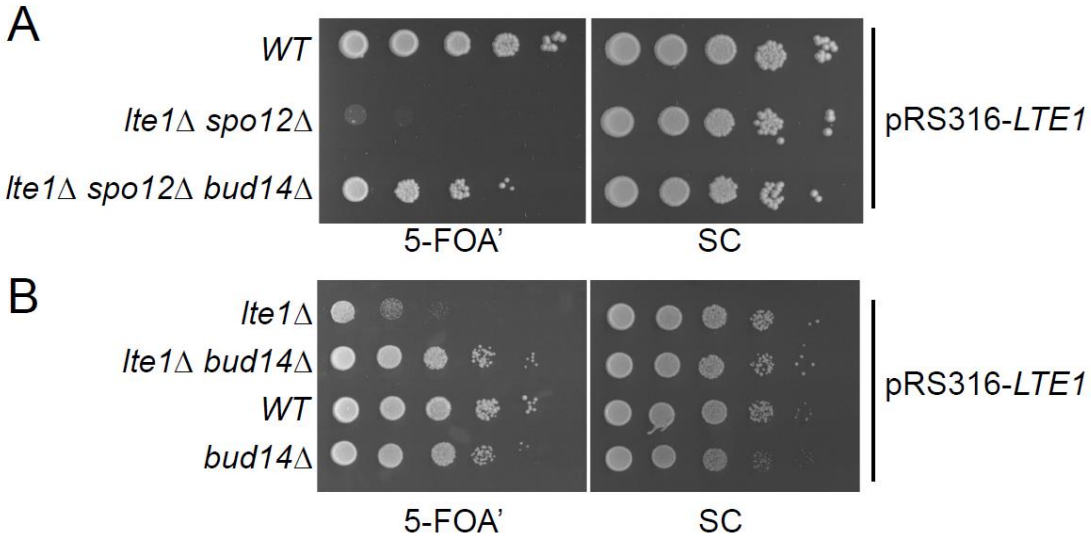

Figure 3. 1. Deletion of *BUD14* rescues the lethality of cells with impaired mitotic exit. A-B. Deletion of *BUD14* rescues the synthetic lethality of *lte1*Δ*spo12*Δ double mutant cells at 30 °C (A) and *lte1*Δ cells at colder temperatures at 16 °C (B). The strains were previously complemented with the plasmids bearing the wild-type copy of *LTE1*. 5-FOA plates are for negatively selecting the *URA3*-based plasmids (pRS316-*LTE1*). Therefore, only the growth of cells that have lost these plasmids is possible on 5-FOA plates where the genetic interactions can easily be tracked.

Chapter 4: **RESULTS**

4.1 ***Bud14 inhibits mitotic exit***

Previously in our lab, we identified *BUD14* as a mitotic exit inhibiting gene. Accordingly, deletion of *BUD14* rescued synthetic of mitotic exit deficient *lte1Δspo12Δ* cells (Kocakaplan D., 2020, Figure 3.1A). We hypothesized that deletion of *BUD14* should promote the growth of mitotic exit network (MEN) *ts* mutants if it is an inhibitor of mitotic exit. MEN is a signaling cascade required for exiting mitosis so that cells can down regulate M-CDK activity and return to the G1 phase, where later they can start a new cycle (Shirayama et al., 1994). Components of the MEN are essential genes. Therefore we made use of temperature sensitive (*ts*) alleles of MEN genes (Jaspersen et al., 1998), which allowed conditional inactivation of the gene function as the temperature raises. We deleted *BUD14* in different MEN-*ts* mutants and checked the growth phenotype at different temperatures. We also deleted *BFA1*, a known mitotic exit inhibitor, in those MEN-ts mutants to allow for comparison of the phenotype. Deletion of *BFA1* rescued the lethality of *mob1-67*, *dbf2-2, cdc15-1 and cdc5-10* ts mutants at 33 ^{o}C, 37 ^{o}C, 35 ^{o}C and 35 ^{o}C respectively (Figure 1A). Deletion of *BUD14* promoted the growth of *mob1-67*, *dbf2-2*, and *cdc15-1* mutants at 33 ^{o}C, 35 ^{o}C and 35 ^{o}C respectively (Figure 1A). Rescue by *BUD14* deletion was milder than that of *BFA1* deletion. Furthermore, *BUD14* deletion did not rescue the growth of the *cdc5-10* while *BFA1* deletion did (Figure 1A). Cdc5 is a polo-like kinase found at the very upstream of SPOC. It phosphorylates Bfa1 to inactivate it and as a result MEN is activated (Geymonat et al., 2003). Bud14 may be counteracting the activity of Cdc5 or acting on its target Bfa1; that could be the reason why *BUD14* deletion did not promote the growth of *cdc15-10* cells. *cdc14-2* mutant was not rescued by deletion of *BFA1* or *BUD14* (Figure 1A). Cdc14 is the essential phosphatase activated at the very downstream of the MEN pathway. The fact that the deletion of *BUD14* or *BFA1* does not rescue *cdc14-2* may indicate a role upstream of MEN pathway for Bfa1 and Bud14. Function of Bfa1 upstream of MEN is already well established (Pereira & Schiebel, 2005b).

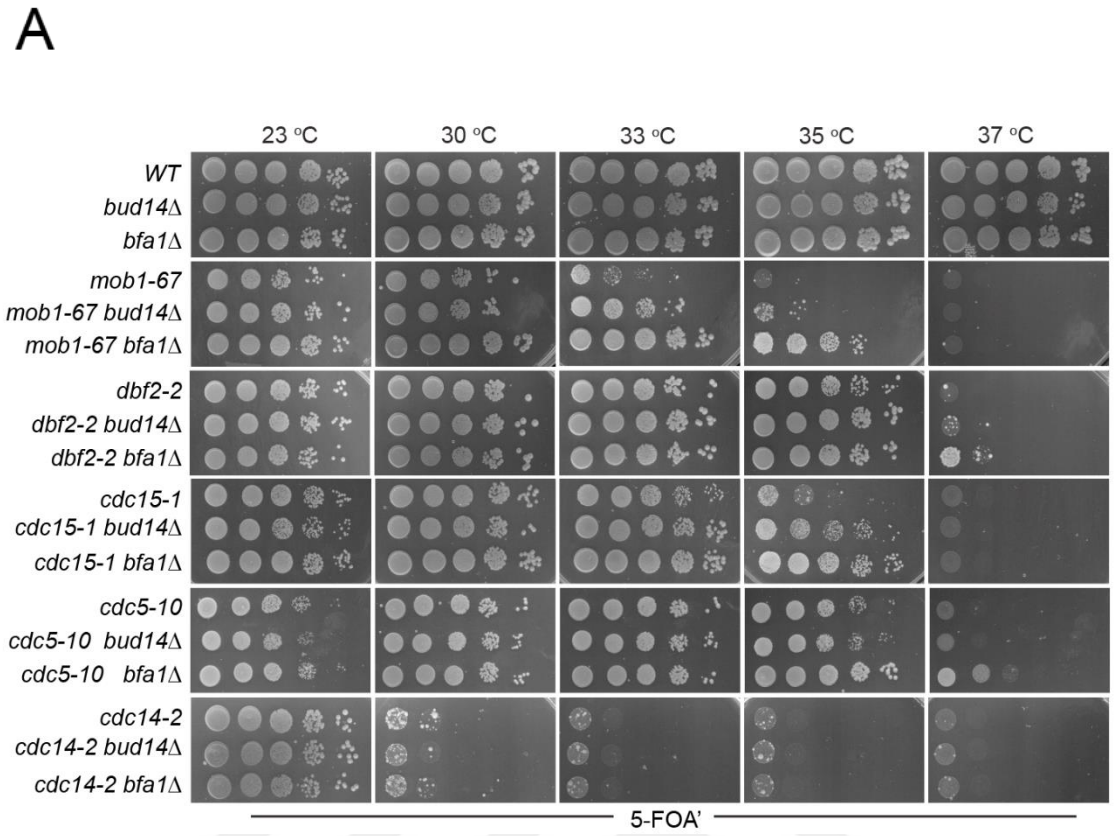

Figure 4. 1: Deletion of *BUD14* rescues the lethality of cells with impaired mitotic exit. A. Deletion of *BUD14* promotes the growth of *mob1-67*, *dbf2-2*, and *cdc15*-1 mutants at 33 °C, 35 °C and 35 °C respectively. Serial dilutions of indicated strains (YPH499, DKY056, HKY177, ESM2285, DKY058, HKY180, ESM2283, DKY060, AKY4095, ESM2282, DKY061, HKY182, JOY79, DKY179, HKY183, GPY491, DKY057, AKY4094) were spotted on the indicated plates. The plates then were incubated at given temperatures for 2-3 days. All the MEN-ts strains were previously complemented with the plasmids bearing the wild-type copy of the corresponding ts allele. 5-FOA plates are for negatively selecting the *URA3*-based plasmids (pRS316 together with the wild type gene copy of the corresponding MEN mutation). Therefore, only the growth of cells that have lost these plasmids is possible on 5-FOA plates where the genetic interactions can easily be tracked.

4.2 *BUD14 deletion causes SPOC deficiency*

The elements of bipartite GTPase activating complex (GAP), Bfa1 and Bub2, and the SPOC kinase Kin4 are known to be the key components of the Spindle Position Checkpoint (SPOC). This checkpoint prevents cell cycle progression by inhibiting MEN in the presence of spindle mispositioning at anaphase. Thus, we wanted to check if Bud14 has a role in SPOC. To answer this question, we examined the activity of SPOC in *bud14*Δ cells. Firstly, we needed to create a *kar9*Δ background to induce spindle misalignment. Kar9 (Adenomatous Polyposis Coli (APC) homolog, a tumor suppressor in mammalian

cells) is a microtubule and actin associated protein. It links the astral microtubules with the actin cables, that ensures the proper alignment of the mitotic spindle in the mother-to-daughter polarity axis (Rita K. Miller & Rose, 1998). It was previously shown that *KAR9* deletion induces spindle misalignment at the temperature of 30 °C and above (Miller & Rose, 1998). However, the misaligned spindle of these cells can still be corrected by the help of another spindle positioning pathway dependent on Dynein, a minus-end directed motor protein (Li et al., 1993). Cells with functional SPOC are arrested at anaphase in the presence of spindle misalignment, while cells having SPOC deficiency are able to continue cell cycle progression, giving rise to the formation of multinucleated or enucleated cell populations. SPOC functionality was assessed by calculating the SPOC deficiency index of the cell populations. SPOC deficiency index shows the ratio of cells with SPOC deficient phenotypes to cells with misaligned spindles. We observed that deletion of *BFA1* and *KIN4* resulted in a significant increase in the SPOC deficiency index in *kar9*Δ background as expected (Figure 2A). Deletion of *BUD14* also caused an increase in SPOC deficiency index, which suggests that Bud14 has a role in the maintenance of ploidy upon spindle mispositioning (Figure 2A). We also observed that the index was the highest in *bfa1*Δ cells. Bfa1 is the main SPOC effector protein; therefore, it is expected to observe the highest SPOC deficiency index in *bfa1*Δ cells. Also, deletion of *BUD14* did not increase the percentage in *bfa1*Δ background. This may suggest that Bud14 might act in the same pathway with Bfa1. Interestingly, we also observed that the increase in the SPOC deficiency index was greater in the double mutant *bud14*Δ*kin4*Δ than in either of the single mutants *bud14*Δ and *kin4*Δ. This result suggests that Bud14 and Kin4 work in parallel to each other (Figure 2A).

It has been shown that Bud14 has a regulatory role in dynein activity at the bud cortex (Knaus et al., 2005). Thus, we wanted to check whether the reason of the increase in the SPOC deficiency phenotype in *bud14*Δ*kar9*Δ cells was due to the lack of Dynein activity which in turn would prevent re-aligning of the anaphase spindle. Thus, if this is the case, we hypothesized that there should not be a significant increase in the cells with SPOC deficient phenotype in a background lacking Dynein activity. For this purpose, we used *dyn1*Δ cells that lack the heavy chain of Dynein. We observed that there was a significant increase in the SPOC deficiency index in *bud14*Δ*dyn1*Δ cells compared to the wild-type cells (Figure 2B). Also, as expected, we observed a similar trend in *kin4*Δ*dyn1*Δ cells (Figure 2B). Similar to the experiment in the *kar9*Δ background, SPOC deficiency index

of the double mutant *bud14*Δ*kin4*Δ was greater than the single mutants *bud14*Δ and *kin4*Δ (Figure 2B). All in all, these data indicate that *bud14*Δ cells are SPOC deficient independently of Bud14 function in Dynein activation and the role of Bud14 in SPOC is likely parallel to that of Kin4.

Next, we wanted to check the timing of mitotic exit in *bud14*Δ cells with normally aligned and misaligned anaphase spindles. To monitor anaphase duration, we monitored the mitotic spindle. For this, we used cells in which Tubulin was tagged with GFP. We performed the experiment in a *kar9*Δ background to simultaneously observe cells with misaligned spindles and cells with normally aligned spindles. Logarithmic phase cultures bearing corresponding gene manipulations were shifted to 30 ^{o}C, and then imaged under fluorescence time-lapse microscopy every 1 minute for 90 minutes. To calculate the duration of anaphase, the time elapsed between the start of fast spindle elongation and the spindle breakdown, which are indications of anaphase onset and mitotic exit respectively, was used. As expected, while the misaligned anaphase spindle of *kin4*Δ*kar9*Δ cells was observed to be broken, most of the *kar9*Δ cells with misaligned spindles were kept arrested with an intact spindle during the time-lapse movie (Figure 2C, *kar9*Δ red triangles vs *kar9*Δ*kin4*Δ black squares). We observed that the spindle of *bud14*Δ*kar9*Δ cells with misaligned spindles was also broken, which indicates that these cells are SPOC deficient (Figure 2C, *kar9*Δ*bud14*Δ, black squares). Interestingly, we detected that the timing of spindle breakage of misaligned cells was almost same as normally aligned cells in *bud14*Δ*kin4*Δ background, whereas the timing in single mutants *bud14*Δ and *kin4*Δ was slightly higher during spindle misalignment than normal alignment. Hence, we can say these data support the idea that Bud14 and Kin4 work in parallel to each other to regulate SPOC. These data altogether show that Bud14 functions as a part of SPOC, that arrests the cells in anaphase in the presence of spindle misalignment.

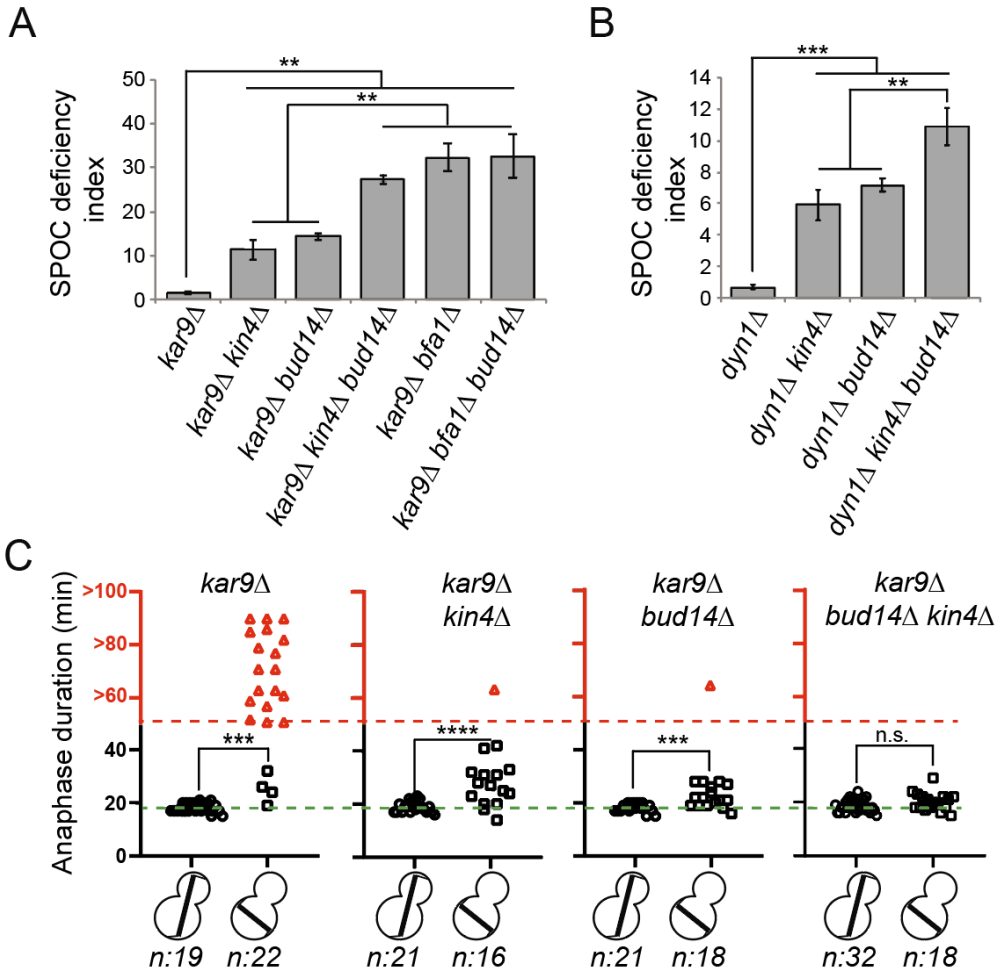

Figure 4. 2: Deletion of Bud14 causes SPOC deficiency phenotype upon spindle mispositioning. A-B. SPOC deficiency index of the indicated yeast strains in *kar9*Δ (A) and *dyn1*Δ (B) backgrounds (AKY260, AKY321, SEY032, AKY4068, AKY315, HKY175; SHM562, ESM2156, AKY2917, AKY2918). Logarithmically growing cells were shifted to 30 °C and then fixed with ethanol. Fixed cells were stained with DAPI and visualized under fluorescence microscopy. Graphs were plotted with the average of percentages of three independent experiments. A minimum of 100 cells were counted from each strain in each experiment. Data are represented as mean ± SEM. Error bars show standard deviation. **C.** Single cell analysis of SPOC functionality in the indicated strains (AKY346, AKY351, SEY032, AKY4068). Anaphase duration of cells with misaligned and normally aligned spindles was calculated and plotted as dot-plots. How the timing was calculated is shown in the cartoon on the right side. Red data points represent the cells with intact spindle during the time lapse movie. In this case, plotted values are the time duration when these cells were observed in anaphase through the time lapse movie. Hence, the actual anaphase duration is greater than the value plotted in the graph, emphasized in the red part of the y-axis, indicated above the red dashed line, with addition of the ">" symbol. Green dashed line shows the mean value of the duration of anaphase in cells with normally aligned spindles. Significancy analysis was performed using students' t-test. **: $p<0.001$, ***: $p<0.0001$, ****: $p<0.00001$, n.s. $p>0.05$ n: sample size.

4.3 *SPOC regulatory function of Bud14 is not dependent on its formin regulatory role*

It has been previously found that Bud14 plays a role in inhibition of the yeast formin, Bnr1, and this function of Bud14 is important for the proper architecture and function of actin cables. It displaces Bnr1 FH2 domain from growing barbed ends, inhibiting actin polymerization to regulate the length of filament. It regulates actin cable formation through its formin-regulatory motif (amino acids 135-150) (Chesarone, Gould, Moseley, & Goode, 2009). In our lab, it was previously shown that a mutant version of Bud14 (*bud14-5A*) that lacks the formin regulatory function is functional in terms of mitotic exit inhibition (Kocakaplan D., 2020, Data not shown). The formin-regulatory motif is disrupted in this mutant by substituting five alanine amino acids at the residues found at 135 and 137–140 on Bud14 (Eskin, Rankova, Johnston, Alioto, & Goode, 2016). When this form of Bud14 was expressed on a centromeric plasmid, it rescued the SPOC deficient phenotype in *bud14*Δ*kar9*Δ and *lte1*Δ*bud14*Δ backgrounds (Kocakaplan D., 2020). These findings suggest that the role of Bud14 in mitotic inhibition is independently of its role in formin regulation.

Here, we revisited the role of Bud14 in actin regulation using different mutants. Bud14 functions together with Kel1 and Kel2 in controlling Bnr1-mediated actin cable formation as well as polarized cell growth, and cytokinesis (Gould et al., 2014). Kel1 and Kel2, or Kelch proteins, associate with Bud14, and they altogether form a stable 520-kDa complex with a stoichiometry of 2:2:1 Bud14/Kel1/Kel2 (Gould et al., 2014). These proteins are shown to colocalize to the polarity site interdependently (Gould et al., 2014). We wanted to check whether SPOC regulatory function of Bud14 is dependent on its actin regulatory role via the Kel1-Kel2-Bud14 complex. We hypothesized if Bud14/Kel1/Kel2 complex is important for SPOC functionality, deletion of *KEL1* or *KEL2* should cause SPOC deficiency like *bud14*Δ cells. To address this question, we analyzed the functionality of SPOC in *kel1*Δ and *kel2*Δ cells upon spindle misalignment. However, *kel1*Δ*kar9*Δ or *kel2*Δ*kar9*Δ cells did not display an increase in SPOC deficiency index (Figure 3A). This data indicates that the function of Bud14 in the regulation of SPOC is independent of its role in controlling the formation of actin cables via the Bud14/Kel1/Kel2 complex.

We next asked whether deletion of *KEL1* or *KEL2* rescue the lethality of *lte1*Δ*spo12*Δ double mutants and the cold sensitivity of *lte1Δ* cells as deletion of *BUD14* does. We observed that the cold sensitivity of *lte1*Δ background was rescued by *KEL1* deletion which was also reported earlier by others (Höfken & Schiebel, 2002) (Figure 3B). In contrast to *KEL1* or *BUD14* deletion, only a minor rescue in the cold sensitivity of *lte1*Δ was observed when *KEL2* was deleted (Figure 3B). *KEL1* deletion also rescued lethality of *lte1*Δ*spo12*Δ cells but to a much lesser extent than deletion of *BUD14* (Figure 3B). Deletion of *KEL2*, however, did not rescue *lte1*Δ*spo12*Δ synthetic lethality. In line with previous research findings, these data indicate a mitotic exit inhibitory function of *KEL1* and to some extend for *KEL2* (Höfken & Schiebel, 2002; Geymonat, Spanos, Jensen, & Sedgwick, 2010). Thus, our data is in line with previous reports that Kel1 and Kel2 has a mitotic inhibitory function (Geymonat et al., 2010). But our data further indicate that the mitotic exit inhibitory function of Kel1 and Kel2 is different from that of Bud14.

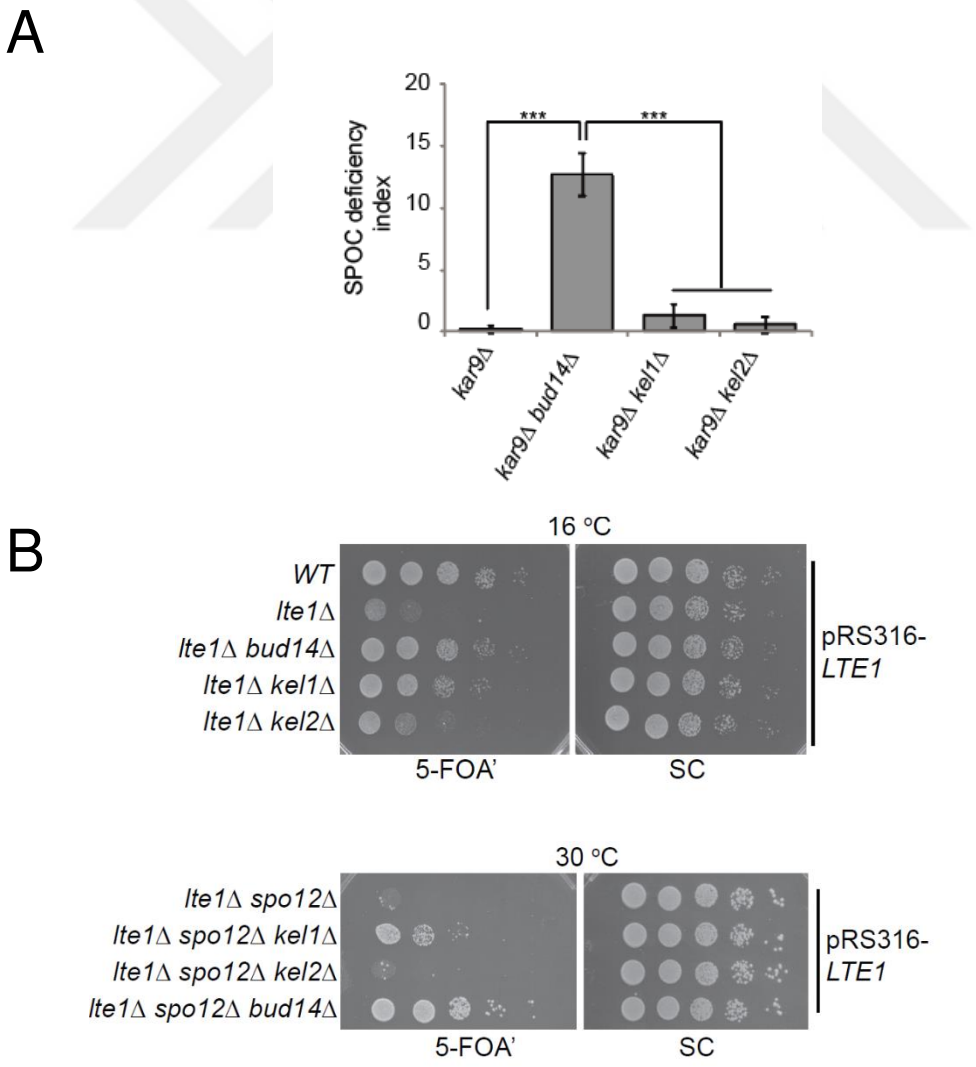

Figure 4. 3: Formin regulatory function of Bud14 does not account for its role in SPOC. A. End-point analysis of SPOC functionality of the indicated strains (AKY260, YDA101, HKY130, HKY140). Temperature shifted cells were first fixed with ethanol and then stained with DAPI. Fixed cells, afterwards, were counted by microscopy and their percentages were plotted. Graphs are average of three independent experiments. A minimum of 100 cells were counted from each strain in each experiment. Error bars show standard deviation. **B.** The indicated strains bearing *LTE1* on *URA3*-based *pRS316* plasmid were first serially diluted (ESM356, FAY145, DKY069, HKY133, HKY134; AKY2526, HKY135, HKY136, AKY2916). Then, each dilution of each strain was spotted on 5-FOA and SC plates and grown at indicated temperatures. 5-FOA negatively selects for *URA3* containing plasmids, therefore cells lose their pRS316-*LTE1* plasmids on 5-FOA plates and genetic interactions can be observed on this plate.

4.4 *Bud14 inhibits mitotic exit through its interaction with Glc7*

Bud14 is known to be a regulatory subunit of the type I Protein phosphatase (PP1) Glc7 in budding yeast (Knaus et al., 2005). Therefore, we asked if Bud14 performs its mitotic exit inhibitory role through Glc7. To address this question, we impaired Glc7-Bud14 interaction using a mutant version of Bud14 that is unable to bind Glc7 (Bud14-F379A) (Knaus et al., 2005). Previously, in our lab, it was observed that deletion of *BUD14* rescued the growth of *lte1*Δ cells at 16 ºC (Figure 3.1B) . Introducing wild type *BUD14* but not the *bud14-F379A* mutant into *lte1*Δ*bud14*Δ cells restored cold sensitivity of *lte1*Δ cells (Kocakaplan D., 2020, Data not shown). We concluded that Glc7-Bud14 interaction is essential for mitotic exit inhibitory function of Bud14.

Next, we used a temperature sensitive *GLC7* mutant *glc7-12 (glc7-ts)* (Andrews & Stark, 2000) to investigate whether Bud14-Glc7 interaction is important for SPOC regulatory function of Bud14. We observed that the SPOC deficiency index was increased in both *glc7-ts kar9*Δ and *bud14-F379A kar9*Δ cultures, meaning that these cells have accumulated multinucleated cells (Figure 4A). This data indicates SPOC regulatory function of Bud14 is dependent on its interaction with Glc7.

It has been reported that the temperature sensitive allele of *GLC7,* which is *glc7-10*, accumulated a population of large budded cells with an unmigrated nucleus at 37 ºC (Andrews & Stark, 2000). In our lab, it was previously shown that *glc7-12* mutant has partially rescued the synthetic lethality of *lte1*Δ*spo12*Δ at 33 ºC even though *BUD14* is functional (Kocakaplan D., 2020). This indicates that the interaction between Bud14 and Glc7 is necessary for the SPOC regulatory function of Bud14 if *glc7-12* is partially inactive at 33 ºC. Thus, we wanted to check whether *glc7-12* is partially inactive at the same temperature at which the partial rescue was observed. To address this question, we

performed a temperature shift assay, and observed the phenotype of the cells. We observed that the percentage of large-budded cells with unmigrated nucleus was increased with the temperature in *glc7-12* cells as opposed to *GLC7* cells (Figure 4B). Most of the *glc7-12* cells were dead at 37 ^{o}C, thus we could not count the phenotype at this temperature (Data not shown). Therefore, we can conclude that *glc7-12* is partially inactive at 33 ^{o}C, and Bud14-Glc7 interaction is needed for the functionality of SPOC in the presence of misalignment. It is known that Hydroxyurea (HU) treatment results in dNTP depletion, causing replication for stalling and the activation of DNA damage checkpoint (Zegerman & Diffley, 2009). It was previously shown that Glc7 is important for removing the phosphorylated Rad53, that is essential for recovery from HU-induced S phase replication fork stalling (Bazzi et al., 2010). It was shown that *glc7* mutants were hypersensitive to HU treatment, showing that Glc7 contributes to cell viability upon replicative stress (Bazzi, Mantiero, Trovesi, Lucchini, & Longhese, 2010). Therefore, we asked if *glc7-12* mutants are sensitive to HU treatment to further ensure our strain is a *glc7-ts* mutant. To do so, we performed a growth assay in the presence of HU and checked the growth phenotype of *glc7-12* cells at different temperatures. We observed that as opposed to *GLC7* cells, the viability of *glc7-12* cells was gradually decreased at the temperatures above 30 ^{o}C in the presence of HU (Figure 4C). Importantly, the viability of *glc7-12* cells was drastically reduced at 35 ^{o}C and completely lost at 37 ^{o}C regardless of the HU treatment (Figure 4C). This further supports that *glc7-12* cells are sensitive to higher temperatures. These data altogether indicate that glc7-12 is a temperature sensitive allele of GLC7, and it leads to formation of large- budded cell populations with unmigrated nucleus as well as sensitivity to the presence of HU.

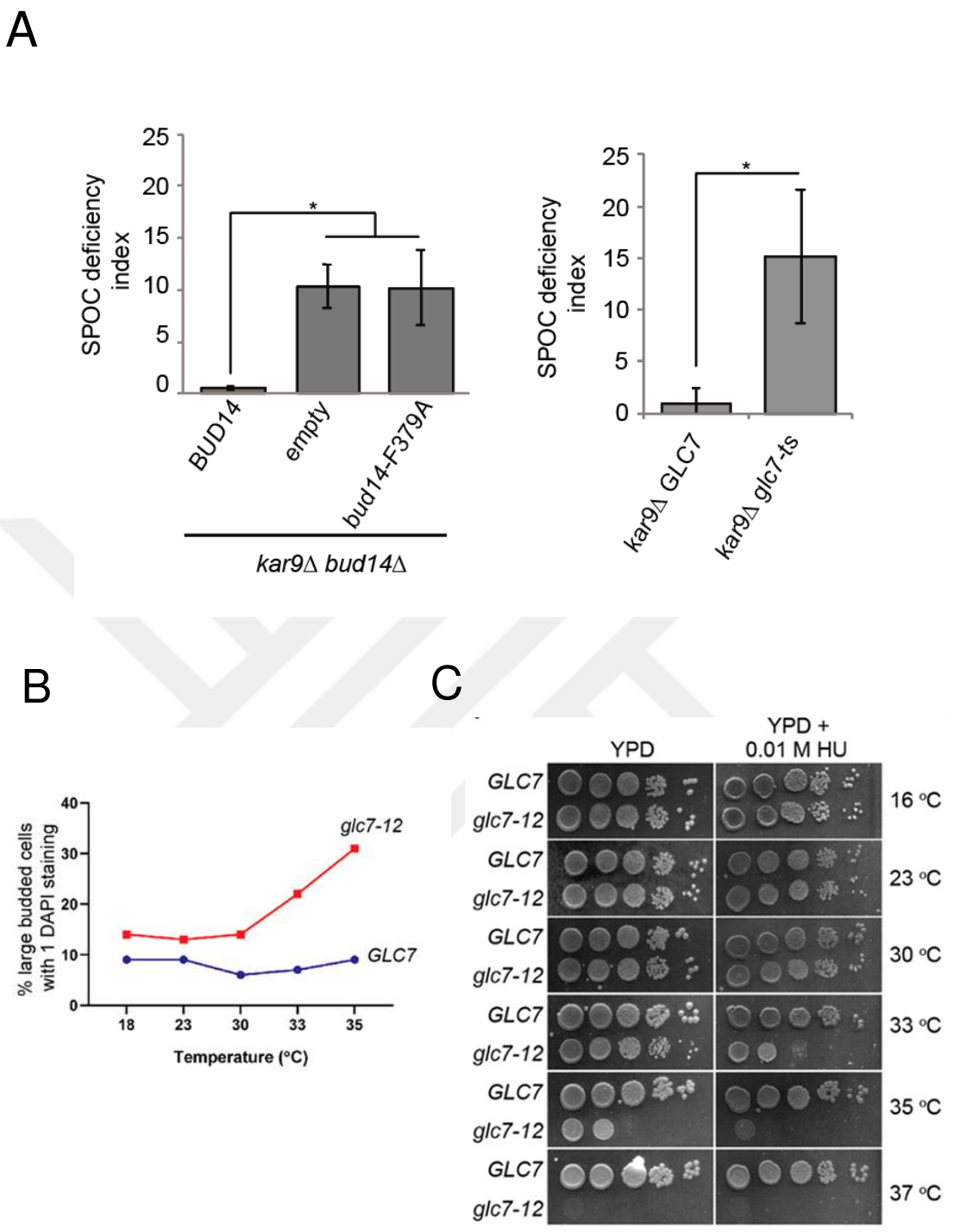

Figure 4. 4: Bud14 inhibits mitotic exit though its interaction with Glc7. A. End-point analysis of SPOC functionality of the indicated strains (DKY145, DKY147, DKY149; AKY4078, AKY4079). Temperature shifted cells were first fixed with ethanol and then stained with DAPI. Fixed cells, afterwards, were counted by microscopy and their percentages were plotted. Graphs are average of three independent experiments. A minimum of 100 cells were counted from each strain in each experiment. Error bars show standard deviation. **B.** End-point analysis of *GLC7* functionality of the indicated strains (DKY070, DKY071). Temperature shifted cells were first fixed with ethanol and then stained with DAPI. Fixed cells, afterwards, were counted by microscopy and their

percentages were plotted. A minimum of 100 cells were counted from each strain. **C.** *glc7-12* mutant is sensitive to HU-induced S phase arrest. Serial dilutions of indicated strains were spotted on the indicated plates (DKY070, DKY081). The plates then were incubated at given temperatures for 2-3 days.

4.5 *More Bfa1 localizes to SPBs in the absence of BUD14.*

The functionality of SPOC is strongly dependent on the change in SPB localization of Bfa1-Bub2 complex. Bfa1-Bub2 complex preferentially localizes to daughter SPB (dSPB) during anaphase in the presence of a normally positioned spindle (Pereira et al., 2000). In the presence of spindle misalignment, however, Bfa1-Bub2 complex dissociates from dSPB, resulting localization of low levels of Bfa1-Bub2 at both SPBs (Caydasi & Pereira, 2009). Thus, we wanted to check if this unique localization phenotype of Bfa1-Bub2 changes in the absence of *BUD14*. To address this question, we tracked the SPB-bound levels of Bfa1-GFP in wild type and *bud14*Δ cells with normally aligned anaphase spindles (spindle length >3µm) (Figure 5A). We detected that the localization of Bfa1-GFP increased at SPBs in *bud14*Δ cells when compared to wild type cells. We also noticed that this difference was more pronounced at the dSPB.

Next, we hypothesized that if the change in the localization of Bfa1-GFP is due to the absence of *BUD14*, then increased Bfa1 localization should return to the wild type cells when *BUD14* is given back on a plasmid. To do so, we performed the same experiment with *BUD14* complemented cells in wild type and *bud14*Δ backgrounds. Importantly, we observed that increased Bfa1-GFP signal at the dSPB of *bud14*Δ cells returned to wild type levels when *BUD14* was introduced back (Figure 5B). Therefore, these data altogether show that Bud14 restricts the localization of Bfa1 to the SPBs at anaphase. We have shown that the interaction of Bud14 with Glc7 is essential for SPOC functionality. Thus, we wanted to check if Bud14-Glc7 interaction is required for limiting the SPB-bound levels of Bfa1. To address this question, we performed the same experiment with cells complemented either with *BUD14* or *BUD14-F379A* in *bud14*Δ background (Figure 5C). We observed that increased Bfa1-GFP signal at the dSPB of *bud14*Δ cells was reduced when *BUD14* was introduced back. However, the signal did not significantly change when the plasmid bearing *BUD14-F379A* was given back. These data altogether indicate that Bud14 restricts the localization of Bfa1 to the SPBs at anaphase, and this requires Glc7 interaction.

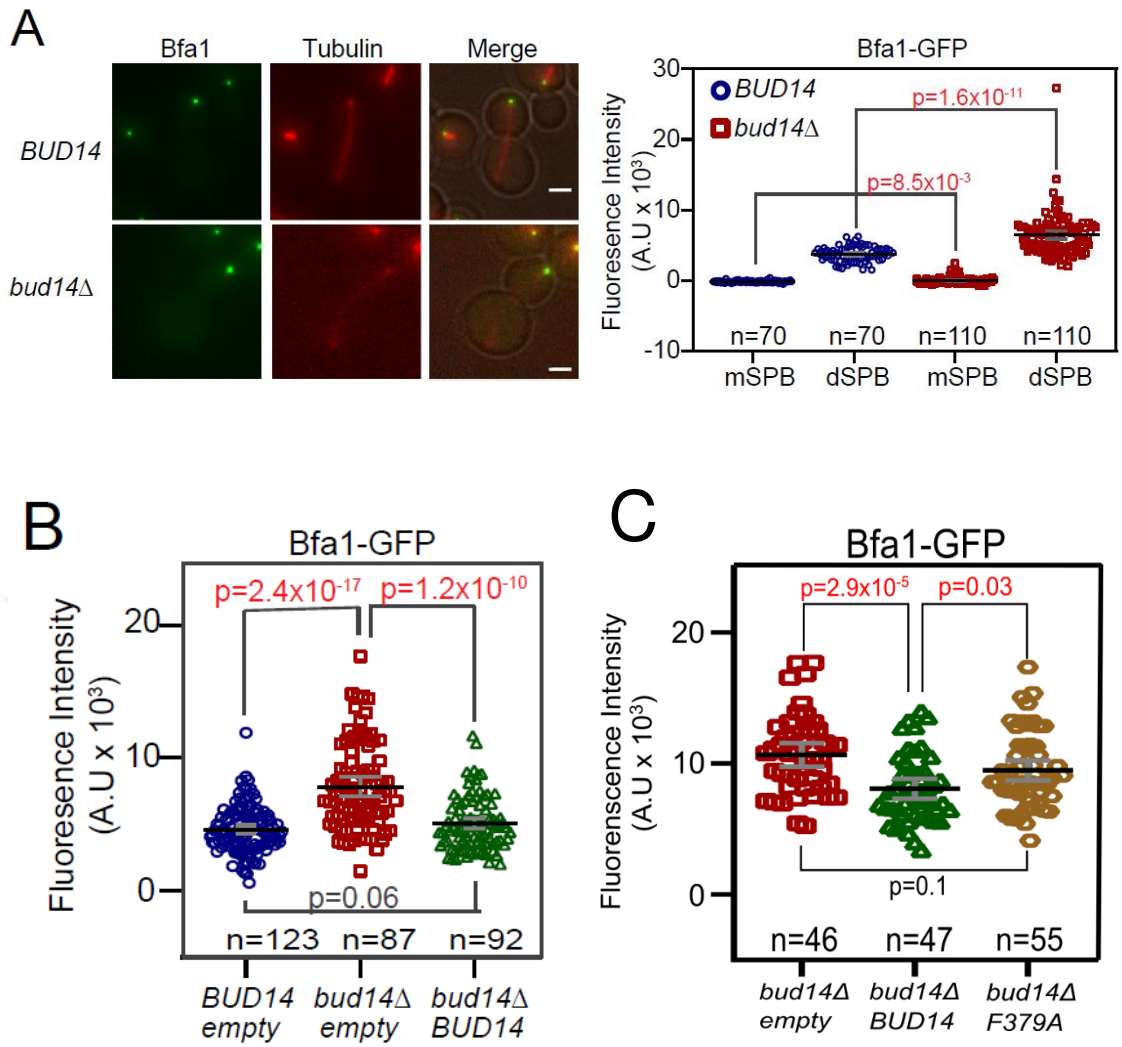

Figure 4. 5: SPB localization of Bfa1 increases in the absence of BUD14. A. Quantification of Bfa1-GFP signal intensity at the SPBs of *BFA1*-GFP mCherry-*TUB1* or *BFA1*-GFP mCherry-*TUB1 bud14*Δ cells (AKY4011, AKY4012). The signal intensity of Bfa1-GFP with normal aligned anaphase spindles was measured and then plotted on the right. Black lines represent the mean value, and grey lines show standard deviation. Representative still images of cells were shown on the left. **B.** Bfa1-GFP signal intensities at the dSPB were plotted in *BUD14* and *bud14*Δ cells bearing empty plasmid (blue and red), as well as *bud14*Δ cells bearing a *BUD14* containing plasmid (green) (HKY114, HKY115, HKY116). **C.** Bfa1-GFP signal intensities at the dSPB were plotted in bud14Δ cells bearing empty plasmid (red), a *BUD14* containing plasmid (green) and *bud14-F379A* plasmid (yellow) (HKY115, HKY116, HKY190). Pairwise comparisons of intensities among indicated strains were performed using Students' t-test. p-values were shown on the graph. n: sample size. Scale bar: 2 µm.

4.6 *In the absence of BUD14, More Bfa1-Bub2 and Tem1 localizes at the SPBs in both metaphase and anaphase*

Bfa1 associates with Bub2 to form a bipartite GAP that regulates the activity of Tem1 (Geymonat et al., 2002). Bfa1-Bub2 also recruits Tem1 at the SPBs (Molk et al., 2004). Thus, we asked whether SPB-bound levels of Bub2-GFP and Tem1-GFP also change similar to Bfa1 levels in the absence of *BUD14*. We observed that dSPB-bound levels of Bub2-GFP and Tem1-GFP was higher in *bud14*Δ cells than wild type cells in anaphase (Figure 5A). Thus, not only Bfa1 but also Bub2 and Tem1 levels are increased at SPBs in the absence of *BUD14* during anaphase. We also analyzed the effect of *BUD14* deletion on the localization of Bfa1-Bub2 and Tem1 during metaphase. We observed that, similar to the cells in anaphase, absence of *BUD14* caused an increase in SPB-bound levels of Bfa1-Bub2 and Tem1 before anaphase onset (spindle length = 1,5-2 µm) (Figure 6B). These data indicate that Bud14 deletion increases the SPB-bound levels of Bfa1-Bub2 and Tem1, and such increase is not restricted to anaphase but also present in metaphase.

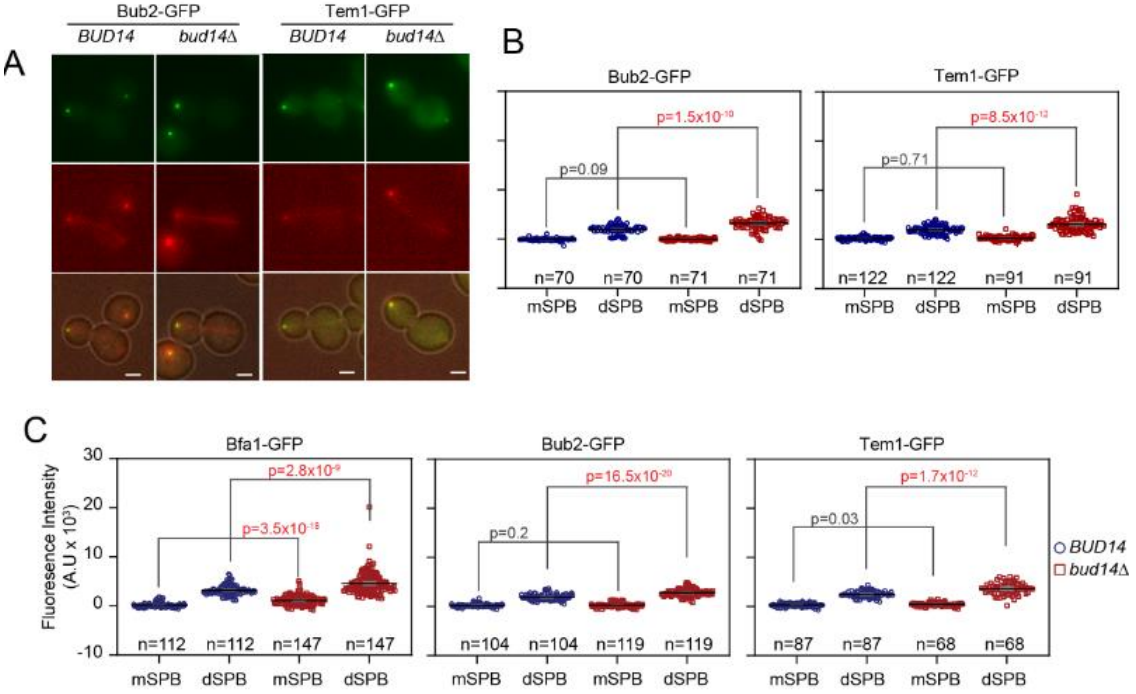

Figure 4. 6: Deletion of Bud14 results in an increase in the SPB-localization of Bfa1-Bub2 and Tem1. A. Representative still images of cells were shown (AKY4007, AKY4008, AKY4009, AKY4013). **B.** Bub2-GFP and Tem1-GFP signal intensity quantifications at the SPBs in cells with normal aligned anaphase spindles in wild type and *bud14*Δ background were plotted (AKY4007, AKY4008, AKY4009, AKY4013). Black and grey lines in the dot plots are the mean value and standard deviation, respectively. **C.** SPB-bound signal intensity quantification of Bfa1-GFP, Bub2-GFP and

Tem1-GFP in cells with metaphase spindles (spindle length = 1,5-2 µm). Graph is plotted as described in A. Pairwise comparisons of intensities among indicated strains (AKY4007, AKY4008, AKY4009, AKY4011, AKY4012, AKY4013). were performed using Students' t-test. p-values were shown on the graph. n: sample size. Scale bar: 2 µm.

4.7 *Deletion of BUD14 does not affect Mob1 localization*

Mob1, a regulatory protein associating with Dbf2, is essential for the phosphorylation of Dbf2, a very downstream event of MEN. Dbf2-Mob1 localizes first to both SPBs in anaphase, and then moves to the bud neck just before the actin assembly (Yoshida & Toh-e, 2001). It has been previously shown that Mob1 localizes to SPBs in metaphase in the absence of *BFA1* (Pereira, Manson, Grindlay, & Schiebel, 2002; Caydasi et al., 2012). Importantly, Mob1 localization at the SPBs can also be used as marker for MEN activity (Pereira et al., 2002). We have found that deletion of *BUD14* affects the SPB-bound levels of Bfa1. Thus, we wanted to check whether the SPB-bound levels of Mob1-GFP changes in metaphase and anaphase upon *BUD14* deletion. To address this question, we tracked the SPB-bound levels of Mob1-GFP in wild type and *bud14*Δ cells with metaphase spindles (1.5 µm<spindle length<3µm), and with normally aligned anaphase spindles (spindle length >3µm). We detected that Mob1 localized to both SPBs in metaphase in *bfa1*Δ cells, but no metaphase localization was detected in *bud14*Δ and *kin4*Δ cells (Figure 7A). Next, we hypothesized that Kin4 and Bud14 may act together on the localization of Mob1. If this is the case, then we would expect to see SPB localization of Mob1 in metaphase in *bud14*Δ*kin4*Δ cells. We observed that there was no SPB localization of Mob1-GFP in metaphase cells of *bud14*Δ *kin4*Δ background (Figure 7A). Also, there was no change in the SPB-bound levels of Mob1-GFP signal in *bud14*Δ in anaphase (Figure 7B). These data altogether indicate that deletion of *BUD14* does affect neither the SPB localization of Mob1 in metaphase nor the SPB-bound levels of Mob1 in anaphase. Thus, similar to Kin4, Bud14 does not inhibit the MEN in cells with normally aligned spindles.

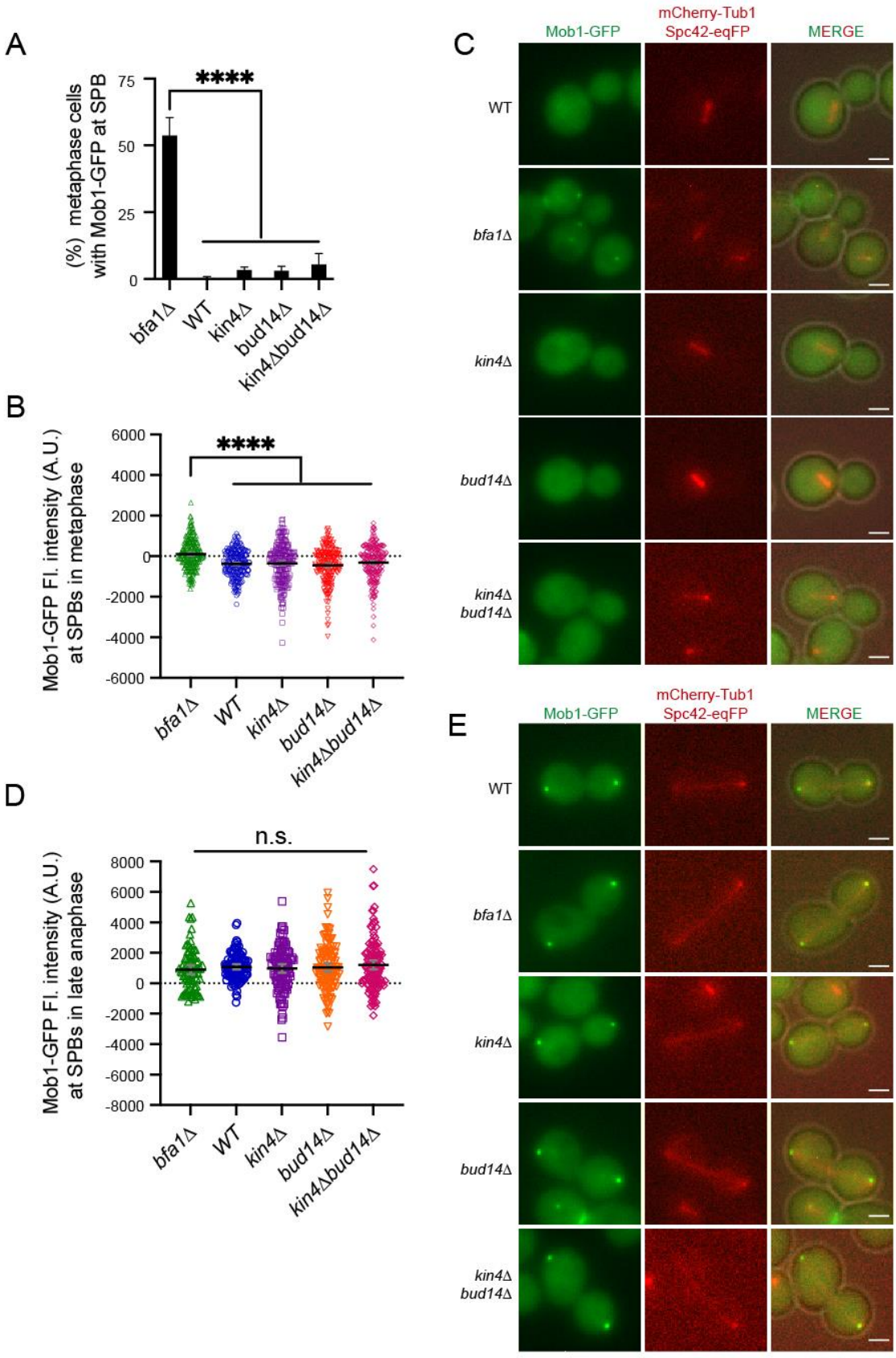

Figure 4. 7: The SPB-localization of Mob1 does not change in the absence of Bud14. **A.** Percentage of metaphase cells with Mob1-GFP signal at the SPBs of the indicated cells (HKY171, HKY171, HKY173, HKY174, AKY4112). Cells were counted by microscopy

and their percentages were plotted. Graphs are average of three independent experiments. A minimum of 100 cells were counted from each strain in each experiment. Error bars show standard deviation. **B.** Quantification of Mob1-GFP signal intensity at the SPBs of Mob1-GFP mCherry-*TUB1* cells and Mob1-GFP mCherry-*TUB1* in *bfa1*Δ, *kin4*Δ, *bud14*Δ and *kin4*Δ*bud14*Δ backgrounds. The signal intensity of Mob1-GFP at the SPBs of cells with a metaphase spindle was plotted. Black lines represent the mean value, and grey lines show standard deviation. Pairwise comparisons of intensities among indicated strains were performed using Students' t-test. p-values were shown on the graph. **C.** Quantification of Mob1-GFP signal intensity at the SPBs of Mob1-GFP mCherry-*TUB1* cells and Mob1-GFP mCherry-*TUB1* in *bfa1*Δ, *kin4*Δ, *bud14*Δ and *kin4*Δ*bud14*Δ backgrounds. The signal intensity of Mob1-GFP at the SPBs of cells with anaphase spindle was plotted. Black lines represent the mean value, and grey lines show standard deviation. The signal intensity of Mob1-GFP in cells with normally aligned anaphase spindles was measured and then plotted. Pairwise comparisons of intensities among indicated strains were performed using Students' t-test. p-values were shown on the graph. **D.** Representative still images of metaphase cells. **E.** Representative still images of anaphase cells n: sample size. Scale bar: 2 µm.

4.8 *SPOC regulatory function of Bud14 is parallel to the Kin4 branch of SPOC*

Upon spindle mispositioning, Kin4 phosphorylates Bfa1, increasing the turnover rate of Bfa1-Bub2 complex at SPBs (Pereira & Schiebel, 2005a). Kin4 phosphorylation creates a docking site on Bfa1 Bmh1 binds. Recruitment of Bmh1 onto Bfa1 causes the displacement of it from the SPBs, providing the symmetric Bfa1 localization upon spindle mispositioning (Caydasi et al., 2014). Consequently, SPB localization of Bfa1-GFP changes from asymmetric (more at the dSPB than mSPB) to more symmetric (similar at both SPBs) upon spindle mispositioning. Thus, we wanted to check whether Bfa1 localization changes from asymmetric to symmetric levels in cells with misaligned anaphase spindles in the absence of *BUD14*. To measure the asymmetry index of Bfa1 signal at SPBs, the ratio of Bfa1-GFP at SPBs both in cells with correctly aligned and misaligned anaphase spindles were analyzed (Figure 7A). We observed that Bfa1-GFP asymmetry changed to symmetric upon spindle mispositioning in *kar9*Δ cells (Figure 8A). In *kin4*Δ*kar9*Δ cells, on the other hand, no change in the asymmetry was observed (Figure 8A). Importantly, we have observed that Bfa1-GFP asymmetry was significantly decreased in *bud14*Δ*kar9*Δ cells like *kar9*Δ cells (Figure 8A). We also analyzed the behavior of Bfa1-GFP in living cells through time-lapse experiments, and we observed that Bfa1-GFP asymmetry changes to symmetric in *bud14*Δ*kar9*Δ cells while there was no change in *kin4*Δ*kar9*Δ cells (Figure 8B). Therefore, these data show that SPB localization of Bfa1 does change in the absence of *BUD14* upon spindle mispositioning. This further supports our findings that Bud14 does not work on Kin4 branch of SPOC.

A

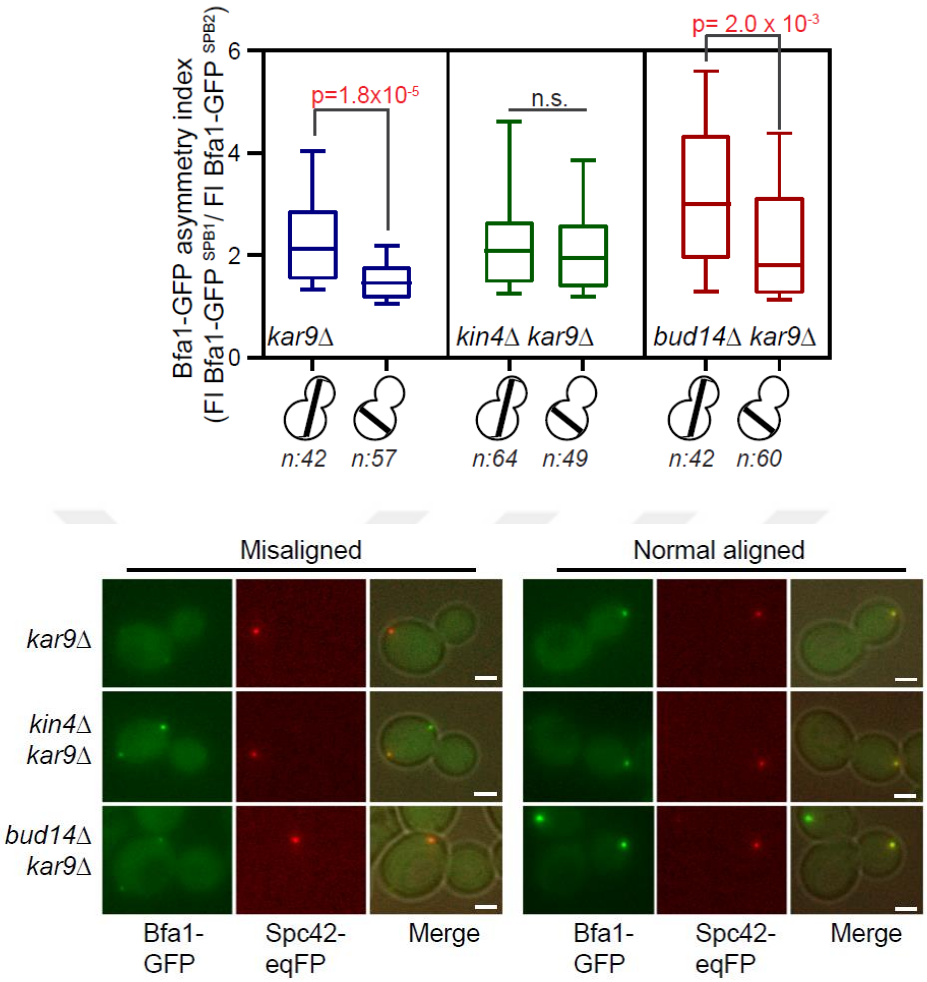
Bfa1-GFP asymmetry index
(FI Bfa1-GFP SPB1/ FI Bfa1-GFP SPB2)
p=1.8x10-5
n.s.
p= 2.0 x 10-3
kar9Δ
kin4Δ kar9Δ
bud14Δ kar9Δ
n:42
n:57
n:64
n:49
n:42
n:60
Misaligned
Normal aligned
kar9Δ
kin4Δ kar9Δ
bud14Δ kar9Δ
Bfa1-GFP
Spc42-eqFP
Merge
Bfa1-GFP
Spc42-eqFP
Merge

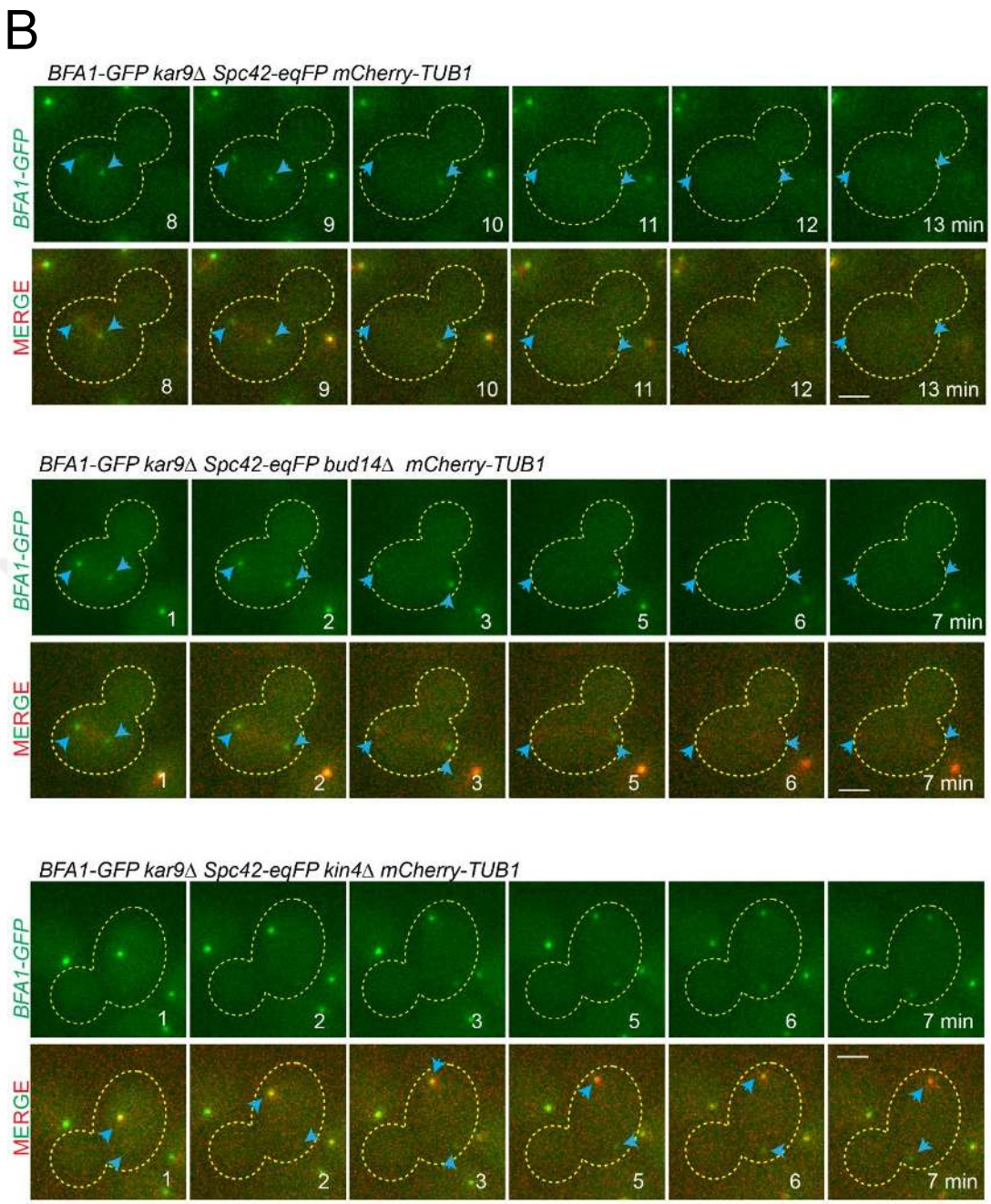

Figure 4. 8: Bud14 does not work through Kin4 branch of SPOC. A. Analysis of asymmetric localization of Bfa1-GFP at the SPBs in *kar9*Δ, *kar9*Δ*kin4*Δ and *kar9*Δ*bud14*Δ background cells with correctly aligned and misaligned anaphase spindles (AKY043, BKY032, DKY081). Bfa1-GFP signal intensity ratio at the SPBs were plotted as Box and Whisker where SPB1 always corresponds to SPB with the brighter Bfa1-GFP signal. The box represents first and third quartile while the whiskers show 10-90 percentile of the data. The horizontal line in the box indicates the median of the data. Representative still images of cells are shown on the right. Pairwise comparisons of intensities among indicated strains were assessed using Students' t-test. p-values were shown on the graph. n: sample size. Scale bar: 2 µm. **B.** Representative frames from Bfa1-GFP time-lapse series in *kar9*Δ, *kar9*Δ*bud14*Δ and *kar9*Δ*kin4*Δ cells (HKY099, HKY100, HKY101). The dashed line outlines the boundary of the cells. SPBs are shown with blue arrows. Time points is indicated on the frames. Scale bar: 2 µm.

4.9 *Localization of Bud14 at bud cortex reduces during late anaphase*

It has been reported that Bud14 localizes at bud tips, bud cortex and bud neck in a cell cycle dependent manner (Knaus et al., 2005). Thus, we wanted to check whether the localization of Bud14 changes in cells with misaligned and normally aligned anaphase spindles. We observed that there was an enriched Bud14-GFP signal at the bud cortex of the cells with normally aligned spindles during early- and mid-anaphase (Figure (8A, spindle length 3-5µm and 5-6µm). On the other hand, bud cortex localization of Bud14-GFP signal was significantly reduced upon mispositioning (Figure 9A). Also, Bud14-GFP signal at bud cortex was greatly decreased in cells with correctly aligned spindles during late anaphase (spindle length >6µm), that is found to be due to prolonged anaphase arrest (Kocakaplan., D. 2020).

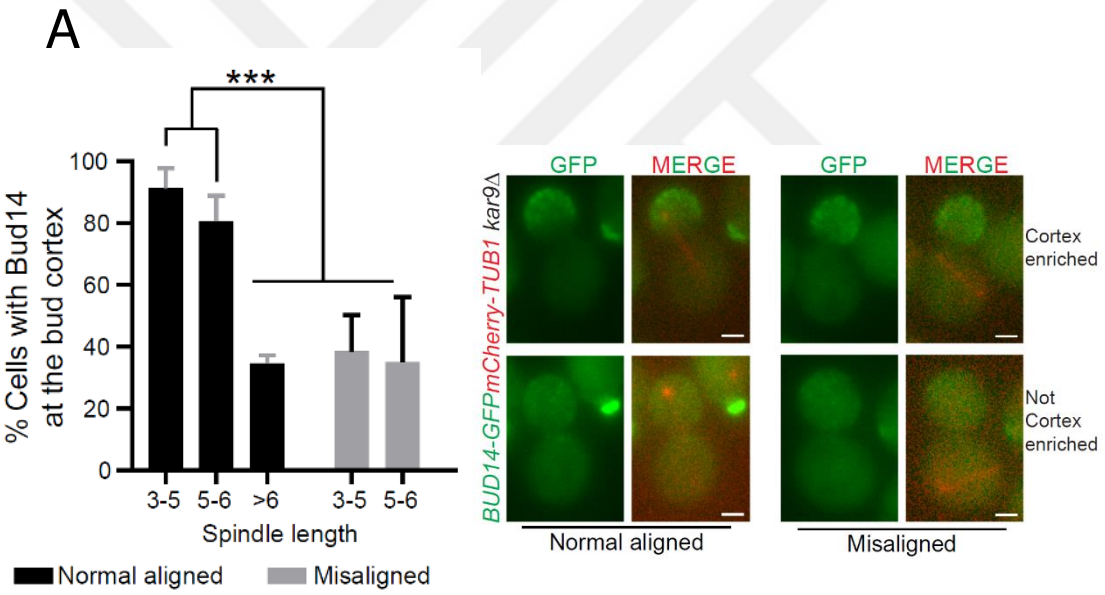

Figure 4. 9: Bud cortex localization of Bud14 changes upon prolonged spindle mispositioning. A. Percentage of anaphase cells with Bud14-GFP signal at bud cortex in cells with normally aligned and misaligned anaphase spindles (AKY4070). mCherry-*TUB1* was used as a spindle marker. Chi-square test was performed for pairwise comparison of percentage of cells with Bud14-GFP cortex enrichment ($p<0.0001$). Representative still images for cells with or without Bud14-GFP cortex enrichment were shown on the left. Scale bar: 2 µm.

Chapter 5: **DISCUSSION**

Positioning of the mitotic spindle is essential for the maintenance of ploidy during cell division. In budding yeast, site of cytokinesis is determined at the early stages of the cycle; therefore, alignment of the mitotic spindle in the mother-to-daughter polarity axis is crucial, so tightly regulated. SPOC is a surveillance mechanism monitoring the positioning of the mitotic spindle in the polarity axis. It inhibits mitotic exit in the presence of spindle mispositioning. SPOC is mainly controlled by the localization and phosphorylation of certain proteins. The activity of Bfa1, being the most downstream effector of the checkpoint, is tightly regulated by phosphorylation status with respect to the spindle orientation. It is phosphorylated by the polo like kinase Cdc5 in cells with normally aligned spindle and the mother specific SPOC kinase Kin4 in response to spindle mispositioning. These phosphorylation events in turn control the localization of Bfa1-Bub2 complex at the SPB and so the activity and localization of the GTPase Tem1 therein. Although the control of Bfa1 activity in a phosphorylation-dependent manner has been identified, the knowledge on phosphatases counteracting these kinases remains elusive. In this study we identified that Bud14 plays a novel role in the regulation of SPOC. It affects both the SPB-bound levels of Bfa1-Bub2 complex, and the phosphorylation status in anaphase (Kocakaplan D., 2020). We further showed in our lab that Glc7-Bud14 promote dephosphorylation of hyperphosphorylated Bfa1 (work of Cansu Dilege) and Bud14 interacts with Bfa1 (work of İdil Kırdök). Our work supports a model where Bfa1-Bub2 is activated by Bud14 (Figure 4.1).

In this thesis, we showed that Glc7-Bud14 is a novel SPOC component blocking the mitotic exit upon spindle mispositioning. We showed that deletion of *BUD14* promoted the growth of several temperature sensitive MEN mutants (*cdc15-1*, *dbf2-2* and *mob1-67*) (Figure 3.1A), the cold sensitivity of *lte1*Δ cells, and *lte1*Δ*spo12*Δ synthetic lethality. Also, we observed that deletion of *BUD14* resulted in a significant increase in the multinucleated cell populations upon spindle misalignment induced by deletion of *KAR9* or *DYN1* (Figure 3.2A-B). This finding indicates that *bud14*Δ cells are SPOC deficient, and they fail to arrest cell cycle progression in response to spindle misalignment during anaphase. Moreover, we observed that there was an increase in the SPOC deficiency phenotype in *glc7-ts kar9*Δ background, meaning that these cells have accumulated

multinucleated cells (Figure 3.4A). This data indicates SPOC regulatory function of Bud14 is dependent on its interaction with Glc7 (Figure 3.4A). Furthermore, we observed that during fluorescence-based time-lapse experiments *bud14*Δ*kar9*Δ cells exited mitosis with similar timing regardless of the spindle position (Figure 3.2C). Therefore, we concluded that deletion of *BUD14* affects the timing of mitotic exit and is important for inhibiting the progression of cell cycle upon spindle mispositioning.

We showed that Bud14 does not work in the Kin4 branch of SPOC. We observed that there was an additive decrease in the duration of anaphase in *kin4*Δ*bud14*Δ cells with misaligned spindles as compared to cells with single gene deletions of either *KIN4* or *BUD14* (Figure 3.2C). We also detected that *kin4*Δ*bud14*Δ cells were completely unable to inhibit cell cycle progression, while cells with single gene deletions could delay the exit from mitosis upon spindle misalignment (Figure 3.2C). Importantly, asymmetric localization of Bfa1 at SPBs changed into symmetric in *bud14*Δ cells whereas it was still asymmetric in *kin4*Δ cells upon spindle misorientation (Figure 3.8A). These findings imply that Kin4 can still act on Bfa1 even if *BUD14* is absent. Thus, these data altogether suggest that Bud14 works in parallel to Kin4, regulating SPOC to arrest cells in anaphase in the presence of spindle misalignment (Figure 3.8A-B).

We detected that deletion of *BUD14* resulted in an increase in the SPB localization of Bfa1, Bub2 and Tem1, especially at the dSPB, promoting the asymmetric localization of Bfa1-Bub2 complex (Figure 3.5 and Figure 3.6), and this function of Bud14 depends on its interaction with Glc7 (Figure 3.5C). It has been known that the asymmetric localization of Bfa1-Bub2 complex depends on Cdc5. It was previously shown that the asymmetric localization of Bfa1 changes into symmetric in cells with defective Cdc5 activity (Kim et al, 2012). This result also may support our model that Bud14 counteracts Cdc5 phosphorylation of Bfa1 during anaphase. It is also possible that Bud14 may act on other proteins that regulate the SPB or SPB localization of Bfa1-Bub2 complex. This increased SPB localization of Bfa1-Bub2 in the absence of *BUD14* leads to an increase in the localization of Tem1 at the SPBs, activating MEN. Thus, it is possible that Bud14 exerts its SPOC regulatory function by limiting the SPB localization of Bfa1-Bub2 complex, so the SPB localization of Tem1 to delay mitotic exit. It may also be suggestive for the fact that dephosphorylation of Bfa1-Bub2 GAP complex by the activity of Bud14-Glc7 limits their SPB-localization, inhibiting the progression of cell cycle.

We observed that bud cortex specific localization of Bud14 gradually disappeared in a cell cycle dependent manner (Figure 3.9). We detected that Bud14 fell off from the bud cortex in late anaphase in both normally aligned and misaligned cells. Interestingly, during fluorescence-based time-lapse experiments, we detected that it started to localize bud neck in cells with normally aligned spindle, but no bud neck localization was detected in cells with misaligned spindle (Kocakaplan D., 2020). Therefore, during most of the time the cell spends in the misaligned state, Bud14 is found spread through the cytoplasm, where it is able to reach on Bfa1-Bub2 complex in the presence of spindle misalignment during anaphase. Therefore, Bud14-Glc7 may be dephosphorylating Bfa1 that was released from the SPBs into the cytoplasm during spindle mispositioning. Importantly, we found that a mutant form of Bud14 (*bud14-sh3*Δ) that cannot localize to the bud cortex is also unable to function as a mitotic exit inhibitor (Kocakaplan 2020), but this form of Bud14 was also unable to interact with Glc7 (Knaus et al., 2005) or Bfa1 (Work of İdil Kırdök, Data not shown). Thus, ability of Bud14 to interact with the cell cortex is also crucial for its function in SPOC.

It remains elusive how the alignment of mitotic spindle is sensed, and how this information is transmitted to the SPOC machinery for the activation of the checkpoint is not known yet. It has been found that treatment of cells with a microtubule depolymerizing drug nocodazole caused the activation of SPOC (Caydasi & Pereira, 2009). This finding suggests that SPOC may be sensing the interaction between microtubule and cell cortex. Bud14-Glc7 complex are known to be involved in the regulation of microtubule-cortex interactions (Knaus et al., 2005). Therefore, the complex may sense such interactions, and this may be how SPOC is activated. Future studies can enlighten if Bud14-Glc7 complex may sense the unattached microtubule-cortex interactions, transmitting the signal to the SPOC machinery.

A SPOC like mechanism exists in *Drosophila melanogaster*, and it is possible to be present in higher eukaryotes (Pereira & Yamashita, 2011). Protein phosphatase I is an essential gene, conserved among the eukaryotes. It has been shown to have various effects on the control of cell cycle (Holder, Poser, & Barr, 2019). Here, we identified Bud14-Glc7 complex is a regulator of SPOC. This work may reveal another function of PP1 in higher eukaryotes. If this function of PP1 exists in the higher eukaryotes, especially in mammalian cells, then a homolog pathway of SPOC can be identified. As we indicated, SPOC deficiency results in genomic instability and aneuploidy, which are hallmarks of

cancer (Hanahan & Weinberg, 2011). Identification of the regulation of these possible pathways can be a good target for anti-cancer therapeutic studies.

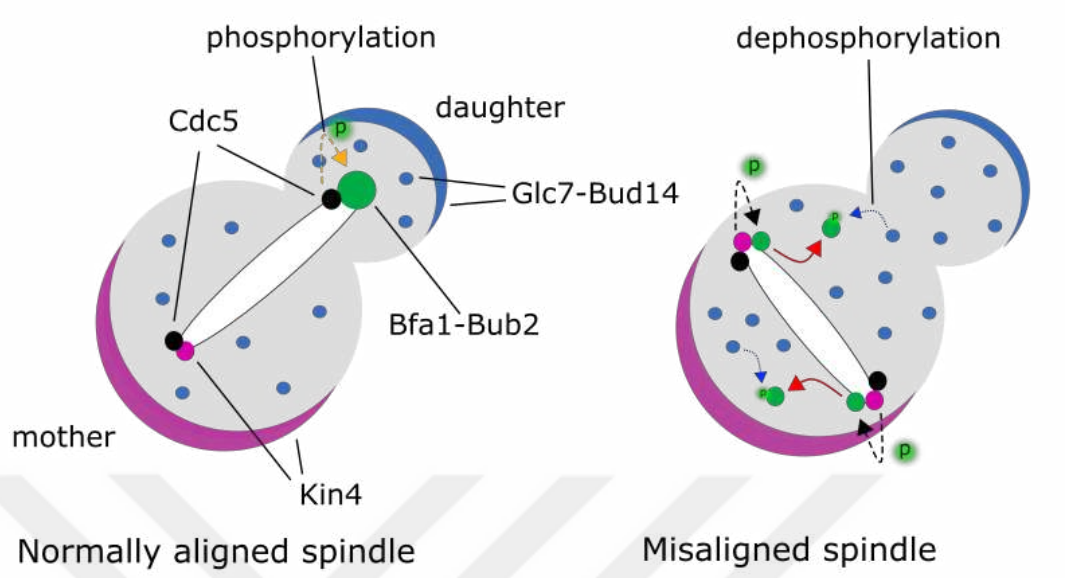

Figure 5. 1: Model for SPOC regulatory function of Bud14. Bfa1 preferentially localizes to the dSPB in cells with normally aligned anaphase spindles in mother-to-daughter polarity axis (cartoon on the left). Cdc5, a polo-like kinase, localizes to the outer plaque of the SPBs in anaphase. Thus, Cdc5 phosphorylates and inactivates the GAP activity of Bfa1-Bub2 complex in the dSPB (orange dashed line). This stimulates the recruitment of more Tem1 to the dSPB, resulting in the activation of exit from mitosis. In the presence of spindle misalignment, Bfa1 localizes to both SPBs dynamically. In this status, Kin4 can localize to both SPBs, and phosphorylates Bfa1 (black dashed line). Phosphorylation of Bfa1 by Kin4 leads to rapid dissociation of Bfa1-Bub2 complex from the SPBs (red line). Bfa1 released from the SPB into the cytoplasm can be dephosphorylated by the Glc7-Bud14 complex. This dephosphorylation both restores Bfa1-Bub2 GAP activity and prevents the association of Bfa1 with the SPBs.

Chapter 6: **BIBLIOGRAPHY**

Adames, N. R., & Cooper, J. A. (2000). Microtubule interactions with the cell cortex causing nuclear movements in Saccharomyces cerevisiae. *Journal of Cell Biology*, *149*(4), 863–874. https://doi.org/10.1083/jcb.149.4.863

Adams, I. R., & Kilmartin, J. V. (1999). Localization of core spindle pole body (SPB) components during SPB duplication in Saccharomyces cerevisiae. *Journal of Cell Biology*, *145*(4), 809–823. https://doi.org/10.1083/jcb.145.4.809

Amon, A. (1996). Mother and daughter are doing fine: Asymmetric cell division in yeast. *Cell*, *84*(5), 651–654. https://doi.org/10.1016/S0092-8674(00)81041-7

Andrews, B., & Measday, V. (1998). The cyclin family of budding yeast: Abundant use of a good idea. *Trends in Genetics*, *14*(2), 66–72. https://doi.org/10.1016/S0168-9525(97)01322-X

Andrews, P. D., & Stark, M. J. (2000). Type 1 protein phosphatase is required for maintenance of cell wall integrity, morphogenesis and cell cycle progression in Saccharomyces cerevisiae. *Journal of Cell Science*, *113 (Pt 3*, 507–520.

Asakawa, K., Yoshida, S., Otake, F., & Toh-e, A. (2001). A novel functional domain of Cdc15 kinase is required for its interaction with Tem1 GTPase in Saccharomyces cerevisiae. *Genetics*, *157*(4), 1437–1450.

Azzam, R., Chen, S. L., Shou, W., Mah, A. S., Alexandru, G., Nasmyth, K., … Deshaies, R. J. (2004). Phosphorylation by cyclin B-Cdk underlies release of mitotic exit activator Cdc14 from the nucleolus. *Science (New York, N.Y.)*, *305*(5683), 516–519. https://doi.org/10.1126/science.1099402

Bardin, A J, Visintin, R., & Amon, A. (2000). A mechanism for coupling exit from mitosis to partitioning of the nucleus. *Cell*, *102*(1), 21–31. https://doi.org/10.1016/s0092-8674(00)00007-6

Bardin, Allison J, Boselli, M. G., & Amon, A. (2003). Mitotic exit regulation through distinct domains within the protein kinase Cdc15. *Molecular and Cellular Biology*, *23*(14), 5018–5030. https://doi.org/10.1128/MCB.23.14.5018-5030.2003

Barnum, K., & O'Connell, M. (2014). Cell Cycle Regulation by Checkpoints. *Methods in Molecular Biology*, *1170*, 477–499. https://doi.org/10.1007/978-1-4939-0888-2

Bazzi, M., Mantiero, D., Trovesi, C., Lucchini, G., & Longhese, M. P. (2010). Dephosphorylation of gamma H2A by Glc7/protein phosphatase 1 promotes recovery from inhibition of DNA replication. *Molecular and Cellular Biology*, *30*(1), 131–145. https://doi.org/10.1128/MCB.01000-09

Beach, D. L., Thibodeaux, J., Maddox, P., Yeh, E., & Bloom, K. (2000). The role of the proteins Kar9 and Myo2 in orienting the mitotic spindle of budding yeast. *Current Biology*, *10*(23), 1497–1506. https://doi.org/10.1016/S0960-9822(00)00837-X

Bertazzi, D. T., Kurtulmus, B., & Pereira, G. (2011). The cortical protein Lte1 promotes mitotic exit by inhibiting the spindle position checkpoint kinase Kin4. *The Journal of Cell Biology*, *193*(6), 1033–1048. https://doi.org/10.1083/jcb.201101056

Biggins, S., & Rose, M. D. (1994). Direct interaction between yeast spindle pole body components: Kar1p is required for Cdc31p localization to the spindle pole body. *Journal of Cell Biology*, *125*(4), 843–852. https://doi.org/10.1083/jcb.125.4.843

Bloom, J., & Cross, F. R. (2007). Multiple levels of cyclin specificity in cell-cycle control. *Nature Reviews Molecular Cell Biology*, *8*(2), 149–160. https://doi.org/10.1038/nrm2105

Boettcher, B., & Barral, Y. (2013). The cell biology of open and closed mitosis. *Nucleus (United States)*, *4*(3), 160–165. https://doi.org/10.4161/nucl.24676

Böhmer, R. M., Scharf, E., & Assoian, R. K. (1996). Cytoskeletal integrity is required throughout the mitogen stimulation phase of the cell cycle and mediates the anchorage-dependent expression of cyclin D1. *Molecular Biology of the Cell*, *7*(1), 101–111. https://doi.org/10.1091/mbc.7.1.101

Botstein, D., Chervitz, S. A., & Cherry, J. M. (1997). Yeast as a Model Organism Biodiversity and Ecosystem Function : The Debate Deepens. *Science*, *277*(August).

Botstein, D., & Fink, G. R. (2011). Yeast: An experimental organism for 21st century biology. *Genetics*, *189*(3), 695–704. https://doi.org/10.1534/genetics.111.130765

Breeden, L. L. (2000). Cyclin transcription: Timing is everything. *Current Biology*,

10(16), 586–588. https://doi.org/10.1016/S0960-9822(00)00634-5

Bullitt, E., Rout, M. P., Kilmartin, J. V., & Akey, C. W. (1997). The yeast spindle pole body is assembled around a central crystal of Spc42p. *Cell*, *89*(7), 1077–1086. https://doi.org/10.1016/S0092-8674(00)80295-0

Byers, B., & Goetsch, L. (1974). Duplication of spindle plaques and integration of the yeast cell cycle. *Cold Spring Harbor Symposia on Quantitative Biology*, *38*, 123–131. https://doi.org/10.1101/sqb.1974.038.01.016

Byers, B., Shriver, K., & Goetsch, L. (1978). The role of spindle pole bodies and modified microtubule ends in the initiation of microtubule assembly in Saccharomyces cerevisiae. *Journal of Cell Science*, *30*, 331–352.

Calvert, M. E. K., Lannigan, J. A., Pemberton, L. F., & Signaling, C. (2009). Optimization of Yeast Cell Cycle Analysis and. *Cytometry*, *73*(9), 825–833. https://doi.org/10.1002/cyto.a.20609.OPTIMIZATION

Carter, M., & Shieh, J. (2005). Cell culture techniques. *Principles and Techniques of Biochemistry and Molecular Biology, Sixth Edition*, 71–102. https://doi.org/10.1017/CBO9780511813412.003

Carvalho, P., Gupta, M. L., Hoyt, M. A., & Pellman, D. (2004). Cell cycle control of kinesin-mediated transport of Bik1 (CLIP-170) regulates microtubule stability and dynein activation. *Developmental Cell*, *6*(6), 815–829. https://doi.org/10.1016/j.devcel.2004.05.001

Casamayor, A., & Snyder, M. (2002). Bud-site selection and cell polarity in budding yeast. *Current Opinion in Microbiology*, *5*(2), 179–186. https://doi.org/10.1016/S1369-5274(02)00300-4

Caydasi, A., Khmelinskii, A., Duenas-Sanchez, R., Kurtulmus, B., Knop, M., & Pereira, G. (2017). Temporal and compartment-specific signals coordinate mitotic exit with spindle position. *Nature Communications*, *8*, 1–14. https://doi.org/10.1038/ncomms14129

Caydasi, Ayse K, Ibrahim, B., & Pereira, G. (2010). Monitoring spindle orientation: Spindle position checkpoint in charge. *Cell Division*, *5*(1), 28. https://doi.org/10.1186/1747-1028-5-28

Caydasi, Ayse Koca, Kurtulmus, B., Orrico, M. I. L., Hofmann, A., Ibrahim, B., & Pereira, G. (2010). Elm1 kinase activates the spindle position checkpoint kinase Kin4. *Journal of Cell Biology*, *190*(6), 975–989. https://doi.org/10.1083/jcb.201006151

Caydasi, Ayse Koca, Lohel, M., Grünert, G., Dittrich, P., Pereira, G., & Ibrahim, B. (2012). A dynamical model of the spindle position checkpoint. *Molecular Systems Biology*, *8*, 582. https://doi.org/10.1038/msb.2012.15

Caydasi, Ayse Koca, Micoogullari, Y., Kurtulmus, B., Palani, S., & Pereira, G. (2014). The 14-3-3 protein Bmh1 functions in the spindle position checkpoint by breaking Bfa1 asymmetry at yeast centrosomes. *Molecular Biology of the Cell*, *25*(14), 2143–2151. https://doi.org/10.1091/mbc.E14-04-0890

Caydasi, Ayse Koca, & Pereira, G. (2009). Spindle alignment regulates the dynamic association of checkpoint proteins with yeast spindle pole bodies. *Developmental Cell*, *16*(1), 146–156. https://doi.org/10.1016/j.devcel.2008.10.013

Cenamor, R., Jiménez, J., Cid, V. J., Nombela, C., & Sánchez, M. (1999). The budding yeast Cdc15 localizes to the spindle pole body in a cell-cycle-dependent manner. *Molecular Cell Biology Research Communications : MCBRC*, *2*(3), 178–184. https://doi.org/10.1006/mcbr.1999.0173

Chan, L. Y., & Amon, A. (2009). The protein phosphatase 2A functions in the spindle position checkpoint by regulating the checkpoint kinase Kin4. *Genes and Development*, *23*(14), 1639–1649. https://doi.org/10.1101/gad.1804609

Chesarone, M., Gould, C. J., Moseley, J. B., & Goode, B. L. (2009). Displacement of formins from growing barbed ends by bud14 is critical for actin cable architecture and function. *Developmental Cell*, *16*(2), 292–302. https://doi.org/10.1016/j.devcel.2008.12.001

Cheung, T., & Rando, T. (2008). Molecular regulation of stem cell quiescence. *Accounts of Chemical Research*, *45*(6), 788–802. https://doi.org/10.1038/nrm3591.Molecular

Colman-Lerner, A., Chin, T. E., & Brent, R. (2001). Yeast Cbk1 and Mob2 activate daughter-specific genetic programs to induce asymmetric cell fates. *Cell*, *107*(6), 739–750. https://doi.org/10.1016/s0092-8674(01)00596-7

Costanzo, M., Nishikawa, J. L., Tang, X., Millman, J. S., Schub, O., Breitkreuz, K., … Tyers, M. (2004). CDK activity antagonizes Whi5, an inhibitor of G1/S transcription in yeast. *Cell*, *117*(7), 899–913. https://doi.org/10.1016/j.cell.2004.05.024

Cross, F. R. (1995). Starting the cell cycle: what's the point? *Current Opinion in Cell Biology*, *7*(6), 790–797. https://doi.org/10.1016/0955-0674(95)80062-X

D'Aquino, K. E., Monje-Casas, F., Paulson, J., Reiser, V., Charles, G. M., Lai, L., … Amon, A. (2005). The Protein Kinase Kin4 Inhibits Exit from Mitosis in Response to Spindle Position Defects. *Molecular Cell*, *19*(2), 223–234. https://doi.org/https://doi.org/10.1016/j.molcel.2005.06.005

De Antoni, A., Pearson, C., Cimini, D., Canman, J., Sala, V., Nezi, L., … Musacchio, A. (2005). The Mad1/Mad2 Complex as a Template for Mad2 Activation in the Spindle Assembly Checkpoint. *Current Biology*, *15*. https://doi.org/10.1016/j

De Bruin, R. A. M., McDonald, W. H., Kalashnikova, T. I., Yates, J., & Wittenberg, C. (2004). Cln3 activates G1-specific transcription via phosphorylation of the SBF bound repressor Whi5. *Cell*, *117*(7), 887–898. https://doi.org/10.1016/j.cell.2004.05.025

Donaldson, A. D., & Kilmartin, J. V. (1996). Spc42p: A Phosphorylated Component of the S. cerevisiae Spindle Pole Body (SPB) With an Essential Function During SPB Duplication. *Journal of Cell Biology*, *132*(5), 887–901.

Donaldson, A. D., Raghuraman, M. K., Friedman, K. L., Cross, F. R., Brewer, B. J., & Fangman, W. L. (1998). CLB5-dependent activation of late replication origins in S. cerevisiae. *Molecular Cell*, *2*(2), 173–182. https://doi.org/10.1016/S1097-2765(00)80127-6

Duina, A. A., Miller, M. E., & Keeney, J. B. (2014). Budding yeast for budding geneticists: A primer on the Saccharomyces cerevisiae model system. *Genetics*, *197*(1), 33–48. https://doi.org/10.1534/genetics.114.163188

Echard, A., & O'Farrell, P. H. (2003). The degradation of two mitotic cyclins contributes to the timing of cytokinesis. *Current Biology*, *13*(5), 373–383. https://doi.org/10.1016/S0960-9822(03)00127-1

Eckert-Boulet, N., Rothstein, R., & Lisby, M. (2011). Cell biology of homologous recombination in yeast. *Methods in Molecular Biology (Clifton, N.J.)*, *745*(4), 523–536. https://doi.org/10.1007/978-1-61779-129-1_30

Eskin, J. A., Rankova, A., Johnston, A. B., Alioto, S. L., & Goode, B. L. (2016). Common formin-regulating sequences in Smy1 and Bud14 are required for the control of actin cable assembly in vivo. *Molecular Biology of the Cell*, *27*(5), 828–837. https://doi.org/10.1091/mbc.E15-09-0639

Falk, J. E., Chan, L. Y., & Amon, A. (2011). Lte1 promotes mitotic exit by controlling the localization of the spindle position checkpoint kinase Kin4. *Proceedings of the National Academy of Sciences of the United States of America*, *108*(31), 12584–12590. https://doi.org/10.1073/pnas.1107784108

Fang, G., Yu, H., & Kirschner, M. W. (1999). Control of mitotic transitions by the anaphase-promoting complex. *Philosophical Transactions of the Royal Society B: Biological Sciences*, *354*(1389), 1583–1590. https://doi.org/10.1098/rstb.1999.0502

Farley, F. W., Satterberg, B., Goldsmith, E. J., & Elion, E. A. (1999). Relative dependence of different outputs of the Saccharomyces cerevisiae pheromone response pathway on the MAP kinase Fus3p. *Genetics*, *151*(4), 1425–1444. https://doi.org/10.1093/genetics/151.4.1425

Fitch, I., Dahmann, C., Surana, U., Amon, A., Nasmyth, K., Goetsch, L., … Futcher, B. (1992). Characterization of four B-type cyclin genes of the budding yeast Saccharomyces cerevisiae. *Molecular Biology of the Cell*, *3*(7), 805–818. https://doi.org/10.1091/mbc.3.7.805

Gardner, J. M., & Jaspersen, S. L. (2014). Manipulating the yeast genome: Deletion, mutation, and tagging by PCR. In *Methods in Molecular Biology* (Vol. 1205). https://doi.org/10.1007/978-1-4939-1363-3_5

Geymonat, M., Spanos, A., de Bettignies, G., & Sedgwick, S. G. (2009). Lte1 contributes to Bfa1 localization rather than stimulating nucleotide exchange by Tem1. *The Journal of Cell Biology*, *187*(4), 497–511. https://doi.org/10.1083/jcb.200905114

Geymonat, M., Spanos, A., Jensen, S., & Sedgwick, S. G. (2010). Phosphorylation of

Lte1 by Cdk prevents polarized growth during mitotic arrest in S. cerevisiae. *The Journal of Cell Biology*, *191*(6), 1097–1112. https://doi.org/10.1083/jcb.201005070

Geymonat, M., Spanos, A., Smith, S. J. M., Wheatley, E., Rittinger, K., Johnston, L. H., & Sedgwick, S. G. (2002). Control of mitotic exit in budding yeast. In vitro regulation of Tem1 GTPase by Bub2 and Bfa1. *The Journal of Biological Chemistry*, *277*(32), 28439–28445. https://doi.org/10.1074/jbc.M202540200

Geymonat, M., Spanos, A., Walker, P. A., Johnston, L. H., & Sedgwick, S. G. (2003). In vitro regulation of budding yeast Bfa1/Bub2 GAP activity by Cdc5. *The Journal of Biological Chemistry*, *278*(17), 14591–14594. https://doi.org/10.1074/jbc.C300059200

Goffeau, A., Barrell, B. G., Bussey, H., Davis, R. W., Dujon, B., Feldmann, H., … Oliver, S. G. (1996). Life with 6000 Genes conveniently among the different interna- Old Questions and New Answers The genome . At the beginning of the se- of its more complex relatives in the eukary- cerevisiae has been completely sequenced Schizosaccharomyces pombe indicate. *Science*, *274*(October), 546–567.

Gould, C. J., Chesarone-Cataldo, M., Alioto, S. L., Salin, B., Sagot, I., & Goode, B. L. (2014). Saccharomyces cerevisiae Kelch proteins and Bud14 protein form a stable 520-kDa formin regulatory complex that controls actin cable assembly and cell morphogenesis. *The Journal of Biological Chemistry*, *289*(26), 18290–18301. https://doi.org/10.1074/jbc.M114.548719

Grana, X., & Reddy, E. P. (1995). Cell cycle control in mammalian cells: Role of cyclins, cyclin dependent kinases (CDKs), growth suppressor genes and cyclin-dependent kinase inhibitors (CKIs). *Oncogene*, *11*(2), 211–219.

Grava, S., Schaerer, F., Faty, M., Philippsen, P., & Barral, Y. (2006). Asymmetric recruitment of dynein to spindle poles and microtubules promotes proper spindle orientation in yeast. *Developmental Cell*, *10*(4), 425–439. https://doi.org/10.1016/j.devcel.2006.02.018

Gruneberg, U, Campbell, K., Simpson, C., Grindlay, J., & Schiebel, E. (2000). Nud1p links astral microtubule organization and the control of exit from mitosis. *The EMBO Journal*, *19*(23), 6475–6488. https://doi.org/10.1093/emboj/19.23.6475

Gruneberg, Ulrike, Campbell, K., Simpson, C., Grindlay, J., & Schiebel, E. (2000). Nud1p links astral microtubule organization and the control of exit from mitosis. *EMBO Journal*, *19*(23), 6475–6488. https://doi.org/10.1093/emboj/19.23.6475

Guacci, V., Koshland, D., & Strunnikov, A. (1997). A direct link between sister chromatid cohesion and chromosome condensation revealed through the analysis of MCD1 in S. cerevisiae. *Cell*, *91*(1), 47–57. https://doi.org/10.1016/S0092-8674(01)80008-8

Gupta, M. L., Carvalho, P., Roof, D. M., & Pellman, D. (2006). Plus end-specific depolymerase activity of Kip3, a kinesin-8 protein, explains its role in positioning the yeast mitotic spindle. *Nature Cell Biology*, *8*(9), 913–923. https://doi.org/10.1038/ncb1457

Gupta, M. L. J., Carvalho, P., Roof, D. M., & Pellman, D. (2006). Plus end-specific depolymerase activity of Kip3, a kinesin-8 protein, explains its role in positioning the yeast mitotic spindle. *Nature Cell Biology*, *8*(9), 913–923. https://doi.org/10.1038/ncb1457

Hanahan, D., & Weinberg, R. A. (2011). Hallmarks of cancer: The next generation. *Cell*, *144*(5), 646–674. https://doi.org/10.1016/j.cell.2011.02.013

Hartwell, L. (1973). Three additional genes required for deoxyribonucleic acid synthesis in Saccharomyces cerevisiae. *Journal of Bacteriology*, *115*(3), 966–974. https://doi.org/10.1128/jb.115.3.966-974.1973

Hartwell, L H, Mortimer, R. K., Culotti, J., & Culotti, M. (1973). Genetic Control of the Cell Division Cycle in Yeast: V. Genetic Analysis of cdc Mutants. *Genetics*, *74*(2), 267–286.

Hartwell, Leland H., Culotti, J., Pringle, J. R., & Reid, B. J. (1974). Genetic control of the cell division cycle in yeast. *Science*, *183*(4120), 46–51. https://doi.org/10.1126/science.183.4120.46

Hershko, A., & Ciechanover, A. (1998). The ubiquitin system. *Nature*, *458*(7237), 421. https://doi.org/10.1038/458421a

Herskowitz, I. (1988). Life cycle of the budding yeast Saccharomyces cerevisiae. *Microbiological Reviews*, *52*(4), 536–553. https://doi.org/10.1128/mmbr.52.4.536-

553.1988

Höfken, T., & Schiebel, E. (2002). A role for cell polarity proteins in mitotic exit. *The EMBO Journal*, *21*(18), 4851–4862. https://doi.org/10.1093/emboj/cdf481

Höfken, T., & Schiebel, E. (2004). Novel regulation of mitotic exit by the Cdc42 effectors Gic1 and Gic2. *The Journal of Cell Biology*, *164*(2), 219–231. https://doi.org/10.1083/jcb.200309080

Holder, J., Poser, E., & Barr, F. A. (2019). Getting out of mitosis: spatial and temporal control of mitotic exit and cytokinesis by PP1 and PP2A. *FEBS Letters*, *593*(20), 2908–2924. https://doi.org/10.1002/1873-3468.13595

Hoyt, M. A., Totis, L., & Roberts, B. T. (1991). S. cerevisiae genes required for cell cycle arrest in response to loss of microtubule function. *Cell*, *66*(3), 507–517. https://doi.org/10.1016/0092-8674(81)90014-3

Hu, F., Wang, Y., Liu, D., Li, Y., Qin, J., & Elledge, S. J. (2001). Regulation of the Bub2/Bfa1 GAP complex by Cdc5 and cell cycle checkpoints. *Cell*, *107*(5), 655–665. https://doi.org/10.1016/s0092-8674(01)00580-3

Hughes, T. R. (2002). Yeast and drug discovery. *Functional & Integrative Genomics*, *2*(4–5), 199–211. https://doi.org/10.1007/s10142-002-0059-1

Hwang, E., Kusch, J., Barral, Y., & Huffaker, T. C. (2003). Spindle orientation in Saccharomyces cerevisiae depends on the transport of microtubule ends along polarized actin cables. *Journal of Cell Biology*, *161*(3), 483–488. https://doi.org/10.1083/jcb.200302030

Iliakis, G., Wang, Y., Guan, J., & Wang, H. (2003). DNA damage checkpoint control in cells exposed to ionizing radiation. *Oncogene*, *22*(37 REV. ISS. 3), 5834–5847. https://doi.org/10.1038/sj.onc.1206682

Janke, C., Magiera, M. M., Rathfelder, N., Taxis, C., Reber, S., Maekawa, H., … Knop, M. (2004). A versatile toolbox for PCR-based tagging of yeast genes: New fluorescent proteins, more markers and promoter substitution cassettes. *Yeast*, *21*(11), 947–962. https://doi.org/10.1002/yea.1142

Jaspersen, S., & Winey, M. (2004). The budding yeast spindle pole body: Structure, duplication, and function. *Annual Review of Cell and Developmental Biology*, *20*,

1–28. https://doi.org/10.1146/annurev.cellbio.20.022003.114106

Jaspersen, S L, Charles, J. F., Tinker-Kulberg, R. L., & Morgan, D. O. (1998). A late mitotic regulatory network controlling cyclin destruction in Saccharomyces cerevisiae. *Molecular Biology of the Cell*, *9*(10), 2803–2817. https://doi.org/10.1091/mbc.9.10.2803

Jaspersen, Sue L., Giddings, T. H., & Winey, M. (2002). Mps3p is a novel component of the yeast spindle pole body that interacts with the yeast centrin homologue Cdc31p. *Journal of Cell Biology*, *159*(6), 945–956. https://doi.org/10.1083/jcb.200208169

Kaibuchi, K., Miyazaki, J., Minato, N., Nomura for plasmids, N., Mizuno, H., Ohba, F., … Li, J. J. (2001). *Cyclin-dependent kinases prevent DNA re-replication through multiple mechanisms*. *411*(JUNE), 2–7. Retrieved from www.nature.com

Khmelinskii, A., Lawrence, C., Roostalu, J., & Schiebel, E. (2007). Cdc14-regulated midzone assembly controls anaphase B. *The Journal of Cell Biology*, *177*(6), 981–993. https://doi.org/10.1083/jcb.200702145

Kilmartin, J. V, & Goh, P. Y. (1996). Spc110p: assembly properties and role in the connection of nuclear microtubules to the yeast spindle pole body. *The EMBO Journal*, *15*(17), 4592–4602.

King, S. M., Hyams, J. S., & Luba, A. (1982). Ultrastructure of mitotic spindles isolated from a cell division cycle mutant of the yeast, Saccharomyces cerevisiae. *European Journal of Cell Biology*, *28*(1), 98–102. Retrieved from http://europepmc.org/abstract/MED/6751829

Knaus, M., Cameroni, E., Pedruzzi, I., Tatchell, K., De Virgilio, C., & Peter, M. (2005). The Bud14p-Glc7p complex functions as a cortical regulator of dynein in budding yeast. *The EMBO Journal*, *24*(17), 3000–3011. https://doi.org/10.1038/sj.emboj.7600783

Knop, M., & Schiebel, E. (1997). Spc98p and Spc97p of the yeast gamma -tubulin complex mediate binding to the spindle pole body via their interaction with Spc110p. *The EMBO Journal*, *16*(23), 6985–6995. https://doi.org/10.1093/emboj/16.23.6985

Knop, Michael, & Schiebel, E. (1998). Receptors determine the cellular localization of a γ-tubulin complex and thereby the site of microtubule formation. *EMBO Journal*, *17*(14), 3952–3967. https://doi.org/10.1093/emboj/17.14.3952

Knop, Michael, Siegers, K., Pereira, G., Zachariae, W., Winsor, B., Nasmyth, K., & Schiebel, E. (1999). Epitope tagging of yeast genes using a PCR-based strategy: More tags and improved practical routines. *Yeast*, *15*(10 B), 963–972. https://doi.org/10.1002/(SICI)1097-0061(199907)15:10B<963::AID-YEA399>3.0.CO;2-W

Korinek, W. S., Copeland, M. J., Chaudhuri, A., & Chant, J. (2000). Molecular linkage underlying microtubule orientation toward cortical sites in yeast. *Science (New York, N.Y.)*, *287*(5461), 2257–2259. https://doi.org/10.1126/science.287.5461.2257

Küntzel, H., Schulz, A., & Ehbrecht, I. M. (1996). Cell cycle control and initiation of DNA replication in Saccharomyces cerevisiae. *Biological Chemistry*, *377*(7–8), 481–487.

Lee, C. S., & Haber, J. E. (1998). Mating-type gene switching in saccharomyces cerevisiae. *Mobile DNA III*, 491–514. https://doi.org/10.1128/9781555819217.ch23

Lesage, G., & Bussey, H. (2006). Cell Wall Assembly in Saccharomyces cerevisiae. *Microbiology and Molecular Biology Reviews*, *70*(2), 317–343. https://doi.org/10.1128/mmbr.00038-05

Li, Y. Y., Yeh, E., Hays, T., & Bloom, K. (1993). Disruption of mitotic spindle orientation in a yeast dynein mutant. *Proceedings of the National Academy of Sciences of the United States of America*, *90*(21), 10096–10100. https://doi.org/10.1073/pnas.90.21.10096

Liakopoulos, D., Kusch, J., Grava, S., Vogel, J., & Barral, Y. (2003). Asymmetric loading of Kar9 onto spindle poles and microtubules ensures proper spindle alignment. *Cell*, *112*(4), 561–574. https://doi.org/10.1016/S0092-8674(03)00119-3

Lim, H. H., Goh, P. Y., & Surana, U. (1998). Cdc20 is essential for the cyclosome-mediated proteolysis of both Pds1 and Clb2 during M phase in budding yeast. *Current Biology*, *8*(4), 231–237. https://doi.org/10.1016/s0960-9822(98)70088-0

Longhese, M. P., Foiani, M., Muzi-Falconi, M., Lucchini, G., & Plevani, P. (1998). DNA damage checkpoint in budding yeast. *EMBO Journal*, *17*(19), 5525–5528. https://doi.org/10.1093/emboj/17.19.5525

Luca, F. C., & Winey, M. (1998). MOB1, an essential yeast gene required for completion of mitosis and maintenance of ploidy. *Molecular Biology of the Cell*, *9*(1), 29–46. https://doi.org/10.1091/mbc.9.1.29

Maekawa, H., Priest, C., Lechner, J., Pereira, G., & Schiebel, E. (2007). The yeast centrosome translates the positional information of the anaphase spindle into a cell cycle signal. *The Journal of Cell Biology*, *179*(3), 423–436. https://doi.org/10.1083/jcb.200705197

Malmanche, N., Maia, A., & Sunkel, C. E. (2006). The spindle assembly checkpoint: Preventing chromosome mis-segregation during mitosis and meiosis. *FEBS Letters*, *580*(12), 2888–2895. https://doi.org/10.1016/j.febslet.2006.03.081

Malumbres, M. (2011). Physiological relevance of cell cycle kinases. *Physiological Reviews*, *91*(3), 973–1007. https://doi.org/10.1152/physrev.00025.2010

McCollum, D., & Gould, K. L. (2001). Timing is everything: Regulation of mitotic exit and cytokinesis by the MEN and SIN. *Trends in Cell Biology*, *11*(2), 89–95. https://doi.org/10.1016/S0962-8924(00)01901-2

McNally, F. J. (2013). Mechanisms of spindle positioning. *Journal of Cell Biology*, *200*(2), 131–140. https://doi.org/10.1083/jcb.201210007

Mendenhall, M. D., & Hodge, A. E. (1998). Regulation of Cdc28 Cyclin-Dependent Protein Kinase Activity during the Cell Cycle of the Yeast Saccharomyces cerevisiae. *Microbiology and Molecular Biology Reviews*, *62*(4), 1191–1243. https://doi.org/10.1128/mmbr.62.4.1191-1243.1998

Miller, R K, & Rose, M. D. (1998). Kar9p is a novel cortical protein required for cytoplasmic microtubule orientation in yeast. *The Journal of Cell Biology*, *140*(2), 377–390. https://doi.org/10.1083/jcb.140.2.377

Miller, Rita K., & Rose, M. D. (1998). Kar9p is a novel cortical protein required for cytoplasmic microtubule orientation in yeast. *Journal of Cell Biology*, *140*(2), 377–390. https://doi.org/10.1083/jcb.140.2.377

Miller, Rita K, Heller, K. K., Frise, L., Wallack, D. L., Loayza, D., Gammie, A. E., & Rose, M. D. (1998). The Kinesin-related Proteins, Kip2p and Kip3p, Function Differently in Nuclear Migration in Yeast. *Molecular Biology of the Cell*, *9*(August), 2051–2068.

Mitchison, T. J., & Salmon, E. D. (2001). Mitosis: A history of division. *Nature Cell Biology*, *3*(1), 17–21. https://doi.org/10.1038/35050656

Miyazaki, W. Y., & Orr-Weaver, T. L. (1994). Sister-chromatid cohesion in mitosis and meiosis. *Annual Review of Genetics*, *28*(29), 167–187. https://doi.org/10.1146/annurev.ge.28.120194.001123

Moens, P. B., & Rapport, E. (1971). Spindles, spindle plaques, and meiosis in the yeast Saccharomyces Cerevisiae. *Journal of Cell Biology*, *50*(2), 344–361. https://doi.org/10.1083/jcb.50.2.344

Molk, J. N., Schuyler, S. C., Liu, J. Y., Evans, J. G., Salmon, E. D., Pellman, D., & Bloom, K. (2004). The differential roles of budding yeast Tem1p, Cdc15p, and Bub2p protein dynamics in mitotic exit. *Molecular Biology of the Cell*, *15*(4), 1519–1532. https://doi.org/10.1091/mbc.e03-09-0708

Moore, J. K., Chudalayandi, P., Heil-Chapdelaine, R. A., & Cooper, J. A. (2010). The spindle position checkpoint is coordinated by the Elm1 kinase. *Journal of Cell Biology*, *191*(3), 493–503. https://doi.org/10.1083/jcb.201006092

Moore, J. K., D'Silva, S., & Miller, R. K. (2006). The CLIP-170 homologue Bik1p promotes the phosphorylation and asymmetric localization of Kar9p. *Molecular Biology of the Cell*, *17*(1), 178–191. https://doi.org/10.1091/mbc.e05-06-0565

Morgan, D. O. (1995). Principles of CDK regulation. *Nature*, Vol. 374, pp. 131–134. https://doi.org/10.1038/374131a0

MORTIMER, R. K., & JOHNSTON, J. R. (1959). Life Span of Individual Yeast Cells. *Nature*, *183*(4677), 1751–1752. https://doi.org/10.1038/1831751a0

Moseley, J. B., & Goode, B. L. (2006). The Yeast Actin Cytoskeleton: from Cellular Function to Biochemical Mechanism. *Microbiology and Molecular Biology Reviews*, *70*(3), 605–645. https://doi.org/10.1128/mmbr.00013-06

Nasmyth, K. (1993). Regulating the HO endonuclease in yeast. *Current Opinion in*

Genetics & Development, *3*(2), 286–294. https://doi.org/10.1016/0959-437x(93)90036-o

Nicklas, R. B., & Arana, P. (1992). Evolution and the meaning of metaphase. *Journal of Cell Science*, *102*(4), 681–690.

Norbury, C., & Nurse, P. (1992). Animal cell cycles and their control. *Annual Review of Biochemistry*, *61*, 441–470. https://doi.org/10.1146/annurev.biochem.61.1.441

Nurse, P. (1975). *Genetic control of cell size at cell division in yeast*.

Obaya, A. J., & Sedivy, J. M. (2002). Regulation of cyclin-Cdk activity in mammalian cells. *Cellular and Molecular Life Sciences*, *59*(1), 126–142. https://doi.org/10.1007/s00018-002-8410-1

Oehlen, L. J. W. M., & Cross, F. R. (1994). G1 cyclins CLN1 and CLN2 repress the mating factor response pathway at start in the yeast cell cycle. *Genes and Development*, *8*(9), 1058–1070. https://doi.org/10.1101/gad.8.9.1058

Palmer, R., Sullivan, D., Huffaker, T., & Koshland, D. (1992). Role of Astral Microtubules and Actin in Spindle Orientation and Migration in the Budding Yeast, Saccharomyces cerevisiae. *Journal of Cell Biology*, *119*(2), 379–388.

Paoletti, A., & Bornens, M. (2003). Kar9 asymmetrical loading on spindle poles mediates proper spindle alignment in budding yeast. *Developmental Cell*, *4*(3), 289–290. https://doi.org/10.1016/S1534-5807(03)00065-0

Pereira, G., Höfken, T., Grindlay, J., Manson, C., & Schiebel, E. (2000). The Bub2p spindle checkpoint links nuclear migration with mitotic exit. *Molecular Cell*, *6*(1), 1–10. https://doi.org/10.1016/S1097-2765(05)00017-1

Pereira, G., Manson, C., Grindlay, J., & Schiebel, E. (2002). Regulation of the Bfa1p-Bub2p complex at spindle pole bodies by the cell cycle phosphatase Cdc14p. *The Journal of Cell Biology*, *157*(3), 367–379. https://doi.org/10.1083/jcb.200112085

Pereira, G., & Schiebel, E. (2003). Separase regulates INCENP-Aurora B anaphase spindle function through Cdc14. *Science (New York, N.Y.)*, *302*(5653), 2120–2124. https://doi.org/10.1126/science.1091936

Pereira, G., & Schiebel, E. (2005a). Kin4 kinase delays mitotic exit in response to

spindle alignment defects. *Molecular Cell*, *19*(2), 209–221. https://doi.org/10.1016/j.molcel.2005.05.030

Pereira, G., & Schiebel, E. (2005b). Kin4 kinase delays mitotic exit in response to spindle alignment defects. *Molecular Cell*, *19*(2), 209–221. https://doi.org/10.1016/j.molcel.2005.05.030

Pereira, G., Tanaka, T. U., Nasmyth, K., & Schiebel, E. (2001). Modes of spindle pole body inheritance and segregation of the Bfa1p-Bub2p checkpoint protein complex. *EMBO Journal*, *20*(22), 6359–6370. https://doi.org/10.1093/emboj/20.22.6359

Pereira, G., & Yamashita, Y. M. (2011). Fly meets yeast: checking the correct orientation of cell division. *Trends in Cell Biology*, *21*(9), 526–533. https://doi.org/10.1016/j.tcb.2011.05.004

Pfleger, C. M., & Kirschner, M. W. (2000). The KEN box: an APC recognition signal distinct from the D box targeted by Cdh1. *Genes & Development*, *14*(6), 655–665.

Piatti, S., Böhm, T., Cocker, J. H., Diffley, J. F. X., & Nasmyth, K. (1996). Activation of S-phase-promoting CDKs in late G1 defines a “point of no return” after which Cdc6 synthesis cannot promote DNA replication in yeast. *Genes and Development*, *10*(12), 1516–1531. https://doi.org/10.1101/gad.10.12.1516

Pretorius, I. S. (2017). Synthetic genome engineering forging new frontiers for wine yeast. *Critical Reviews in Biotechnology*, *37*(1), 112–136. https://doi.org/10.1080/07388551.2016.1214945

Qiao, X., Zhang, L., Gamper, A. M., Fujita, T., & Wan, Y. (2010). APC/C-Cdh1: From cell cycle to cellular differentiation and genomic integrity. *Cell Cycle*, *9*(19), 3904–3912. https://doi.org/10.4161/cc.9.19.13585

Rhyu, M. S., & Knoblich, J. A. (1995). Spindle orientation and asymmetric cell fate. *Cell*, *82*(4), 523–526. https://doi.org/10.1016/0092-8674(95)90022-5

Rizk, R. S., DiScipio, K. A., Proudfoot, K. G., & Gupta, M. L. (2014). The kinesin-8 Kip3 scales anaphase spindle length by suppression of midzone microtubule polymerization. *Journal of Cell Biology*, *204*(6), 965–975. https://doi.org/10.1083/jcb.201312039

Robinow, C., & Marak, J. (1966). A FIBER APPARATUS IN THE NUCLEUS OF

THE YEAST CELL. *The Journal of Cell Biology*, (3).

Rock, J. M., & Amon, A. (2009). The FEAR network. *Current Biology : CB*, *19*(23), R1063-8. https://doi.org/10.1016/j.cub.2009.10.002

Roof, D. M., Meluh, P. B., & Rose, M. D. (1992). Kinesin-related proteins required for assembly of the mitotic spindle. *Journal of Cell Biology*, *118*(1), 95–108. https://doi.org/10.1083/jcb.118.1.95

Rout, M. P., & Kilmartin, J. V. (1990). Components of the yeast spindle and spindle pole body. *Journal of Cell Biology*, *111*(5 I), 1913–1927. https://doi.org/10.1083/jcb.111.5.1913

Sanchez, Y., Bachant, J., Wang, H., Hu, F., Liu, D., Tetzlaff, M., & Elledge, S. (1999). Control of the DNA Damage Checkpoint by Chkl and Rad53 Protein Kinases Through Distinct Mechanisms. *Science*, *286*(5442), 1166–1171.

Schaerer, F., Morgan, G., Winey, M., & Philippsen, P. (2001). Cnm67p is a spacer protein of the Saccharomyces cerevisiae spindle pole body outer plaque. *Molecular Biology of the Cell*, *12*(8), 2519–2533. https://doi.org/10.1091/mbc.12.8.2519

Schmoller, K. M., Turner, J. J., Kõivomägi, M., & Skotheim, J. M. (2015). Dilution of the cell cycle inhibitor Whi5 controls budding-yeast cell size. *Nature*, *526*(7572), 268–272. https://doi.org/10.1038/nature14908

Schweitzer, B., & Philippsen, P. (1991). CDC15, an essential cell cycle gene in Saccharomyces cerevisiae, encodes a protein kinase domain. *Yeast (Chichester, England)*, *7*(3), 265–273. https://doi.org/10.1002/yea.320070308

Segal, M, Clarke, D. J., & Reed, S. I. (1998). Clb5-associated kinase activity is required early in the spindle pathway for correct preanaphase nuclear positioning in Saccharomyces cerevisiae. *The Journal of Cell Biology*, *143*(1), 135–145. https://doi.org/10.1083/jcb.143.1.135

Segal, Marisa, & Bloom, K. (2001). Control of spindle polarity and orientation in Saccharomyces cerevisiae. *Trends in Cell Biology*, *11*(4), 160–166. https://doi.org/10.1016/S0962-8924(01)01954-7

Seshan, A., & Amon, A. (2005). Ras and the Rho effector Cla4 collaborate to target and anchor Lte1 at the bud cortex. *Cell Cycle*, *4*(7), 940–946.

https://doi.org/10.4161/cc.4.7.1785

Seshan, A., Bardin, A. J., & Amon, A. (2002). Control of Lte1 localization by cell polarity determinants and Cdc14. *Current Biology : CB*, *12*(24), 2098–2110. https://doi.org/10.1016/s0960-9822(02)01388-x

Seybold, C., & Schiebel, E. (2013). Spindle pole bodies. *Current Biology*, *23*(19), R858–R860. https://doi.org/10.1016/j.cub.2013.07.024

Shah, J., Botvinick, E., Bonday, Z., Furnari, F., Berns, M., & Cleveland, D. (2004). Dynamics of Centromere and Kinetochore Proteins: Implications for Checkpoint Signaling and Silencing. *Current Biology*, *14*. https://doi.org/10.1016/j

Sheeman, B., Carvalho, P., Sagot, I., Geiser, J., Kho, D., Hoyt, M. A., & Pellman, D. (2003). Determinants of S. cerevisiae dynein localization and activation: Implications for the mechanism of spindle positioning. *Current Biology*, *13*(5), 364–372. https://doi.org/10.1016/S0960-9822(03)00013-7

Sherr, C. J., & Roberts, J. M. (1999). CDK inhibitors: Positive and negative regulators of G1-phase progression. *Genes and Development*, *13*(12), 1501–1512. https://doi.org/10.1101/gad.13.12.1501

Shirayama, M., Matsui, Y., & Toh-E, A. (1994). The yeast TEM1 gene, which encodes a GTP-binding protein, is involved in termination of M phase. *Molecular and Cellular Biology*, *14*(11), 7476–7482. https://doi.org/10.1128/mcb.14.11.7476-7482.1994

Shou, W, Seol, J. H., Shevchenko, A., Baskerville, C., Moazed, D., Chen, Z. W., … Deshaies, R. J. (1999). Exit from mitosis is triggered by Tem1-dependent release of the protein phosphatase Cdc14 from nucleolar RENT complex. *Cell*, *97*(2), 233–244. https://doi.org/10.1016/s0092-8674(00)80733-3

Shou, Wenying, Seol, J. H., Shevchenko, A., Baskerville, C., Moazed, D., Susan Chen, Z. W., … Deshaies, R. J. (1999). Exit from mitosis is triggered by Tem1-dependent release of the protein phosphatase Cdc14 from nucleolar RENT complex. *Cell*, *97*(2), 233–244. https://doi.org/10.1016/S0092-8674(00)80733-3

Sikorski, R. S., & Hieter, P. (1989). A system of shuttle vectors and yeast host strains designed for efficient manipulation of DNA in Saccharomyces cerevisiae.

Genetics, *122*(1), 19–27.

Slaughter, B. D., Smith, S. E., & Li, R. (2009). Symmetry breaking in the life cycle of the budding yeast. *Cold Spring Harbor Perspectives in Biology*, *1*(3), 1–19. https://doi.org/10.1101/cshperspect.a003384

Stegmeier, F., & Amon, A. (2004). Closing mitosis: the functions of the Cdc14 phosphatase and its regulation. *Annual Review of Genetics*, *38*, 203–232. https://doi.org/10.1146/annurev.genet.38.072902.093051

Stegmeier, F., Visintin, R., & Amon, A. (2002). Separase, polo kinase, the kinetochore protein Slk19, and Spo12 function in a network that controls Cdc14 localization during early anaphase. *Cell*, *108*(2), 207–220. https://doi.org/10.1016/s0092-8674(02)00618-9

Stirling, D. A., Welch, K. A., & Stark, M. J. (1994). Interaction with calmodulin is required for the function of Spc110p, an essential component of the yeast spindle pole body. *The EMBO Journal*, *13*(18), 4329–4342.

Straight, A F, Shou, W., Dowd, G. J., Turck, C. W., Deshaies, R. J., Johnson, A. D., & Moazed, D. (1999). Net1, a Sir2-associated nucleolar protein required for rDNA silencing and nucleolar integrity. *Cell*, *97*(2), 245–256. https://doi.org/10.1016/s0092-8674(00)80734-5

Straight, Aaron F, Marshall, W. F., Sedat, J. W., & Murray, A. W. (1997). *Mitosis in Living Budding Yeast: Anaphase A But No Metaphase Plate*. (July).

Sudakin, V., Chan, G. K. T., & Yen, T. J. (2001). Checkpoint inhibition of the APC/C in HeLa cells is mediated by a complex of BUBR1, BUB3, CDC20, and MAD2. *Journal of Cell Biology*, *154*(5), 925–936. https://doi.org/10.1083/jcb.200102093

Sun, S., & Heitman, J. (2011). Is sex necessary? *BMC Biology*, *9*(May 2014). https://doi.org/10.1186/1741-7007-9-56

Taylor, S., & Peters, J.-M. (2008). Polo and Aurora kinases: lessons derived from chemical biology. *Current Opinion in Cell Biology*, *20*(1), 77–84. https://doi.org/10.1016/j.ceb.2007.11.008

Ten Hoopen, R., Cepeda-García, C., Fernández-Arruti, R., Juanes, M. A., Delgehyr, N., & Segal, M. (2012). Mechanism for astral microtubule capture by cortical Bud6p

priming spindle Polarity in S. cerevisiae. *Current Biology*, *22*(12), 1075–1083. https://doi.org/10.1016/j.cub.2012.04.059

Toyn, J. H., & Johnston, L. H. (1993). Spo12 is a limiting factor that interacts with the cell cycle protein kinases Dbf2 and Dbf20, which are involved in mitotic chromatid disjunction. *Genetics*, *135*(4), 963–971.

Traverso, E. E., Baskerville, C., Liu, Y., Shou, W., James, P., Deshaies, R. J., & Charbonneau, H. (2001). Characterization of the Net1 cell cycle-dependent regulator of the Cdc14 phosphatase from budding yeast. *The Journal of Biological Chemistry*, *276*(24), 21924–21931. https://doi.org/10.1074/jbc.M011689200

Tvegård, T., Soltani, H., Skjølberg, H. C., Krohn, M., Nilssen, E. A., Kearsey, S. E., … Boye, E. (2007). A novel checkpoint mechanism regulating the G1/S transition. *Genes and Development*, *21*(6), 649–654. https://doi.org/10.1101/gad.421807

Udden, M. M., & Finkelstein, D. B. (1978). Reaction order of Saccharomyces cerevisiae alpha factor mediated cell cycle arrest and mating inhibition. *Journal of Bacteriology*, *133*(3), 1501–1507. https://doi.org/10.1128/jb.133.3.1501-1507.1978

Uhlmann, F, Lottspeich, F., & Nasmyth, K. (1999). Sister-chromatid separation at anaphase onset is promoted by cleavage of the cohesin subunit Scc1. *Nature*, *400*(6739), 37–42. https://doi.org/10.1038/21831

Uhlmann, Frank, Lottspelch, F., & Nasmyth, K. (1999). Sister-chromatid separation at anaphase onset is promoted by cleavage of the cohesin subunit Scc1. *Nature*, *400*(6739), 37–42. https://doi.org/10.1038/21831

Usui, T., Ogawa, H., & Petrini, J. H. (2001). A DNA damage response pathway controlled by Tel1 and the Mre11 complex. *Molecular Cell*, *7*(6), 1255–1266. https://doi.org/10.1016/s1097-2765(01)00270-2

Visintin, R, & Amon, A. (2001). Regulation of the mitotic exit protein kinases Cdc15 and Dbf2. *Molecular Biology of the Cell*, *12*(10), 2961–2974. https://doi.org/10.1091/mbc.12.10.2961

Visintin, R, Craig, K., Hwang, E. S., Prinz, S., Tyers, M., & Amon, A. (1998). The phosphatase Cdc14 triggers mitotic exit by reversal of Cdk-dependent phosphorylation. *Molecular Cell*, *2*(6), 709–718. https://doi.org/10.1016/s1097-

2765(00)80286-5

Visintin, R, Prinz, S., & Amon, A. (1997). CDC20 and CDH1: a family of substrate-specific activators of APC-dependent proteolysis. *Science (New York, N.Y.)*, *278*(5337), 460–463. https://doi.org/10.1126/science.278.5337.460

Visintin, Rosella, Craig, K., Hwang, E. S., Prinz, S., Tyers, M., & Amon, A. (1998). The phosphatase Cdc14 triggers mitotic exit by reversal of Cdk-dependent phosphorylation. *Molecular Cell*, *2*(6), 709–718. https://doi.org/10.1016/S1097-2765(00)80286-5

Visintin, Rosella, Prinz, S., & Amon, A. (1997). CDC20 and CDHI: A Family of Su bstrate-Specif ic Activators of APC-~ependent Proteolysis. *Science*, 2–5.

Wang, X., Tsai, J. W., Imai, J. H., Lian, W. N., Vallee, R. B., & Shi, S. H. (2009). Asymmetric centrosome inheritance maintains neural progenitors in the neocortex. *Nature*, *461*(7266), 947–955. https://doi.org/10.1038/nature08435

Wang, Y., & Burke, D. J. (1997). Cdc55p, the B-type regulatory subunit of protein phosphatase 2A, has multiple functions in mitosis and is required for the kinetochore/spindle checkpoint in Saccharomyces cerevisiae. *Molecular and Cellular Biology*, *17*(2), 620–626. https://doi.org/10.1128/MCB.17.2.620

Wang, Y., Hu, F., & Elledge, S. J. (2000). The Bfa1/Bub2 GAP complex comprises a universal checkpoint required to prevent mitotic exit. *Current Biology : CB*, *10*(21), 1379–1382. https://doi.org/10.1016/s0960-9822(00)00779-x

Wäsch, R., & Cross, F. R. (2002). APC-dependent proteolysis of the mitotic cyclin Clb2 is essential for mitotic exit. *Nature*, *418*(6897), 556–562. https://doi.org/10.1038/nature00856

Wigge, P. A., Jensen, O. N., Holmes, S., Souès, S., Mann, M., Kilmartin, J. V, … Cell, W. L. M. (1998). *Analysis of the*. *141*(4), 967–977.

Woodruff, J. B., Drubin, D. G., & Barnes, G. (2009). Dynein-driven mitotic spindle positioning restricted to anaphase by She1p inhibition of dynactin recruitment. *Molecular Biology of the Cell*, *20*(13), 3003–3011. https://doi.org/10.1091/mbc.e09-03-0186

Woodruff, J. B., Drubin, D. G., & Barnes, G. (2010). Mitotic spindle disassembly

occurs via distinct subprocesses driven by the anaphase-promoting complex, Aurora B kinase, and kinesin-8. *The Journal of Cell Biology*, *191*(4), 795–808. https://doi.org/10.1083/jcb.201006028

Yeh, E., Skibbens, R. V., Cheng, J. W., Salmon, E. D., & Bloom, K. (1995). Spindle dynamics and cell cycle regulation of dynein in the budding yeast, Saccharomyces cerevisiae. *Journal of Cell Biology*, *130*(3), 687–700. https://doi.org/10.1083/jcb.130.3.687

Yin, H., Pruyne, D., Huffaker, T. C., & Bretscher, A. (2000). Myosin V orientates the mitotic spindle in yeast. *Nature*, *406*(6799), 1013–1015. https://doi.org/10.1038/35023024

Yoshida, S, & Toh-e, A. (2001). Regulation of the localization of Dbf2 and mob1 during cell division of saccharomyces cerevisiae. *Genes & Genetic Systems*, *76*(2), 141–147. https://doi.org/10.1266/ggs.76.141

Yoshida, Satoshi, Asakawa, K., & Toh-e, A. (2002). Mitotic exit network controls the localization of Cdc14 to the spindle pole body in Saccharomyces cerevisiae. *Current Biology : CB*, *12*(11), 944–950. https://doi.org/10.1016/s0960-9822(02)00870-9

Zachariae, W., & Nasmyth, K. (1999). Whose end is destruction: Cell division and the anaphase-promoting complex. *Genes and Development*, *13*(16), 2039–2058. https://doi.org/10.1101/gad.13.16.2039

Zegerman, P., & Diffley, J. F. X. (2009). DNA replication as a target of the DNA damage checkpoint. *DNA Repair*, *8*(9), 1077–1088. https://doi.org/10.1016/j.dnarep.2009.04.023

Zhaoxia, S., Hsiao, J., David, F., & Stern, D. (1997). Rad53 FHA Domain Associated with Phosphorylated Rad9 in the DNA Damage Checkpoint. *Genomic Instability and Immortality in Cancer*, *281*(74), 149–157. https://doi.org/10.1007/978-1-4615-5365-6_10

Zhou, B. S., & Elledge, S. J. (2000). Checkpoints in Perspective. *Nature*, *408*(November), 433–439.

Chapter 7: **APPENDIX**

7.1 ***Table of Strains***

Table 7. 1: Table showing the stains used in this thesis.

Strain Name	**Description**	**Reference**
AKY038	*ESM356 Bfa1-GFP-kanMX6 Spc42-eqFP- hphNT1 mCherry-Tub1-URA3*	This study
AKY043	*ESM356 BFA1-GFP-kanMX6 Spc42-eqFP-hphNT1 kar9Δ::klTRP1 pRS316-KAR9*	(Caydasi & Pereira, 2009)
AKY2526	*FAY145 lte1Δ::kanMX6 pRS316-LTE1 spo12Δ::natNT2*	(Caydasi et al., 2017)
AKY260	*ESM356 kar9Δ::HIS3MX6 pRS316-KAR9*	(Caydasi et al., 2017)
AKY2916	*FAY145 lte1Δ::kanMX6 pRS316-LTE1 spo12Δ::natNT2 bud14Δ::HIS3MX6*	This study
AKY2917	*YPH499 GFP-Tub1-URA3 dyn1Δ::klTRP1 bud14Δ::HIS3MX6*	This study
AKY2918	*YPH499 GFP-Tub1-URA3 dyn1Δ::klTRP1 kin4Δ::hphNT1 bud14Δ::HIS3MX6*	This study
AKY315	*ESM356 kar9Δ::HIS3MX6 pRS316-KAR9 bfa1Δ::klTRP1*	(Caydasi et al., 2017)
AKY321	*ESM356 kar9Δ::HIS3MX6 pRS316-KAR9 kin4Δ::klTRP1*	(Caydasi et al., 2017)
AKY346	*YPH499 kar9Δ::klTRP1 pRS316-KAR9 GFP-Tub1-ADE2*	(Caydasi et al., 2010)
AKY351	*YPH499 kar9Δ::klTRP1 pRS316-KAR9 kin4Δ::HIS3MX6 GFP-Tub1-ADE2*	(Caydasi et al., 2010)
AKY4007	*ESM356 Bub2-GFP-kanMX6 Spc42-eqFP-hphNT1 mCherry-Tub1-URA3*	This study

AKY4008	*ESM356 Tem1-GFP-kanMX6 Spc42-eqFP-hphNT1 bud14Δ::HIS3MX6 mCherry-Tub1-URA3*	This study
AKY4009	*ESM356 Bub2-GFP-kanMX6 Spc42-eqFP-hphNT1 bud14Δ::klTRP1 mCherry-Tub1-URA3*	This study
AKY4011	*ESM356 Bfa1-GFP-kanMX6 Spc42-eqFP-hphNT1 bud14Δ::klTRP1 mCherry-Tub1-URA3*	This study
AKY4012	*ESM356 Bfa1-GFP-kanMX6 Spc42-eqFP-hphNT1 mCherry-Tub1-URA3*	This study
AKY4013	*ESM356 Tem1-GFP-kanMX6 Spc42-eqFP-hphNT1 mCherry-Tub1-URA3*	This study
AKY4040	*ESM356 Spc42-eqFP-hphNT1 BUD14-GFP-his3MX6 mCherry-Tub1-URA3*	This study
AKY4068	*YPH499 kar9Δ::klTRP1 pRS316-KAR9 GFP-Tub1-ADE2 bud14Δ::HIS3MX6 kin4Δ::hphNT1*	This study
AKY4070	*ESM356 Spc42-eqFP-hphNT1 BUD14-GFP-his3MX6 mCherry-Tub1-URA3 kar9Δ::klTRP1*	This study
AKY4078	*PAY704 MATa ade2-1 his3-11,15 leu2-3,112 ura3-1 can1-100 ssd1-d2 glc7::LEU2 trp1-1::GLC7::TRP1 kar9Δ::hphNT1*	This study
AKY4079	*PAY701 MATa ade2-1 his3-11,15 leu2-3,112 ura3-1 can1-100 ssd1-d2 glc7::LEU2 trp1-1::glc7-12::TRP1 kar9Δ::hphNT1*	This study
AKY4088	*ESM356 Mob1-GFP-kanMX6 Spc42-eqFP-hphNT1 kin4Δ::natNT2 bud14Δ::HIS3MX6*	This study
AKY4094	*YPH499 cdc14-2 pRS316-CDC14 bfa1Δ::klTRP3*	This study
AKY4095	*YPH499 dbf2-2 pRS316-DBF2 bfa1Δ::klTRP3*	This study
AKY4102	*ESM356 Mob1-GFP-kanMX6 Spc42-eqFP-hphNT1 kin4Δ::natNT2 bud14Δ::HIS3MX6 mCherry-Tub1-LEU2*	This study
BKY032	*ESM356 BFA1-GFP-kanMX6 Spc42-eqFP-hphNT1 kar9Δ::klTRP1 pRS316-KAR9 kin4Δ::HIS3MX6*	(Caydasi & Pereira, 2009)
DKY056	*YPH499 bud14Δ::kITRP3*	This study
DKY057	*YPH499 cdc14-2 pRS316-CDC14 bud14Δ::klTRP3*	This study

DKY058	*YPH499 mob1-67 pRS316-MOB1 bud14Δ::klTRP3*	This study
DKY060	*YPH499 dbf2-2 pRS316-DBF2 bud14Δ::klTRP3*	This study
DKY061	*YPH499 cdc15-1 pRS316-CDC15 bud14Δ::klTRP3*	This study
DKY069	*FAY145 lte1Δ::kanMX6 pRS316-LTE1 bud14Δ::HIS3MX6*	This study
DKY070	*PAY704 MATa ade2-1 his3-11,15 leu2-3,112 ura3-1 can1-100 ssd1-d2 glc7::LEU2 trp1-1::GLC7::TRP1*	This study
DKY071	*PAY701 MATa ade2-1 his3-11,15 leu2-3,112 ura3-1 can1-100 ssd1-d2 glc7::LEU2 trp1-1::glc7-12::TRP1*	This study
DKY081	*ESM356 BFA1-GFP-kanMX6 Spc42-eqFP hphNT1 kar9Δ::klTRP1 pRS316-KAR9 bud14Δ::HIS3MX6*	This study
DKY145	*ESM356 kar9Δ::HIS3MX6 bud14Δ::klTRP1 pRS316*	This study
DKY147	*ESM356 kar9Δ::HIS3MX6 bud14Δ::klTRP1 pMK125*	This study
DKY149	*ESM356 kar9Δ::HIS3MX6 bud14Δ::klTRP1 pMK131*	This study
DKY179	*YPH499 cdc5-10 pRS316-CDC5 bud14Δ::klTRP3*	This study
ESM2156	*YPH499 GFP-Tub1-URA3 dyn1Δ::klTRP1 kin4Δ::hphNT1*	(Pereira & Schiebel, 2005a)
ESM2282	*YPH499 cdc15-1 pRS316-CDC15*	(Caydasi et al., 2017)
ESM2283	*YPH499 dbf2-2 pRS316-DBF2*	(Caydasi et al., 2017)
ESM2285	*YPH499 mob1-67 pRS316-MOB1*	(Caydasi et al., 2017)
ESM356	*MATa ura3-52 leu2Δ1 his3Δ200 trp1Δ63*	(Pereira et al., 2001)

FAY145	*MATa ura3-52 his3Δ200 leu2Δ1 lte1Δ::kanMX6 pRS316-LTE1*	(Bertazzi et al., 2011)
GPY1054	*ESM356 Mob1-GFP-kanMX6 Spc42-eqFP-hphNT1*	This study
GPY491	*YPH499 cdc14-2 pRS316- CDC14*	(Caydasi et al., 2017)
HKY099	*ESM356 BFA1-GFP-kanMX6 Spc42-eqFP-hphNT1 kar9Δ::klTRP1 pRS316-KAR9 mCherry-Tub1-LEU2*	This study
HKY100	*ESM356 BFA1-GFP-kanMX6 Spc42-eqFP-hphNT1 kar9Δ::klTRP1 pRS316-KAR9 kin4Δ::HIS3MX6 mCherry-Tub1-LEU2*	This study
HKY101	*ESM356 BFA1-GFP-kanMX6 Spc42-eqFP-hphNT1 kar9Δ::klTRP1 pRS316-KAR9 bud14Δ::HIS3MX6 mCherry-Tub1-LEU2*	This study
HKY114	*ESM356 Bfa1-GFP-kanMX6 Spc42-eqFP-hphNT1 mCherry-Tub1-LEU2 pRS416*	This study
HKY115	*ESM356 Bfa1-GFP-kanMX6 Spc42-eqFP-hphNT1 bud14Δ::klTRP1 mCherry-Tub1-LEU2 pRS416*	This study
HKY116	*ESM356 Bfa1-GFP-kanMX6 Spc42-eqFP-hphNT1 bud14Δ::klTRP1 mCherry-Tub1-LEU2 pRS416-BUD14*	This study
HKY133	*FAY145 lte1Δ::kanMX6 pRS316-LTE1 kel1Δ::hphNT1*	This study
HKY134	*FAY145 lte1Δ::kanMX6 pRS316-LTE1 kel2Δ::hphNT1*	This study
HKY135	*FAY145 lte1Δ::kanMX6 pRS316-LTE1 spo12Δ::natNT2 kel1Δ::hphNT1*	This study
HKY136	*FAY145 lte1Δ::kanMX6 pRS316-LTE1 spo12Δ::natNT2 kel2Δ::hphNT1*	This study
HKY139	*ESM356 kar9Δ::HIS3MX6 pRS316-KAR9 kel1Δ::hphNT1*	This study
HKY140	*ESM356 kar9Δ::HIS3MX6 pRS316-KAR9 kel2Δ::hphNT1*	This study

HKY155	*ESM356 BUD14-TAP-kanMX6*	This study
HKY171	*ESM356 Mob1-GFP-kanMX6 Spc42-eqFP-hphNT1 mCherry-Tub1-LEU2*	This study
HKY172	*ESM356 Mob1-GFP-kanMX6 Spc42-eqFP-hphNT1 mCherry-Tub1-LEU2 bud14Δ::HIS3MX6*	This study
HKY173	*ESM356 Mob1-GFP-kanMX6 Spc42-eqFP-hphNT1 mCherry-Tub1-LEU2 kin4Δ::natNT2*	This study
HKY174	*ESM356 Mob1-GFP-kanMX6 Spc42-eqFP-hphNT1 mCherry-Tub1-LEU2 bfa1Δ::natNT2*	This study
HKY175	*YPH499 kar9Δ::klTRP1 pRS316-KAR9 GFP-Tub1-ADE2 bud14Δ::HIS3MX6 bfa1Δ::natNT2*	This study
HKY177	*YPH499 bfa1Δ::klTRP1*	This study
HKY180	*YPH499 mob1-67 pRS316-MOB1 bfa1Δ::klTRP3*	This study
HKY182	*YPH499 cdc15-1 pRS316-CDC15 bfa1Δ::klTRP3*	This study
HKY183	*YPH499 cdc5-10 pRS316-CDC5 bfa1Δ::klTRP3*	This study
HKY190	*ESM356 BFA1-GFP-kanMX6 Spc42-eqFP-hphNT1 bud14Δ::klTRP1 mCherry-TUB1-Leu2 pMK131*	This study
JOY79	*YPH499 cdc5-10 pRS316-CDC5*	(Caydasi et al., 2017)
SEY032	*YPH499 kar9Δ::klTRP3 pRS316-KAR9 GFP-Tub1-ADE2 bud14Δ::HIS3MX6*	This study
SHM562	*YPH499 GFP-Tub1-URA3 dyn1Δ::klTRP1*	(Pereira & Schiebel, 2005a)
YDA101	*ESM356 kar9Δ::HIS3MX6 bud14Δ::klTRP1*	This study
YPH499	*MATa ura3-52 lys2-801 ade2-101 trp1Δ63 his3Δ200 leu2Δ1*	(Sikorski & Hieter, 1989)

7.2 *Table of Plasmids*

Table 7. 2: Table showing the plasmids used in this thesis.

Plasmid Name	**Description**	**Reference**
pAFS125	*GFP-TUB1-URA3* containing integration plasmid.	(Straight et al., 1997)
pAK011	*mCherry-TUB1-URA3* containing integration plasmid.	(Khmelinskii et al., 2007)
pBK067	*mCherry-TUB1-LEU2* containing integration plasmid.	(Caydasi et al., 2014)
pBS9	*pRS316-CDC15*	(Schweitzer & Philippsen, 1991)
pCL33	*pRS316-CDC5*	(Höfken & Schiebel, 2004)
pGW399	*pRS316-KAR9*	(Höfken & Schiebel, 2002)
pMK125	*pRS416 ADH-BUD14*	(Knaus et al., 2005)
pMK131	*pRS416 ADH-BUD14-F379A*	(Knaus et al., 2005)
pRS316	*URA3-dependent CEN-based yeast-E. coli* shuffle plasmid. *AmpR.*	(Sikorski & Hieter, 1989)
pRS416	*URA3-dependent CEN-based yeast-E. coli* shuffle plasmid. *AmpR.*	(Sikorski & Hieter, 1989)
pSM1027	*GFP-TUB1-ADE2 containing integration plasmid.*	
pSM903	*pRS316-LTE1*	(Höfken & Schiebel, 2002)
pSM908	*pRS316-DBF2*	From Elmar Schiebel
pSM926	*pRS316-MOB1*	From Elmar Schiebel

pUG120	*pRS316-CDC14*	(Gruneberg, Campbell, Simpson, Grindlay, & Schiebel, 2000)

7.3 *Table of Primers*

Table 7. 3: Table showing the primers used in this thesis.

BFA1-1	GTGATTCAAATGTTGGGTGAGC
BFA1-2	CGAGTTTTAATCCATTCCACCC
BFA1-S1	TGCGTACGCTGCAGGTCGACAGAAAAAAGTTCGAAAACTTTTGTAGCAGTTGAAAGTTTTGTATGCTA
BFA1-S2	TGTACTCAAGATAACGGTAAAGAAACAGTTATAAGAAGGCTAAAGGGCTAATCGATGAATTCGAGCTCG
BFA1-S3	AATCCTATATGTATGAAATCAGGAACATGGTAATCAATTCGACAAAAGATCGTACGCTGCAGGTCGAC
BUB2-S2	TTGTAGAATTAAACGATAAAATATAATATTTCTTCACATAGTTTAATCGATGAATTCGAGCTCG
BUB2-S3	GACCTATTGGTAGACCACTTGACCGACCCAGACATATATATACCGCGTACGCTGCAGGTCGAC
BUD14-1	CACGACTAAGTAGTTGTCG
BUD14-2	GCAAGAGTCAGACTGACTCG
BUD14-S1	GTGAAATACACGTAGTTTTTAGATAACATTCTCTGCTTGGTAAGAGAATGCGTACGCTGCAGGTCGAC
BUD14-S2	AAGTTCGTTGGATGAGAAAAAGACCAGGCTTTATTGTAAGGACAATATCAATCGATGAATTCGAGCTCG
BUD14-S3	TTGACAGAATGGATGTGTTGATGAAACAATTGGATGAAATTATTCGTAAACGTACGCTGCAGGTCGAC
DYN1-S1	CAGAGCTTAAATTGGAAAGTACGTCAAAACGTTTTTTAGGCAATGCGTACGCTGCAGGTCGAC
DYN1-S2	TGAGAAAACCGCGGACAAGCAAGACACGCGTACCTGAAAAGGCTAATCGATGAATTCGAGCTCG

KAR9-S1	ATCTTTGTCTGTAACAGCCTTAAAGATTTCAGTAGCACTGCC ATGCGTACGCTGCAGGTCGAC
KAR9-S2	AGGATATATAAAAATGTATAAGTATACAGTTTTAGGTTAGT ATCAATCGATGAATTCGAGCTCG
KEL1-1	ATCCTCGGATCCATGTAG
KEL1-2	GCAATCGGACTATTCTGC
KEL1-S1	AGTTAGAGCCCGTTTGCTTCAATTTGCACCTAGAAAATAACT CAAACATGCGTACGCTGCAGGTCGAC
KEL1-S2	ATTGTTATTACACATGAAAAGTGAAATTTCATTACGCATATT GTCTTTTAATCGATGAATTCGAGCTCG
KEL2-1	GCATGGATTGTGCTGATG
KEL2-2	CTGAACAGTTTCGCTTCG
KEL2-S1	GTAACAAAAAAAAAAAATGATTTGGATGAGGCAGGCAACC CCTTAAGTAGCTATGCGTACGCTGCAGGTCGAC
KEL2-S2	ACTTTGTACATATTGACTTCCCAGTGCGTAACAACGTCTTCC AATGACTAATCGATGAATTCGAGCTCG
KIN4-1	AATCGCATCGGTGGGAGAG
KIN4-2	AACAACTTGCCAGCCAAGAC
KIN4-S1	TCGCATAATATTCTATCAGGACATTCCGTATACCTGAATATA TATACATGCGTACGCTGCAGGTCGAC
KIN4-S2	CACTCTATAATATAATGTAATTGTCGATATAACTATGTACTG AAAACTCAATCGATGAATTCGAGCTCG
LTE1-1	GAAGCATGAATTAAGATCATCG
LTE1-2	CCGTTGTAGTTATGTACTGAAG
LTE1-S1	TTGCTTTACATAGCCTCTAGCCATTCAAAGATTCGCTACCCT GAACCATGCGTACGCTGCAGGTCGAC
LTE1-S2	TTTTTTACAAGAGGAATTTGGGAACTGGAGGAAAGTGGCAC AATACCTCAATCGATGAATTCGAGCTCG
MOB1-S2	GCATGGAAGAATACAACCTACAAGCAGACTTATATAAATAT ACAATACTAATCGATGAATTCGAGCTCG
MOB1-S3	CGGCTGATTTTGGTCCGCTGTTAGAATTAGTGATGGAGTTGA GGGATAGGCGTACGCTGCAGGTCGAC
SPO12-1	CCCATTGTATTGCCTCTTCCC

SPO12-2	CGGGTGCCCGCTACTTTATTACAGAGG
SPO12-S1	AACAAAATAACATATACAGTAAGAACAATAGAAAACGTATTTATGCGTACGCTGCAGGTCGA
SPO12-S2	TAGTGTAGCATTTGGCTATTTTTGGATGACTAGAAAGGCAGATTTTTTTAATCGATGAATTCGAGCTCG
TEM1-S2	TAACGCCAACTCTCACATGGTAGCAGGCGGGTATAGTTGTTTTCAATCGATGAATTCGAGCTCG
TEM1-S3	TCCTCGTCGCCCTCATCTAAGGCACCATCGCCGGGCGTTAATACACGTACGCTGCAGGTCGAC

7.4 *Table of Media, Buffers, and Reagents*

Table 7. 4: Table showing the composition of media, buffers, and reagents used in this thesis.

Name	**Description**
TY agar with selective antibiotics (Ampicillin or Kanamycin)	5 g of NaCl (Merck, #106498), 5 g of Yeast Extract (Conda, #1702), 10 g of Tryptone (Biolife, #4122902), 20 g of Agar (Carl Roth, #5210.2), ddH2O up to 1000 mL. 100 µg/mL Ampicillin or 50 Kanamycin µg/mL
10X PCR Buffer	500mM Tris-HCl pH: 9.2 (Sigma, #T1503), 160mM (NH4)2SO4, 17.5mM MgCl2 (Fisher BioReagents, #BP214)
1X Blotting Buffer	25mM Tris, 190mM Glycine (AppliChem, #A1067), 0.025% SDS (Sigma, #75746), 20% methanol (Sigma, #32213)
1X Laemmli Running Buffer	25mM Tris, 192mM Glycine, 0.1% SDS, adjust pH to 8.3
1X PBS	137mM NaCl, 2.7mM KCl (Merck, #104936), 10mM Na2HPO4 (Merck, #106575), 1.76mM KH2PO4 (Fisher BioReagents, #BP362). Adjust pH to 7.2-7.4
1X PBS-T	137mM NaCl, 2.7mM KCl, 10mM Na2HPO4, 1.76mM KH2PO4. Adjust pH to 7.2-7.4 and add Tween-20 in final concentration of 0.02% (AppliChem, #A4974)

1X TAE Buffer	4.84 g of Tris, 1.14 mL of Glacial acetic acid (Isolab, #901016), 2 mL of 0.5M EDTA pH:8.0 (Sigma, #E5134), ddH2O up to 1000 mL.
2mM dNTPs mix	20 µL of dATP (100 mM), 20 µL dCTP (100 mM), 20 µL dTTP (100 mM) and 20 µL dGTP (100 mM), 920 µL ddH2O
5-FOA agar	6.7 g of Yeast Nitrogen Base without amino acids with ammonium sulfate (Conda, #1545), 2 g of SC-URA dropout amino acid mix, 20 g of D-(+)-Glucose, 0.1 g of Uracil (Sigma, #U1128), 1 g of 5-Fluoroorotic acid (USbiological), ddH2O up to 500 mL were mixed and filter-sterilized, then mixed with 20 g of sterile agar in 500 mL ddH2O
6% SET	3 mL of 20% SDS, 0.2 mL of 0,5M EDTA pH: 8.0, 0.3 mL of 1M Tris-HCI pH: 8.0, 6.5 mL of ddH2O
Colloidal Coomassie Brilliant Blue	Mix 100 mL ddH2O and 117 mL of H3PO4. Then, add 100 g of Ammonium sulfate to the warm solution. 1.2 g of Coomassie Brilliant Blue g-250 (Fisher BioReagents, #BP100). Complete the volume to 800 mL with ddH2O. Before use add Methanol final 20%.
Homemade ECL Solutions	Solution 1: 20 mL of 1M Tris-HCI pH: 8.5, 2 mL of 250mM Luminol (in DMSO, Sigma # A-8511), 889 µL of 90mM p-Coumaric acid (in DMSO, Sigma # C-9008), 178 mL of ddH2O Solution 2: 20 mL of 1M Tris-HCI pH: 8.5, 180 mL of ddH2O, 123 µL of 30% Hydrogen peroxide (H2O2, Sigma # H-1009)
HU-DTT	8M Urea (MP Biomedicals, #823048), 5% SDS, 200mM Tris-HCl pH: 6.8, 0.1mM EDTA, Bromophenol blue, 100mM 15 mg/mL DTT (Fisher BioReagnets, #BP172)
LiPEG	100mM LiOAc (Sigma, #L6883), 10mM Tris pH: 8.0, 1mM EDTA pH 8.0, 40% PEG3350 (Sigma, #P4338) ddH2O to complete the desired volume. Filter to sterilize.
LiSORB	100mM Lithium Acetate (LiOAc), 10mM Tris pH: 8.0, 1mM EDTA pH: 8.0, 1M Sorbitol (Merck, #107758), ddH2O to complete the desired volume. Filter to sterilize
P1 Buffer	50mM Tris-HCl pH:8.0, 10mM EDTA pH 8.0, 0.1 mg/mL RNase A
P2 Buffer	200mM NaOH, 1% SDS
P3 Buffer	3M KAc pH: 5.5

Ponceau S	0.2% (w/w) Ponceau S (Sigma #P3504) 3% (w/w) TCA in ddH2O
SC-X (X= URA, LEU, HIS or TRP)	3.4 g of Bacto Yeast Nitrogen Base (YNB) without amino acids with ammonium sulfate, 1 g of SC-X dropout amino acid mix, 10 g of D-(+)-Glucose, 0.05 g of Adenine hemisulfate salt (Sigma # A9126), ddH2O up to 500 mL
SC-X with selective antibiotics (Geneticin, Nourseothricin, or Hygromycin)	1.7 g of Yeast Nitrogen Base without amino acids without ammonium sulfate (Conda, #1553), 1 g of monosodium glutamic acid, 2 g of dropout amino acid mix, 20 g of D-(+)-Glucose, 20 g of Agar, ddH2O up to 500 mL were mixed and autoclaved, then mixed with 20 g of sterile agar in 500 mL ddH2O. 200 mg/L G418, 100 mg/L Nourseothricin or 300 mg/L Hygromycin into autoclaved agar
TY agar	5 g of NaCl, 5 g of Yeast Extract, 10 g of Tryptone, 20 g of Agar, ddH2O up to 1000 mL
TY medium	5 g of NaCl, 5 g of Yeast Extract, 10 g of Tryptone, ddH2O up to 1000 mL
TY medium with selective antibiotics (Ampicillin or Kanamycin)	5 g of NaCl, 5 g of Yeast Extract, 10 g of Tryptone, ddH2O up to 1000 mL. 100 µg/mL Ampicillin or 50 Kanamycin µg/mL
YPAD	5 g of Yeast Extract, 10 g of Peptone (Conda, #1616), 10 g of D-(+)-Glucose, 0.05 g of Adenine hemisulfate salt, ddH2O up to 500 mL
YPD with 0.01M Hydroxyurea	10 g of Yeast Extract, 20 g of Peptone, 20 g of D-(+)-Glucose, 20 g of Agar, ddH2O up to 1000 mL. Filter sterilized HU was added into the autoclaved agar in final concentration of 0.01M HU.
YPD with selective antibiotics (Geneticin, Nourseothricin, or Hygromycin)	10 g of Yeast Extract, 20 g of Peptone, 20 g of D-(+)-Glucose, 20 g of Agar, ddH2O up to 1000 mL. 200 mg/L G418, 100 mg/L Nourseothricin or 300 mg/L Hygromycin in autoclaved agar